PAP-952

THESIS

AIR ENTRAINMENT AND ENERGY DISSIPATION ON A STEPPED BLOCK SPILLWAY

Submitted by

Matthew L. Gaston

Department of Civil Engineering

In partial fulfillment of the requirements

for the degree of Master of Science

Colorado State University

Fort Collins, Colorado

Summer 1995

THESIS

AIR ENTRAINMENT AND ENERGY DISSIPATION ON A STEPPED BLOCK SPILLWAY

Submitted by

Matthew L. Gaston

Department of Civil Engineering

In partial fulfillment of the requirements

for the degree of Master of Science

Colorado State University

Fort Collins, Colorado

Summer 1995

ABSTRACT OF THESIS
EFFECTS OF ENTRAINED AIR
ON A STEPPED BLOCK SPILLWAY

With a recent increase in available precipitation and flood data, estimates of the Probable Maximum Flood (PMF) have been increased. This larger PMF value has meant that many of the dams and their spillways in the United States are now considered inadequate. The U.S. Bureau of Reclamation (USBR), in a cooperative effort with Colorado State University (CSU), has recently concluded a three-part series of tests aimed at examining the use of overlapping concrete wedge-shaped blocks for protection of overtopped dams. This thesis is based on the third and final phase of these tests. The purpose of this phase of tests was to study the effects of aeration on the bulking and the velocity of the flow over these blocks.

The results of the first two phases of tests produced a block that was proven to be stable in flows of 31.6 cfs/ft for four hours. A special facility was constructed at CSU for the second and third phases of tests. This facility, the CSU/USBR Dam Safety Overtopping Facility (DSOF), allowed flows of up to 32.2 cfs/ft, and a vertical drop of approximately 50 feet. The DSOF had four platforms used for taking measurements. However, only the lower three of these were used in the current study. Velocity and air concentration data were collected using two specially designed probes. The velocity probe was made from a modified airplane pitot static tube, and was calibrated for flows of varying air concentrations. The air

concentration probe was based on the principle that the resistivity of air is approximately 1000 times greater than that of water. Using two conductors placed a small distance apart, the air probe used this difference in resistance to detect air bubbles. An integration over a period of time gave air concentration measurements.

Since determining the depth of an aerated flow is very difficult, the concept of using the depth of flow to the point where the air concentration is 90% was used. This depth, called Y_{90}, is the same depth used by many other researchers. Velocity and air concentration profiles were taken at the center of the spillway at locations approximately 57, 101, and 110 feet from the crest. Unit flow rates of 3.3, 9.7, 18.0, 28.2, and 32.2 cfs/ft were tested. This allowed data to be taken in both the uniform and non-uniform regions of flow.

The data collected for this study produced six main conclusions:

1. A terminal velocity was reached for flow rates up through 28.2 cfs/ft. These terminal velocities appear to level off at approximately 38 fps. At the highest unit flow rate of 32.2 cfs/ft, it does not appear that a terminal velocity was achieved.

2. When the flow rate is high enough so cascading flow is no longer present, the difference between the bulked depth measured during the

tests, and the unbulked depth determined from a water surface profile calculation becomes relatively constant (0.25 feet for the present study).

3. If a skimming flow is present, the average air concentration of the flow is no longer affected by the very high roughness of the blocks. In these flows, the average air concentration becomes a function of the slope.

4. Air concentration profiles for a stepped block spillway assume the same general form as those for a smooth surface spillway.

5. In the uniform flow region, the shape of the air concentration profile is independent of unit flow rate.

6. In the uniform flow region, the friction factor becomes independent of unit flow rate.

Matthew L. Gaston
Civil Engineering Department
Colorado State University
Fort Collins, CO 80523
Spring 1995

ACKNOWLEDGMENTS

A sincere thanks is extended to Colorado State University and the United States Bureau of Reclamation for jointly funding this study. Special thanks is extended to my advisor, Dr. James F. Ruff, for his guidance and advice throughout my graduate career at Colorado State, and to Brent Mefford and Kathy Frizell of the USBR for their assistance in collecting and understanding the data. Thanks, also, to Ellen Wohl for serving on my committee. I especially thank my wife, Jana, and my parents, for their support and understanding throughout my graduate career, and especially the last few months of writing this thesis. I would also like to thank Jesse, Lisa, Jason, and Bill, whose assistance in collecting the data made this research possible.

TABLE OF CONTENTS

LIST OF FIGURES

LIST OF TABLES

CHAPTER 1
INTRODUCTION

With the increasing availability of historical data on precipitation and floods, estimates of the Probable Maximum Flood (PMF) have risen, indicating that many embankment dams and their spillways are insufficient. In most cases the options of raising the dam height or increasing the spillway capacity prove to be economically unfeasible. A third option is to let the flood water overtop the dam. This would require some type of measure to protect the downstream face from the resulting erosion that could eventually cause the failure of the dam.

The United States Bureau of Reclamation (USBR) is presently studying the use of overlapping concrete wedge blocks as a protective overlay for overtopped earthen dams. The stability of these blocks has already been proven through tests completed on a near-prototype spillway at the Colorado State University (CSU) Engineering Research Center. In these tests the blocks withstood unit discharges as high as 31.6 cfs/ft (2.94 cms/m) for four hours (Slovensky, 1993).

As more dams are allowed to overtop, many additional factors need to be studied, one of these being self-aerated flow. The study of self-aerated flow is important as it is a parameter that affects such design criteria as velocity and bulking of the flow. Self-aeration is one of the primary characteristics of high-velocity, open-channel flow. Self-aerated flow is the natural phenomenon that occurs in supercritical

open-channel flow when air is entrained at the free surface. Previous studies have shown that as the air concentration in a flow increases, the velocity of the flow also increases, and the drag decreases, (Straub and Anderson, 1958). The increase in velocity corresponds to a decrease in the mean depth, but an increase in the bulked depth of the water (or spray). Design of spillway sidewalls must include the increased height of the flow due to the bulking. The decrease in drag accompanying an aerated flow is thought to be caused by the presence of the air bubbles next to the floor of the spillway which increases the dynamic viscosity. This increase in viscosity results in a thickened viscous sublayer, and a decrease in drag (Chanson, 1992). It is also known that the potential for cavitation damage in aerated flows is much less than that of non-aerated flows due to the cushioning effect of the entrained air.

The present study was the third of a three-part series of tests conducted by the USBR. The first phase, conducted at the USBR Hydraulics Laboratory, determined the optimum block geometry to create the best balance between separation-zone pressure reduction and energy dissipation. What this balance achieved was a block that incorporated the energy dissipating characteristics of a stepped overlay, but allowed velocities high enough to create very low pressures in the separation zone that exists just downstream of each block. Applying the USBR's block design to a 2:1 embankment slope (the slope of the spillway used at CSU) gives a block with a step height to length ratio of 1:4.6, and a tread surface sloped down from horizontal by 15 degrees. For more details of the block design please refer to Chapter 3.

The second phase of the USBR study verified the stability of the wedge block design placed on a gravel filter layer on a near-prototype scale embankment. The purpose of the filter layer was to facilitate drainage of any water that might get through gaps between blocks. A special outdoor facility was built for this purpose at the CSU Engineering Research Center. For results of these tests refer to Slovensky (1993).

The third and final stage of the USBR tests was performed at the same facility as that of phase two. The objectives of this phase of tests and the subject for this report were as follows.

1. Measure the air concentration in the flow over a near-prototype scale embankment and evaluate the air concentration distribution.
2. Measure the velocity in the flow over a near-prototype scale embankment and evaluate the velocity distribution.
3. Use the collected data to develop and verify design criteria for the use of concrete wedge blocks for dam overtopping protection.

Though several tests have been performed on self-aerated flows in open channels, the topic is still relatively new. Because self-aeration requires a supercritical open channel flow, one of the easiest places to find this situation is on a spillway. Figure 1.1 is a diagram of the regions present in a self-aerated flow.

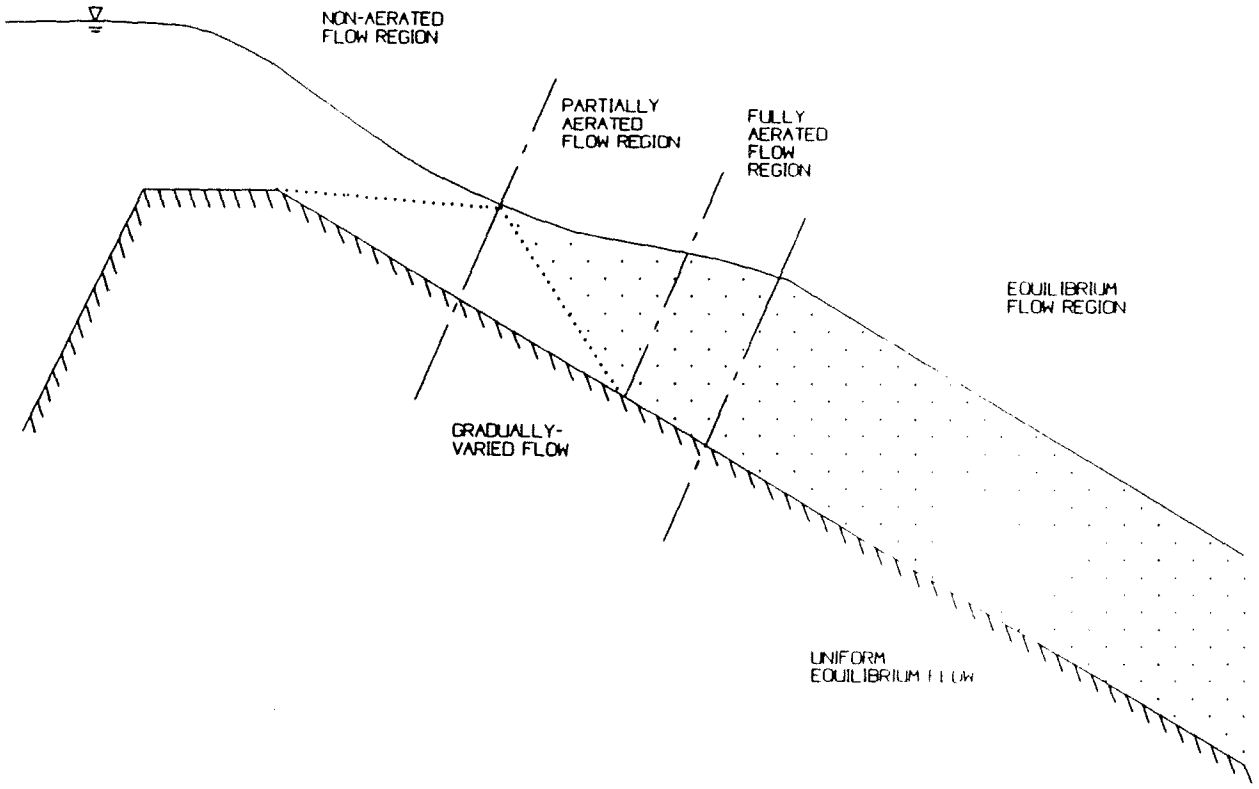

Figure 1.1: Regions of a self-aerated flow

Water coming over the crest of a spillway is at the water surface quite smooth, but at the spillway surface turbulence is being created as a result of the flow being retarded by the solid boundary. This turbulence forms a turbulent boundary layer that keeps expanding in the downstream direction until it reaches the water surface. At this point, known as the point of inception, air entrainment begins. Following the point of inception air bubbles are gradually drawn deeper into the flow profile until the entire flow is aerated. Given sufficient length, the flow will become uniform, with air entrainment and escape being equal. This can be defined as the uniform equilibrium flow region (Chanson, 1993). This mode of air entrainment seems to be the most commonly used method today.

CHAPTER 2
LITERATURE REVIEW

Except for a very limited number, all tests on self-aerated flows have been conducted on laboratory flumes or relatively small scale models, generally about 1:15 scale. The lack of data from large scale models or prototype spillways is due to the difficulties involved with obtaining data on such a structure, as well as the small number of facilities available for obtaining such data. Because of this, much of the available literature deals with the topic of using bottom aerators to induce air into the flow, unlike the present study. This literature is still helpful, though, in determining methods to measure the air concentration and velocity of the flow. Following is a two-part summary of existing contributions in the area of air entrainment on dams and spillways. Given first is a chronological presentation of the developments made by selected authors in the area of air concentration and velocity measurement devices, as well as their major discoveries. The second section is a more detailed look at past theoretical development in the area of air concentration distributions and velocity distributions in self-aerated flows.

LITERATURE REVIEW PART 1: METHODS FOR STUDYING AERATED FLOWS

Ehrenberger, 1926

Ehrenberger was one of the first investigators of the air entrainment process, and his work has influenced many succeeding studies. Ehrenberger describes air-entrained flow as consisting of four different layers, each containing a different air

concentration. The first layer, closest to the surface of the channel, is pure water with no air. The second layer consists of water with a few individual air bubbles mixed in. Above this layer is a region of closely packed air bubbles and water. The fourth and final layer is made up solely of water drops flying through the air. Ehrenberger's experiments were performed in a rectangular flume with discharges ranging from 0.106 to 1.57 cubic feet per second (cfs) on slopes from 15.5 to 76.2 percent. Though somewhat crude in his method, Ehrenberger did take some air concentration measurements using a chute constructed of sheet metal that separated the flow into layers (Killen, 1968). The amount of water and air for each section was then measured to determine the air concentration.

Straub & Anderson, 1958

Lorenz Straub and Alvin Anderson are credited with obtaining the "classic set" of aerated flow measurements. Their tests at the St. Anthony Falls laboratory were performed in a variable sloped flume 50 feet long, 1.5 feet wide, and 1 foot deep. An electrical resistance probe was used to measure the air concentration in the flow. This probe, developed by Lamb and Killen (1950), operated on the principle of measuring the bubbly mixture between two electrodes. Assuming that the conductivity of air is zero, Lamb and Killen showed that Maxwell's equation for specific resistivity of a suspension of spheres could be reduced to an equation involving only the air concentration of bubbles in water as follows:

$$C = \frac{\frac{R_E}{R_{EO}} - 1}{\frac{R_E}{R_{EO}} + 1} \qquad (2.1)$$

in which R_E is the resistance between two electrodes of the air water mixture, and R_{EO} is the resistance between the same two electrodes of the water alone. To measure the velocity of the flow a device was used which timed the travel of a small cloudlet of saltwater as it passed two electrodes spaced three inches apart in the flow path. The air concentration probe and the velocity meter were both calibrated by a comparison between the measured water rate entering the channel and the integrated flow determined by velocity and air concentration traverses over the channel cross section. A typical air concentration profile from Straub and Anderson's tests is shown in Figure 2.1.

Straub and Anderson described aerated flow as consisting of two regions: an upper region consisting of water globules ejected from the main flow that can be described by a cumulative Gaussian probability equation, and a lower region of distributed air bubbles that closely follows an equation for turbulent mixing. Both regions are described in more detail in the next section.

The tests revealed two important concepts. First, it was shown that the flow depth of aerated flow is greater than that for non-aerated flow; thus, a bulking effect,

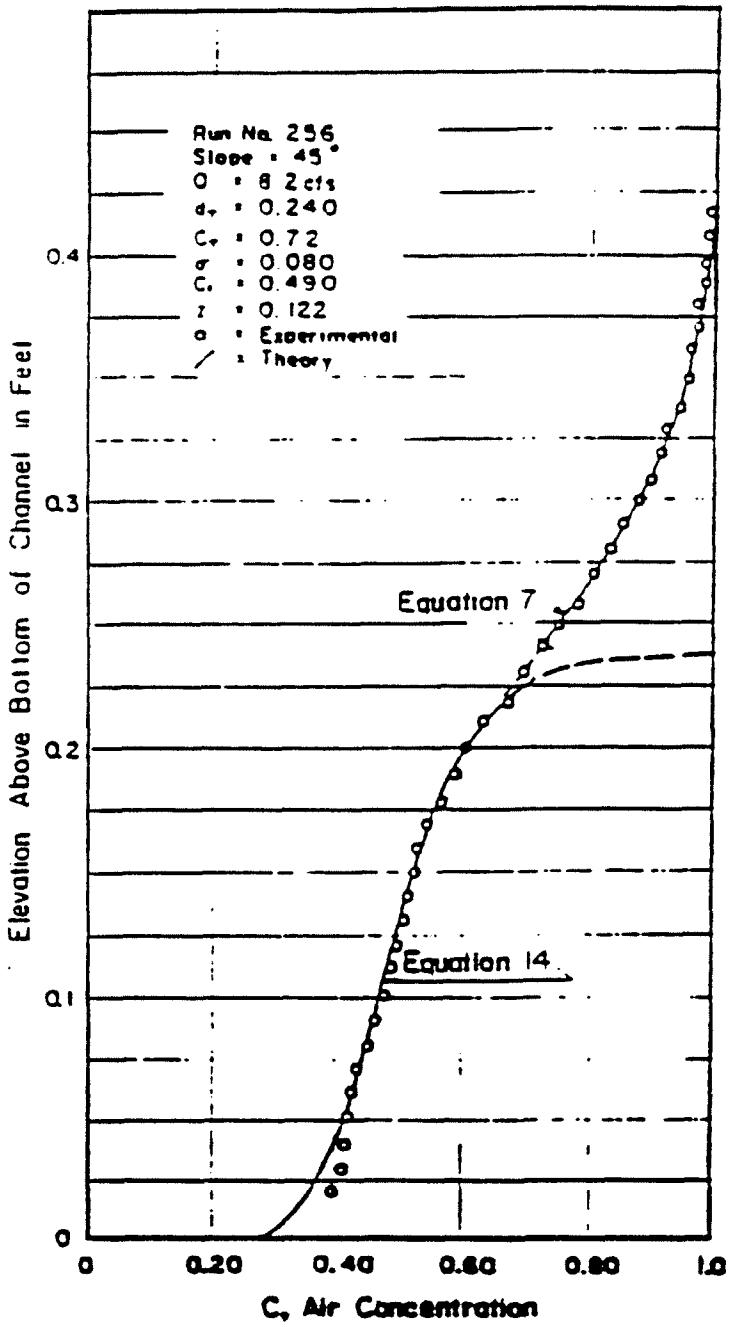

Figure 2.1: Typical air concentration profile found by Straub and Anderson (1958)

or increasing of the flow area, is present in aerated flows that needs to be considered when designing spillway sidewalls. Second, the velocity of an aerated flow was also shown to be greater than that for a non-aerated flow, (Straub & Anderson, 1958). The resulting increase in momentum must be considered when designing an energy dissipater, such as a ski jump, downstream of a spillway (Ackers and Priestley, 1985).

Cain, 1978

Paul Cain studied the developing region of self-aerated flow on the Aviemore Dam spillway in New Zealand at unit flow rates of 2.23 m^2/sec and 3.15 m^2/sec using a combined pressure/air concentration probe. This probe predicted the velocity using measurements of air-concentration and stagnation pressure. The stagnation pressure was measured using a pressure transducer attached to the stagnation point of the probe by a fluid-filled pressure inlet tube. The air concentration was measured by the resistance in the electric field created between two electrodes.

Calibration of the probe was done using a flow simulator. The simulator consisted of a tube in which a known flow rate was present. Upstream of the test section a device was inserted consisting of three hollow airfoil-shaped tubes that were vented to the atmosphere. Connected to these were 18 uniformly spaced 4.7-mm diameter tubes. Flow past these tubes sucked air into the test section where it was

dispersed by turbulence. The calibration was based on the concept that since the 18 air inlet tubes took up approximately 13% of the cross sectional area of the test section then the air concentration in the test section was approximately 13%.

This probe was mounted at five test stations placed every 6.1 meters down spillway bay five of Aviemore Dam. Each station consisted of a steel box lying flush with the spillway surface. Inside each box was a stepper motor that allowed the probe to be set accurately within 0.5 mm to a maximum depth of 352 mm. Measurements were taken with the spillway gate open to 300 mm and 450 mm. Cain found the air concentration to be a function of the inception depth and the distance downstream from the point of inception, as was expected. The velocity distribution, however, was found to be independent of the air concentration, as well as the position on the spillway. This contradicts the findings of most other researchers in that it suggests that the air in suspension has a negligible effect on the velocity distribution of the air-water interface (Cain and Wood, 1981).

Wood, 1983

Ian Wood performed a re-analysis of the classic set of air concentration data taken by Straub and Anderson (1958). He found that a mean air concentration and concentration distribution exist for each slope. In other words, he showed that the average air concentration for uniform flow is a function solely of the slope, and is independent of the upstream geometry.

Figure 2.2 is a plot of the friction factor against the mean air concentration. This plot shows a significant reduction in the friction factor as the air concentration increases. Wood interprets this plot to show that there is no departure from the water value of the friction factor until the mean air concentration reaches 30%, meaning that no drag reduction occurs until the air concentration reaches 30% (Wood, 1983).

Bachmeier, 1987/88

Guido Bachmeier performed tests at the Institute for Hydromechanics of Karlsruhe University in Germany on a 1:15 scale model of the Foz do Areia Dam in Brazil. The purpose of Bachmeier's tests was to determine some dimensioning techniques for bottom aerators used for the prevention of cavitation on dam spillways. A probe consisting of Fischer and Porter rotameter flow meters for water and air was used to measure the air concentration in the flow. Bachmeier used a method for the calibration of his probe which, by comparison with the methods just discussed, appears to be quite accurate. Water and air were each measured separately before mixing so a known concentration was available. The measuring device was then placed in a jet of this mixture for calibration, and the near-linear relationship between voltage and air concentration, shown in Figure 2.3, was achieved (Bachmeier, 1988).

Chanson, 1989, 1992, 1993

Much of the recent work on self-aerated flows has been done by Hubert Chanson. In his experiments, Chanson used a 1:15 scale model of the Clyde Dam

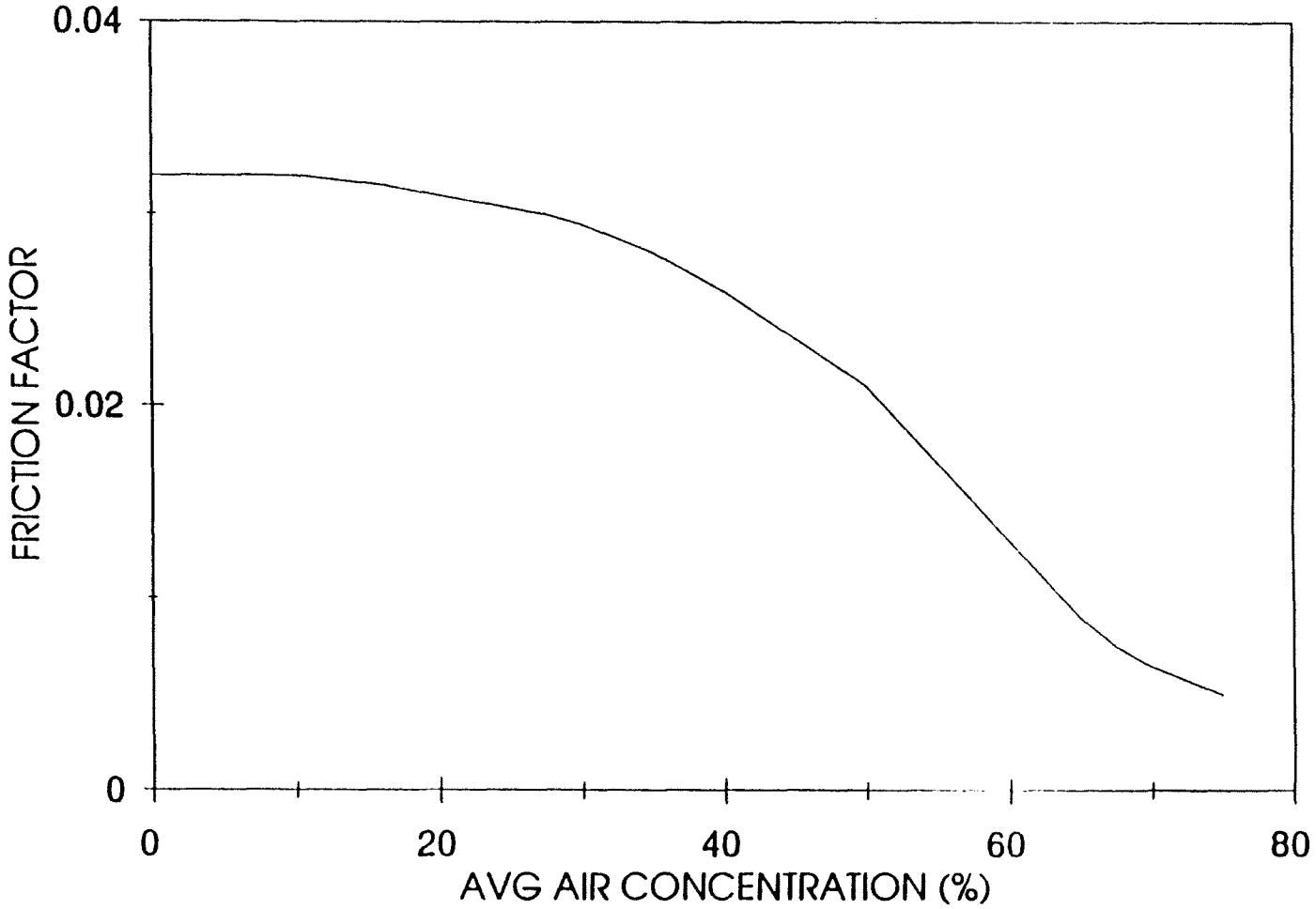

Figure 2.2: Wood's relationship between friction factor and air concentration

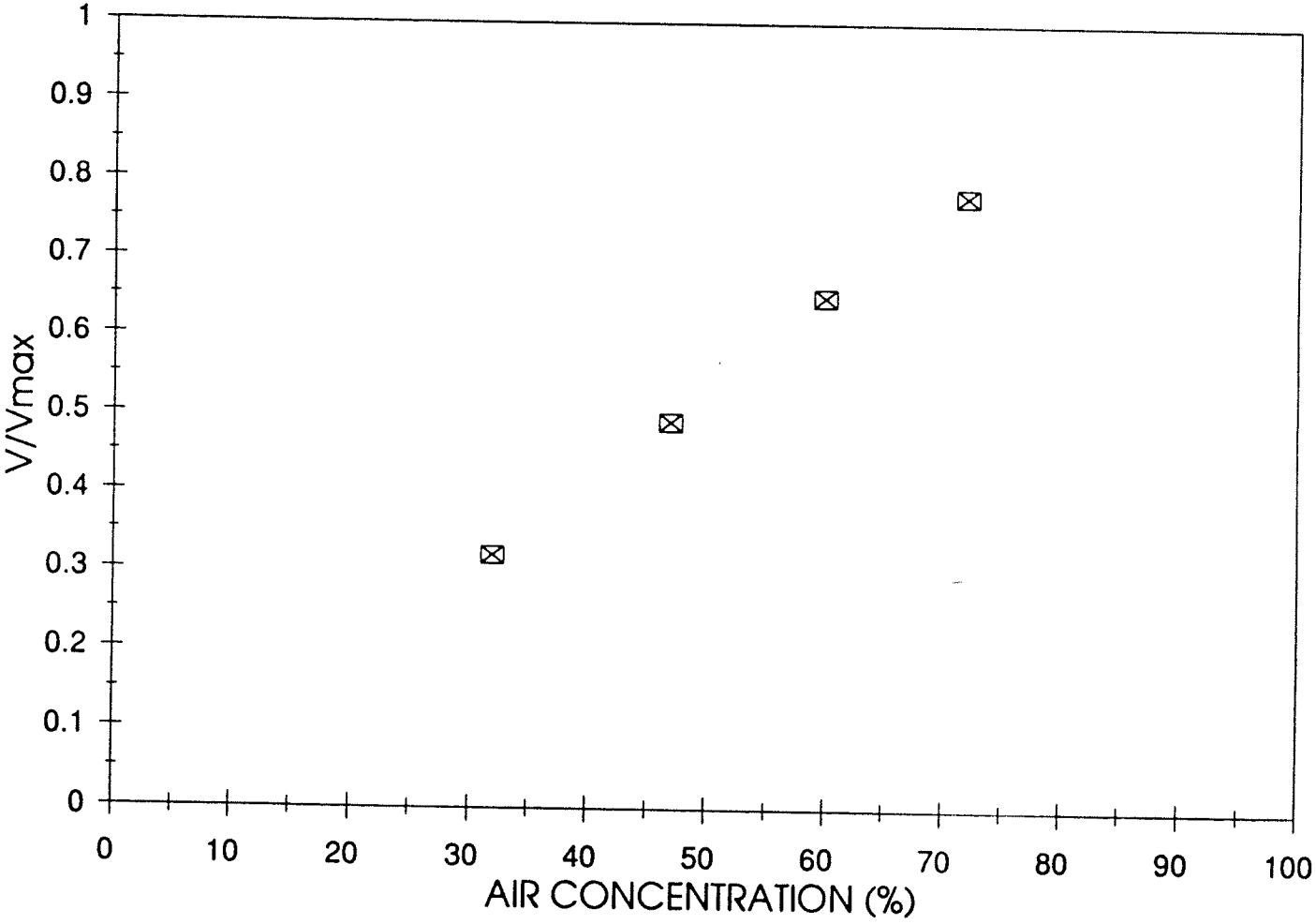

Figure 2.3: Bachmeier's air probe calibration curve

spillway which has a slope of 52.33 degrees. Air-water mixture velocities were measured using a two-tip velocity probe and a cross-correlation probe (Chanson, 1989). No details were found concerning how this probe worked, or how it was calibrated.

Chanson believes that the channel slope, water discharge, and non-aerated friction factor are the quantities needed for a complete description of a uniform aerated flow. Following an analysis of his data Chanson suggests that there exists an air concentration boundary layer. This is consistent with the bottom layer described by Ehrenberger in 1926. Chanson suggests that this boundary layer might in some way interact with the shear stress and velocity distribution next to the channel surface to give a possible explanation to the drag reduction process that takes place in aerated flows.

LITERATURE REVIEW PART 2: THEORY DEVELOPMENT IN AERATED FLOW

MECHANISMS OF ENTRAINMENT

Many explanations have been offered in the past as to the mechanism of self-air-entrainment. Keulegan and Patterson (1940) suggested that air-entrainment may occur due to breaking waves at the free surface of the flow when the Froude number is greater than 1.5. Volkart (1980) suggested the idea that air is entrained by water drops falling back into the flow. Air entrapment caused by turbulent velocity

fluctuations on the free surface was proposed by Hino (1961) and Ervine and Falvey (1987). (Most present researchers in the area of self-aerated flow agree on the theory that air-entrainment is, in part, caused by the growth of the turbulent boundary layer to the free surface of the flow.) Another necessary condition for air-entrainment is that the turbulence level must be large enough to overcome both surface tension and gravity effects (Killen, 1968). In other words, the turbulent velocity normal to the free surface must be great enough to overcome the surface tension pressure of the entrained bubble for the bubble to be carried away. The turbulent velocity must also be greater than the bubble rise velocity component (Rao and Rajaratnam, 1961; Ervine and Falvey, 1987). These conditions can be restated in the following two equations:

$$v^t > \sqrt{\frac{8\sigma}{\rho_w d_b}} \tag{2.2}$$

$$v^t > u_r \cos\alpha \tag{2.3}$$

where v^t= turbulent velocity, σ = surface tension, ρ_w = density of water, d_b =bubble diameter, u_r = bubble rise velocity, and α = slope of the spillway. Equations (2.2) and (2.3) must be satisfied for air-entrainment to occur (Chanson, 1993).

Referring to Figure 1.1 it can be seen that following the point of inception there exist two regions of flow: a gradually varied flow region, and a uniform equilibrium flow region. Following is an explanation of the concepts involved with each, starting with the uniform flow region.

UNIFORM FLOW REGION

VELOCITY DISTRIBUTION:

Certain definitions are essential to the study of aerated flow. Any time one deals with aerated flow the air concentration must be known before any other parameters can be properly described. The air concentration, c, can be defined as the volume of air per volume of air and water for a given flow. The air concentration for the present study was measured using a special probe developed by the USBR, and is described in detail in Chapter 3. Having the air concentration, a characteristic flow depth, d, can then be defined as:

$$d = \int_0^{Y_{90}} (1-c)\, dy \tag{2.4}$$

where Y_{90} is the depth, measured from the channel bottom, where the air concentration is 90%, and the depth, y, is measured perpendicular to the slope (Chanson, 1993; Wood, 1983). Knowing that the discharge per unit width is q_w, the average water velocity for the flow can be defined as:

$$U_w = \frac{q_w}{d} \tag{2.5}$$

Several equations have been proposed in the past to describe the velocity distribution in aerated flow and there is some controversy as to the proper form. The thrust of the disagreement comes from the question of whether the velocity

distribution is dependent on the air concentration. In 1953, Halbronn, et al. proposed the following equation based on Bernoulli's equation using the pitot tube static head difference, P_s - P_a.

$$\rho_w \frac{(1-\lambda c)\, u_w^2}{2g} = P_s - P_a \tag{2.6}$$

Where λ = a coefficient that allows for the ratio of bubble size to total head tube size, and c = air concentration. Lai (1971) used a similar equation and came up with values between 0.91 and 1.09 in his calibration of λ. In calculating his results he simply used a mean value of 1.0, (Wood, 1983). Viparelli (1957) used the following very similar form of the same equation:

$$u_w = \sqrt{2g\delta} \tag{2.7}$$

Where δ is the pitot tube static head difference. It is interesting to note that this equation is independent of the air concentration. Viparelli suggests that this velocity is valid only for layers near the bottom of the channel, and that above a certain layer the velocity should be described by the following equation developed from Gauss's probability equation.

$$q = u_w e^{-1/2} \left(\frac{y-h}{\sigma \delta_{max}} \right)^2 \tag{2.8}$$

where q = water discharge per unit width, y = depth of flow, h = depth associated

with δ_{max}, and δ_{max} = maximum difference in pitot tube static head, and σ = the standard deviation.

Tests were performed by Cain in 1978 on the Aviemore dam in which he took measurements of the velocity of the air-water interfaces, u_w, in the aerated flow. Cain suggests the following equation for flows with mean air concentrations between 0% and 50%. The similarity between Cain's equation and that of Viparelli should be noted in that neither one is dependent on the mean air concentration.

$$\frac{u_w}{u_{c=90}} = \left[\frac{y}{y_{c=90}}\right]^{0.1584} \tag{2.9}$$

Here, $u_{c=90}$ and $y_{c=90}$ correspond to the velocity and depth where the air concentration is equal to 90%. This equation is based on the flow in the developing region, but because it is independent of the air concentration, Wood (1983) proposes that it would also be valid in the uniform flow region. To obtain a distribution from this equation, $u_{c=90}$ must first be known. This can be found by combining the above equation with the continuity equation, thus obtaining:

$$u_{c=90} = \frac{q_w Y_{90}^{0.1584}}{\int_0^{Y_{90}} (1-c)\, y^{0.1584}\, dy} \tag{2.10}$$

Equation (2.9) can then be used to obtain the velocity distribution.

FRICTION FACTOR:

In most recent studies it has been common belief that the air concentration distribution is independent of discharge, and is only dependent on the slope of the channel and the friction in the channel. A description of the friction factor can be obtained by equating the shear stress on the bed of the channel with the component of weight down the slope, and assuming that for very high Reynold's numbers and relatively rough spillways the Reynold's number effects can be neglected (Wood, 1983). This yields the following functional relationship for the uniform air-water mixture friction factor, f_{aw}.

$$f_{aw} = \frac{8g \sin\alpha \; d^3}{q^2} \Phi \left(\frac{d}{k}, \overline{c} \right) \tag{2.11}$$

Here α = channel slope, d = depth of flow, k = relative roughness, and $\overline{c}$ = mean air concentration. Several variations of this equation have been used, the most recent by Chanson (1993). In his equation, Chanson replaces the function, Φ, with $D_H/4d$ and obtains the following result.

$$f_{aw} = \frac{8g \sin\alpha \; d^2}{q_w^2} \left(\frac{D_H}{4} \right) \tag{2.12}$$

where D_H is the hydraulic diameter and is equal to four times the hydraulic radius.

In 1983 Wood reanalyzed Straub and Anderson's (1958) classic set of aerated

flow measurements and showed that when the average air concentration increases, the uniform air-water mixture friction factor decreases. This can be seen in Figure 2.4 developed by Wood (1983) based on Straub and Anderson's data. The plot relates f_{aw} and the non-aerated friction factor, f, to the mean air concentration. Note, also, that as one would expect, as the air concentration goes to zero, f_{aw} and f become equal (i.e., $f_{aw}/f = 1$).

AIR CONCENTRATION DISTRIBUTION

As previously stated, Ehrenberger (1926) described aerated flow in steep channels as consisting of four layers, each having more air and less water the further from the channel bed the measurements were taken. Straub and Anderson (1958) describe aerated flow as consisting of two layers with a transition zone in between. The first layer is the upper region made up of globules and droplets of water that are ejected at arbitrary velocities from the main flow into the atmosphere. The second layer is a region consisting of a distribution of air bubbles through the flow by turbulent transport fluctuations that can be described by some boundary layer equation. The transition zone exists between the two layers at a mean elevation above the channel bottom defined by a transition depth, d_T. Straub, et al. found that the upper region can be described by the Gaussian cumulative probability equation given as:

$$\frac{1-C}{1-C_T} = \frac{2}{h\sqrt{\pi}} \int_{y'}^{\infty} e^{-\left(\frac{y'}{h}\right)^2} dy' \qquad (2.13)$$

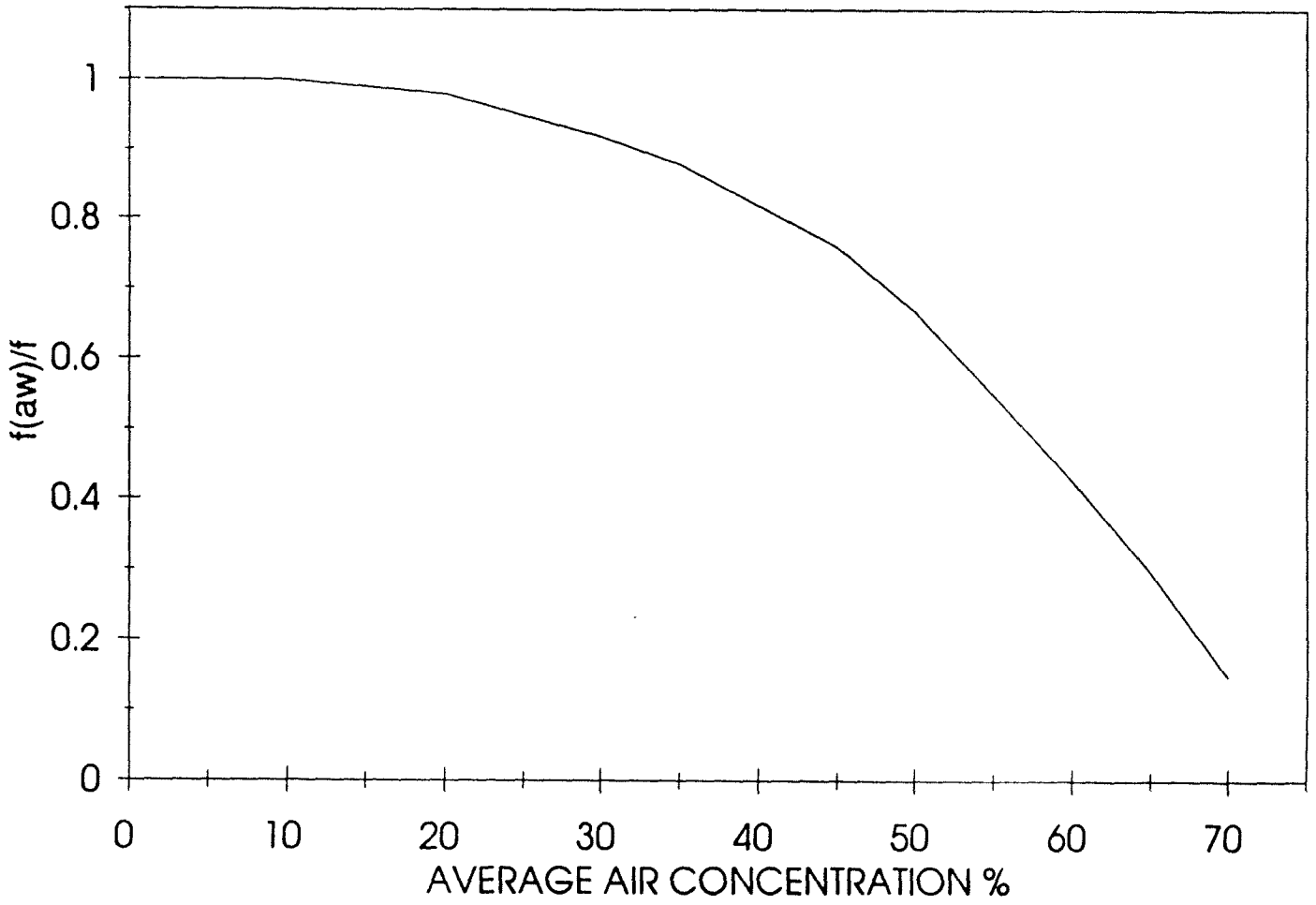

Figure 2.4: Relationship between air concentration and the air-water friction factor

in which C = the air concentration, C_T = concentration at the transition depth, h = a mean height to which water particles are projected above d_T, and y' = the outward normal distance above d_T. The air distribution in the lower region can be described by the following equation for turbulent mixing based on an approximation for the distribution of the mixing parameter:

$$C = C_1\left(\frac{y}{d_T - y}\right)^z \tag{2.14}$$

where

$$z = \frac{u_b}{\beta k\sqrt{\frac{\tau_0}{\rho}}} \tag{2.15}$$

in which C_1 = the concentration at $y = d_T/2$, u_b = the bubble rise velocity, β = a proportionality constant based on the mixing parameters, k = Von Karman's velocity distribution constant, τ_0 = the boundary shear force, and ρ = the density of water.

According to Straub and Anderson the mean air concentration, c, is dependent on the slope of the channel and the unit discharge, q. Wood (1983) reanalyzed Straub and Anderson's data and showed that indeed the air concentration is dependent on slope, but pointed out that Straub and Anderson were not looking solely at the uniform flow region when they concluded that the mean air concentration was dependent on the unit discharge. In Wood's re-analysis of Straub and Anderson's data it was shown that the average air concentration for uniform flow conditions, C_e,

is not dependent on the discharge, and is solely a function of the slope of the channel. Thus, given the slope and the depth at which the air concentration is 90%, it should be possible to obtain the distribution of the equilibrium air concentration.

If Wood's method is used, the uniform equilibrium flow region can be described completely. Table 2.1 gives a fair estimate of the mean air concentration, and if the non-aerated friction factor, f, is known then the aerated friction factor, f_{aw}, can be determined from Figure 2.4.

Table 2.1: Wood's air concentration for given slopes, based on Straub & Anderson's data.

Slope (degrees)	C_e
7.5	0.161
15.0	0.241
22.5	0.310
30.0	0.410
37.5	0.569
45.0	0.622
60.0	0.680
75.0	0.721

This allows the depth, d, to be computed from equation (2.12).

$$f_{aw} = \frac{8g \sin\alpha \; d^2}{q_w^2} \left(\frac{D_H}{4}\right) \qquad (2.12)$$

The average water velocity, U_w, is then found from equation (2.5).

$$U_w = \frac{q_w}{d} \tag{2.5}$$

And Y_{90} is calculated from equation (2.16) as follows:

$$Y_{90} = \frac{d}{(1-C_e)} \tag{2.16}$$

The water velocity distribution can then be found from the fact that the Aviemore dam data showed that $u_{90} = 1.2U_w$, and equation (2.9) (Wood, 1985).

$$\frac{u_w}{u_{c=90}} = \left[\frac{y}{y_{c=90}}\right]^{0.1584} \tag{2.9}$$

GRADUALLY VARIED FLOW REGION

Wood's (1985) description of the gradually varied flow region in a self-aerated flow is probably the most complete. In his analysis Wood determined that to describe this region of flow an entrainment function was needed in conjunction with a modified version of the gradually varied flow equation. Determining that these were dependent upon the Froude number and mean air concentration at a given position on the slope he then developed the following two equations:

$$V_e = q\frac{dC}{dx} = 0.17\,[C_e - \overline{C}]\cos\theta \tag{2.17}$$

$$\frac{dy}{dx} = \frac{\sin\theta - S_f + d\sin\theta \frac{d\theta}{dx}}{\cos\theta - 1.05F_r^2} \tag{2.18}$$

where V_e = the entrainment velocity, θ = the slope angle, F_r^2 = the square of the Froude number = q^2/gd^3, and S_f may be defined by:

$$S_f = \left[\frac{q_w^2 f_e}{8gd^3}\right]\Phi(c) \tag{2.19}$$

in which $\Phi(c) = f_{aw}/f$ and is defined by the curve in Figure 2.4.

Equations (2.17) and (2.18) then become two simultaneous differential equations that can be solved numerically when used with $\Phi(c)$ and C_e for each slope (Wood, 1985).

In summary, previous research has shown that four main regions exist in a self-aerated flow:

1. Non-aerated flow region
2. Partially aerated flow region
3. Fully-aerated flow region
4. Equilibrium flow region

Studies have been conducted which look at all of these regions, but most of these studies took place in smooth-surfaced flumes. The purpose of the present research was to study the fully-aerated flow regions of a spillway with a surface much rougher than those previously researched. The next chapter describes the testing facility and equipment used for this study.

CHAPTER 3
DESCRIPTION OF TESTING FACILITY
TEST PROCEDURES AND SETUP

SUMMARY

The tests at CSU were performed on a near-prototype scale model, the CSU/USBR Dam Safety Overtopping Facility (DSOF). Near-prototype, in this case, means that the vertical drop in the model is similar to that of many small dams currently in operation, but the width was constricted to allow for high unit discharges. There are many advantages that a model this size has over smaller models or flumes. When dealing with aerated flow, for example, one distinct advantage is the fact that surface tension forces in small models tend to be much greater than the entrainment forces, thus creating a very reduced aeration effect. A picture of the DSOF is shown in Figure 3.1. Figures 3.2 and 3.3 show plan and profile views of the testing facility. The main components of the facility are:

- Intake pipeline
- Concrete flume
- Stepped-block overlay and filter material
- Return pipeline and pump
- Measurement platforms and equipment

Following is a detailed description of the facility and equipment used.

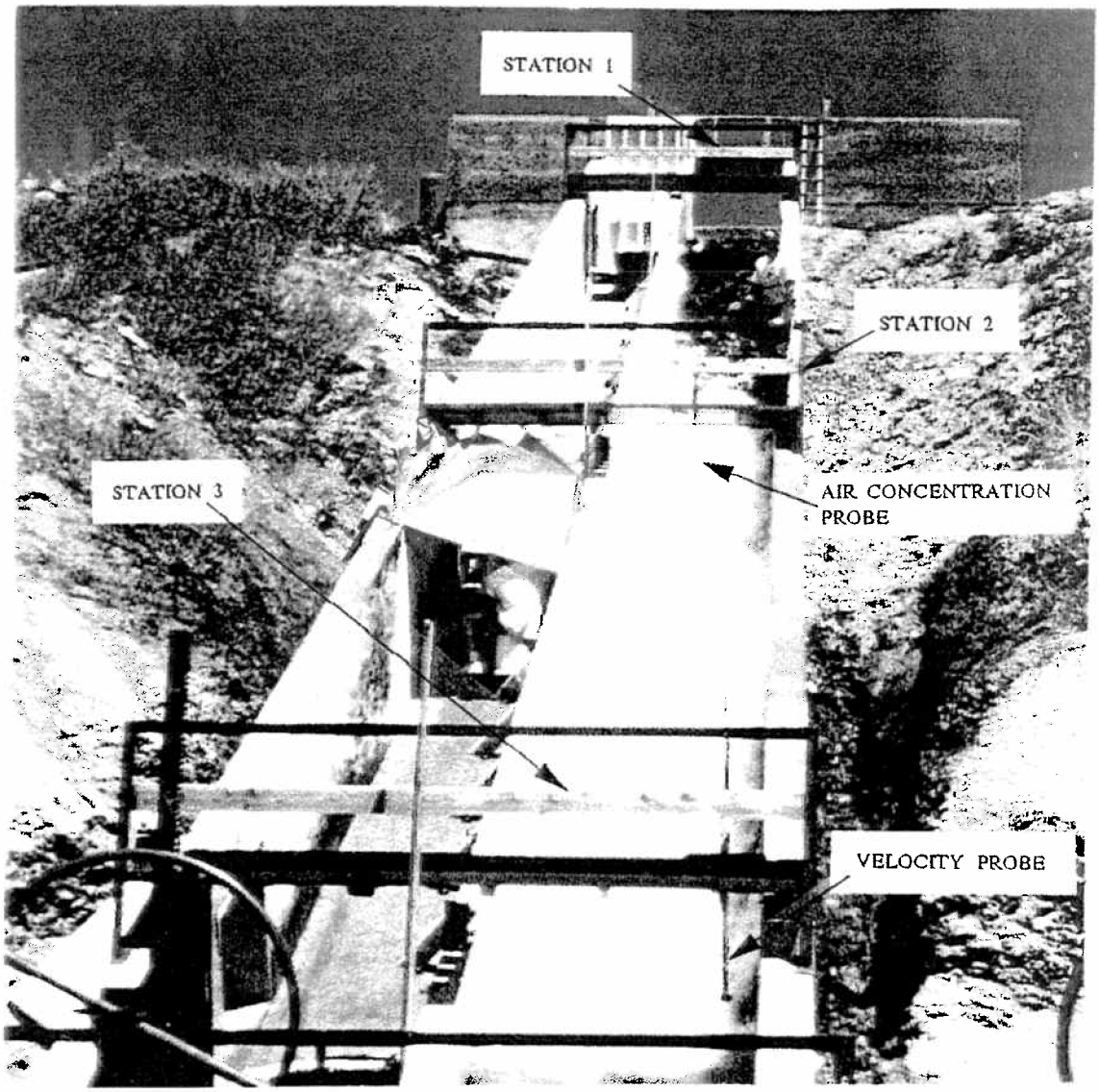

Figure 3.1: CSU/USBR Dam Safety Overtopping Facility

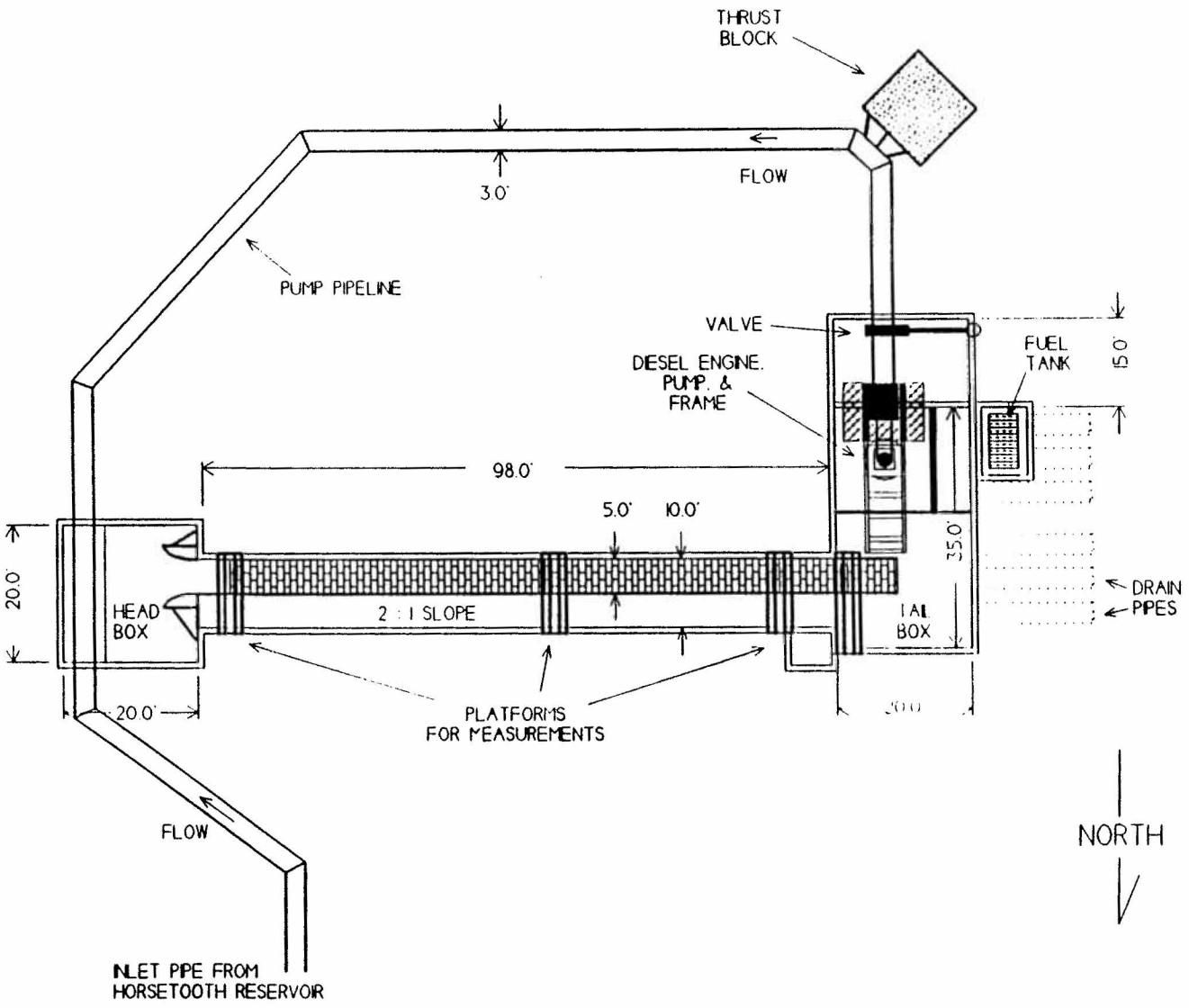

Figure 3.2: Plan view of overtopping facility

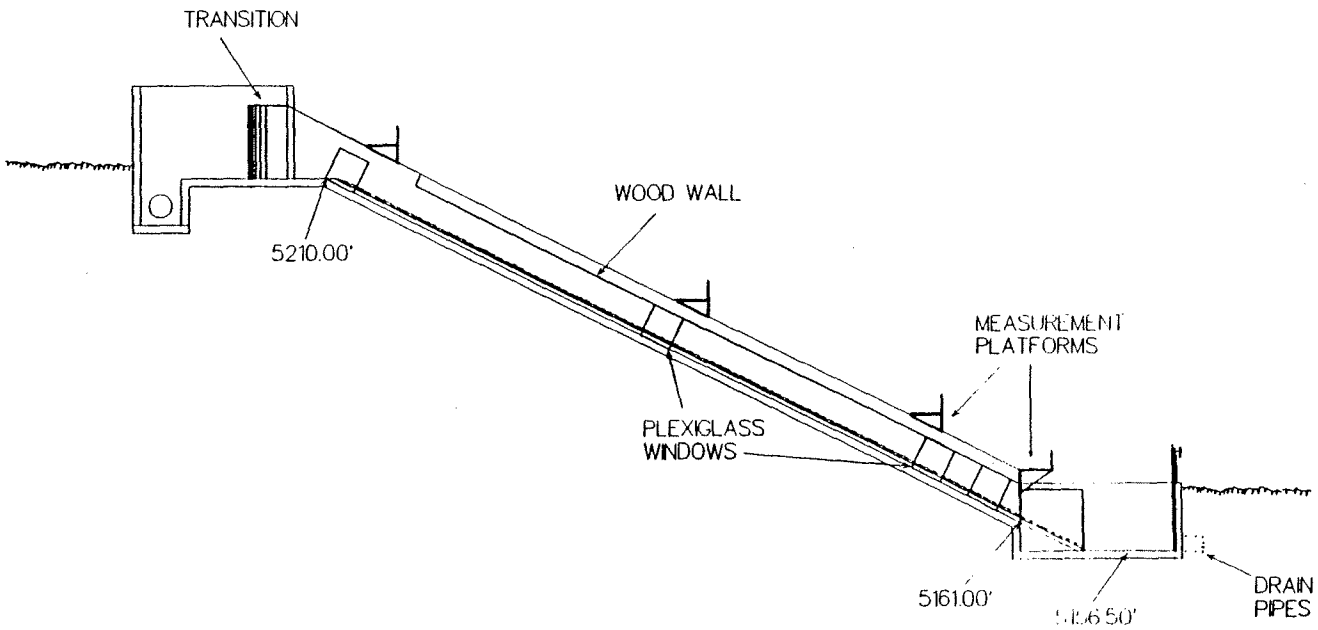

Figure 3.3: Profile view of overtopping facility

DESCRIPTION OF TESTING FACILITY

The CSU/USBR DSOF is a concrete flume 10 feet (3 meters) wide. It is located just west of Ft. Collins, Colorado, at the Engineering Research Center on the Foothills Campus of Colorado State University. For the current tests a temporary wood wall, 4 feet (1.2 meters) high, was placed in the flume to constrict the width to 5 feet (1.5 meters). At a 2H:1V slope, the facility provides approximately 50 feet (15 meters) of vertical drop.

Water is supplied via a 36-inch (914 mm) pipeline from Horsetooth Reservoir which provides a flow of approximately 130 ft^3/s (3.68 m^3/s) dependent upon the reservoir elevation. The pipeline enters a diffuser in the headbox of the flume to distribute the flow more evenly. The tailbox contains six 36-inch (914 mm) drainage pipes, three of which have slide gates to control the water level in the tailbox. These gates, together with stop-logs, can also be used to control the head on a pump which recirculates some of the flow back to the headbox to supply an additional 45 ft^3/s (1.275 m^3/s) when needed, for a total flow of 175 ft^3/s (4.96 m^3/s). The pump is powered by an Aurora Diesel 8V-92T engine that supplies 435 BHP(325 KW) at 2100 rpm. Staff gages in the head box indicate the overtopping head for 175 ft^3/s to be approximately 4.9 feet (1.47 m). A rating curve for the staff gages is given in Figure 3.4.

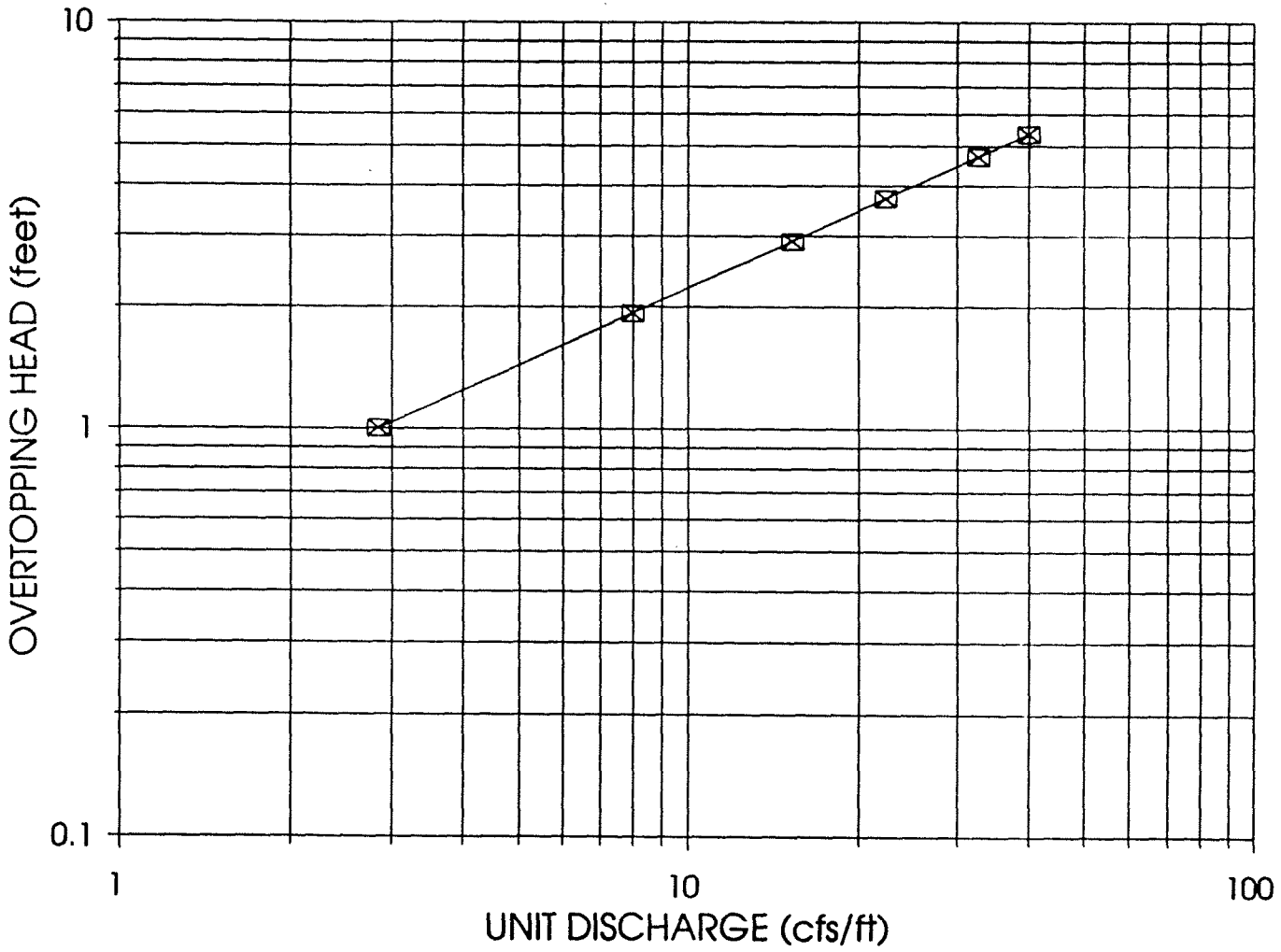

Figure 3.4: Staff gage rating curve

BLOCKS AND DRAINAGE UNDERLAYER

BLOCKS:

The protective overlay used for the present study was a layer of interlocking wedge-shaped concrete blocks placed on a drainage subgrade, six inches (152 mm) thick. Figure 3.5 is a diagram showing the block dimensions. The U.S. Bureau of Reclamation has been studying overtopping protection measures for embankment dams since the early 1980's and has found that these blocks provide an excellent form of embankment protection, (Slovensky, 1993). Through smaller model tests performed at the USBR in Denver, CO, it was determined that the block configuration which best optimized the balance between energy dissipation and separation zone pressure reduction for a 2:1 slope was a block with a step height to length ratio of 1:4.6 and a tread surface sloped down from the horizontal by 15 degrees. This design was consequently used on the near-prototype model.

As shown in Figure 3.5, the blocks have slots on the downstream face. These slots exist to aid in the pressure relief of the subgrade material, thus making the blocks more stable. Stability of the blocks at the base of the flume during a hydraulic jump was a major concern. To alleviate this problem, the first ten rows from the toe of the flume were linked together by 3-inch (76 mm)-long pins placed in holes on the upstream and downstream ends of each block. These pins were placed every foot (0.3 meters) for the width of the flume. In addition, the bottom most row of blocks

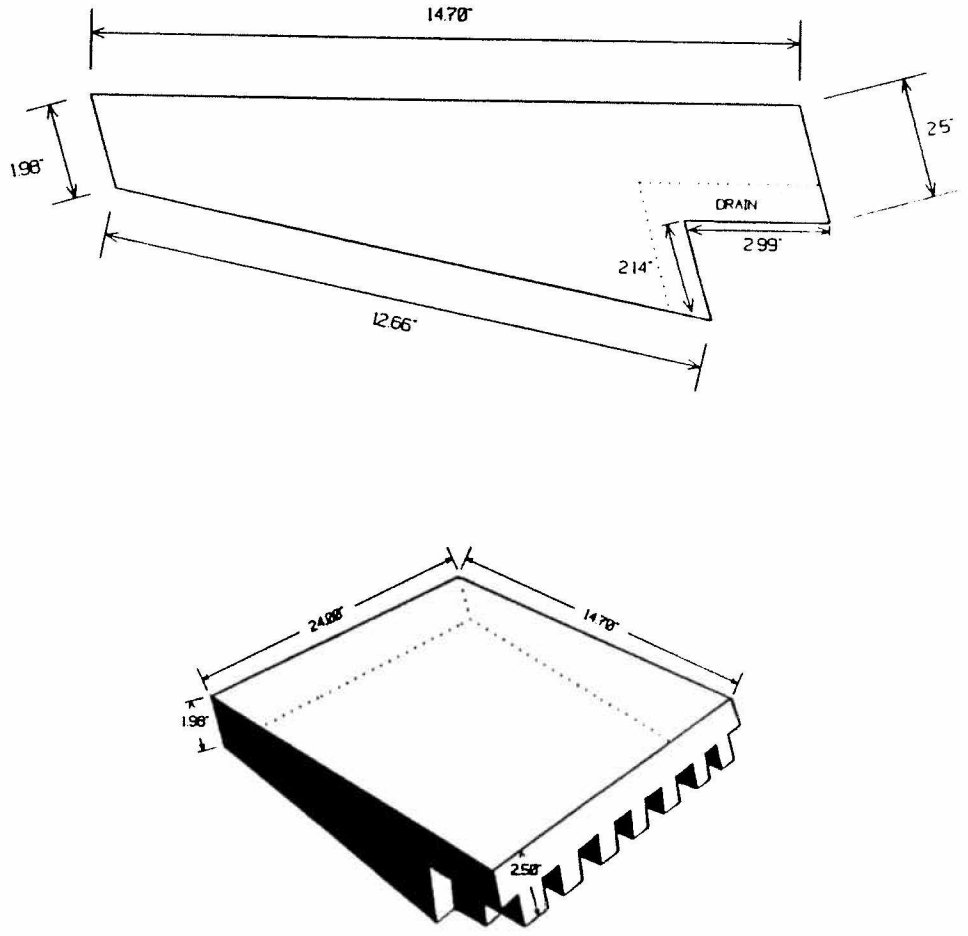

Figure 3.5: Overlapping wedge block dimensions

was fastened to angle iron beneath the blocks by j-bolts. At three other points up the slope blocks were also fastened by j-bolts: at the crest, and at two points mid-slope dividing the slope into thirds. Figure 3.6 shows the typical layout for the blocks and the filter layer.

DRAINAGE SUBGRADE:

The filter material used for these tests consisted of half-inch (average) aggregate, free of fines, placed in a 6-inch (152 mm) layer covering the entire flume floor. To keep the filter material from sliding down the slope during placement, 4-inch (101.3 mm) angle iron, spanning the width of the flume, was placed every 6 feet (1.8 meters) up the spillway. Two-by-six-inch (51 x 152 mm) redwood timbers were fastened to the base of the flume walls for screeding purposes during leveling of the filter material. The timbers were also used to keep the blocks from settling on either end.

DISCHARGE AND OVERTOPPING HEAD

Staff gages for flow measurement were placed in the headbox on the North and South walls. These gages were set so zero corresponded to the crest elevation of the flume, and were calibrated by comparison to a Mapco Nusonics sonic flow meter.

The pump was used to achieve higher flow rates. Pump discharge was

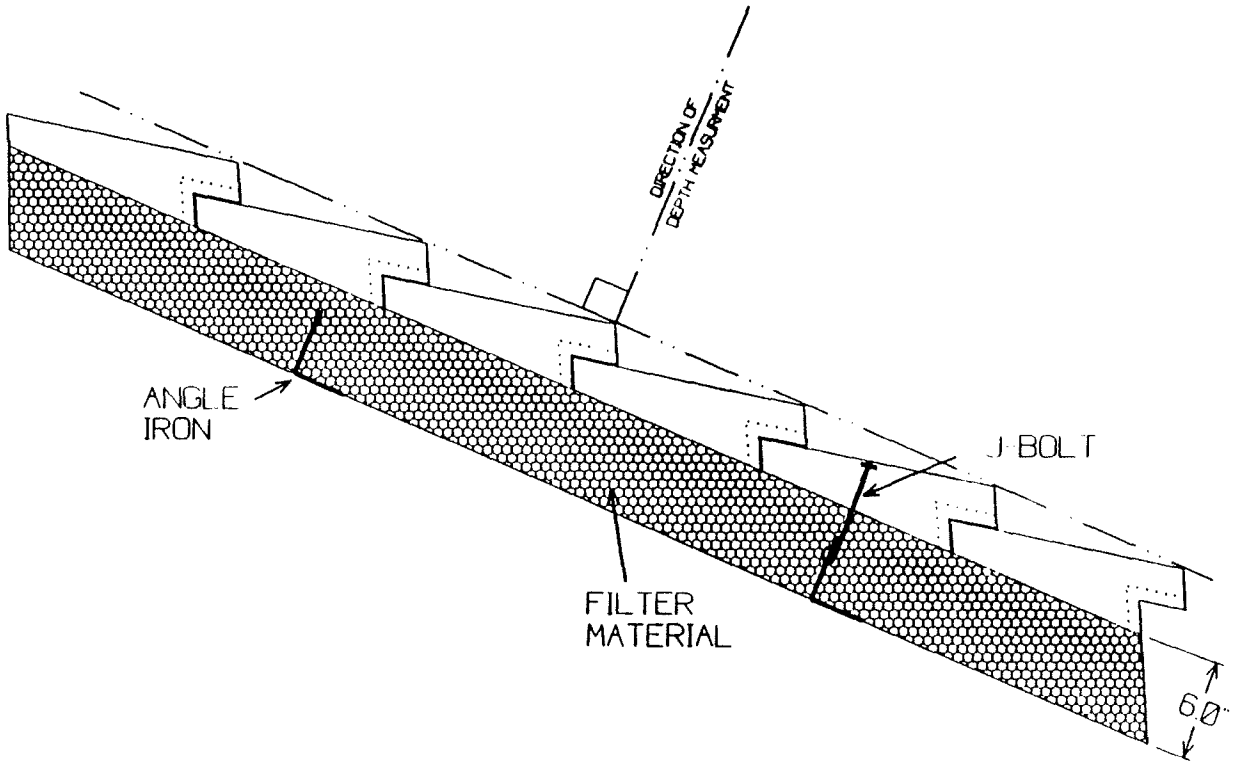

Figure 3.6: Filter layer and block layout

determined by subtracting the flow rate in the Horsetooth line from the total flow determined from the flume rating curve shown in Figure 3.4.

TEST PROCEDURES AND SETUP

For the current study, five different flow rates were tested: 16.6, 48.5, 90.0, 140.9, and 160.9 cfs. On the 5 ft. - wide overtopping facility these correspond to unit flow rates of 3.3, 9.7, 18.0, 28.2, and 32.2 cfs/ft. For each flow rate, measurements of velocity and air concentration were taken.

VELOCITY MEASUREMENTS:

The instrument used to measure velocity needed to be quite sturdy, as the forces it was subjected to were very large. Two velocity measuring devices were destroyed on the same flume in the tests conducted by Slovensky (1993). The probe also needed to be capable of measuring velocities approaching about 60 ft/sec. To accommodate this purpose a converted fuselage-mounted airplane pitot-static tube was used, RMT model 856HW by Rosemount, Inc. The pitot tube had to be modified to work properly in water, since it was originally designed for measurements in air. This entailed sealing two side ports meant for vapor pressure measurements. The probe also had to be calibrated for flows of varying air concentrations. Figure 3.7 is a schematic of the pitot tube used in the current tests.

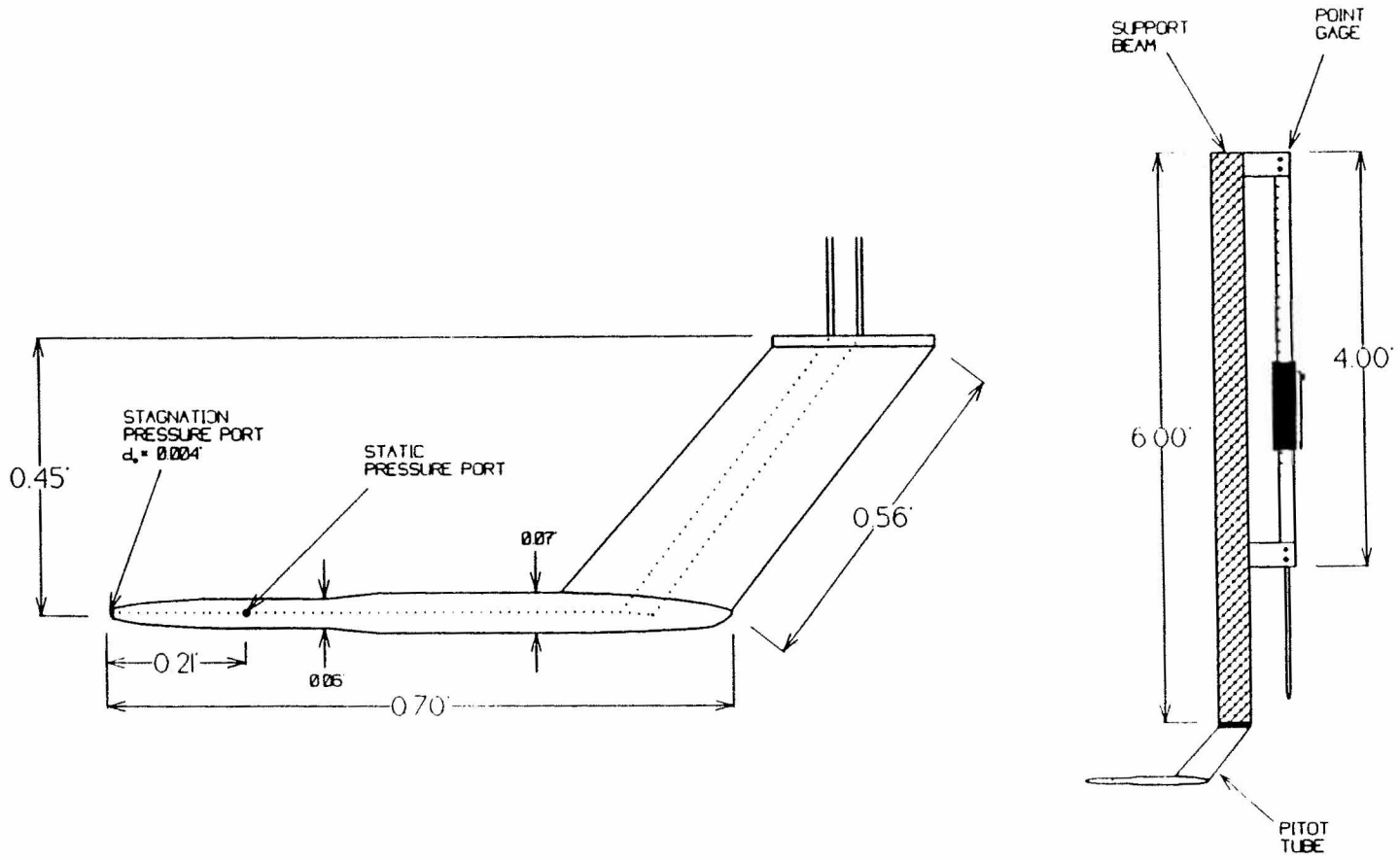

Figure 3.7: Pitot tube velocity meter

The pitot tube measured the pressure difference between the stagnation pressure at the upstream end of the tube, and the static pressure, measured by a port opening parallel to the velocity, located several tube diameters downstream from the tip. A pressure transducer was used to convert these pressures to a voltage difference that was read from a Hewlett Packard 3457A multimeter. This voltage was then corrected for a zero velocity reading. Normally this voltage could simply be converted to a velocity, since pitot tubes are usually used in flows of 100% water or 100% air. However, since the pitot tube in the present study was to take velocity measurements in a mixture of water and air, it needed to be calibrated in flows of varying air concentration.

The same setup used to calibrate the air concentration probe, described in the next section, was used to calibrate the velocity probe. This system used two flow meters to measure the amounts of water and air entering the main jet of flow. With a known flow and a known orifice opening, the velocity at these different air concentrations was known. A diagram of this calibration setup is shown in Figure 3.8. During calibration, velocities were taken at air concentrations of 0%, 40%, 58%, and 68%. The curves for each of these flow rates were fit to an equation of the following form:

$$V = Cp^{0.5} \tag{3.1}$$

where C is a constant determined for each air concentration, and p is the differential pressure read by the pitot tube. These curves are shown in Figure 3.9. The constant,

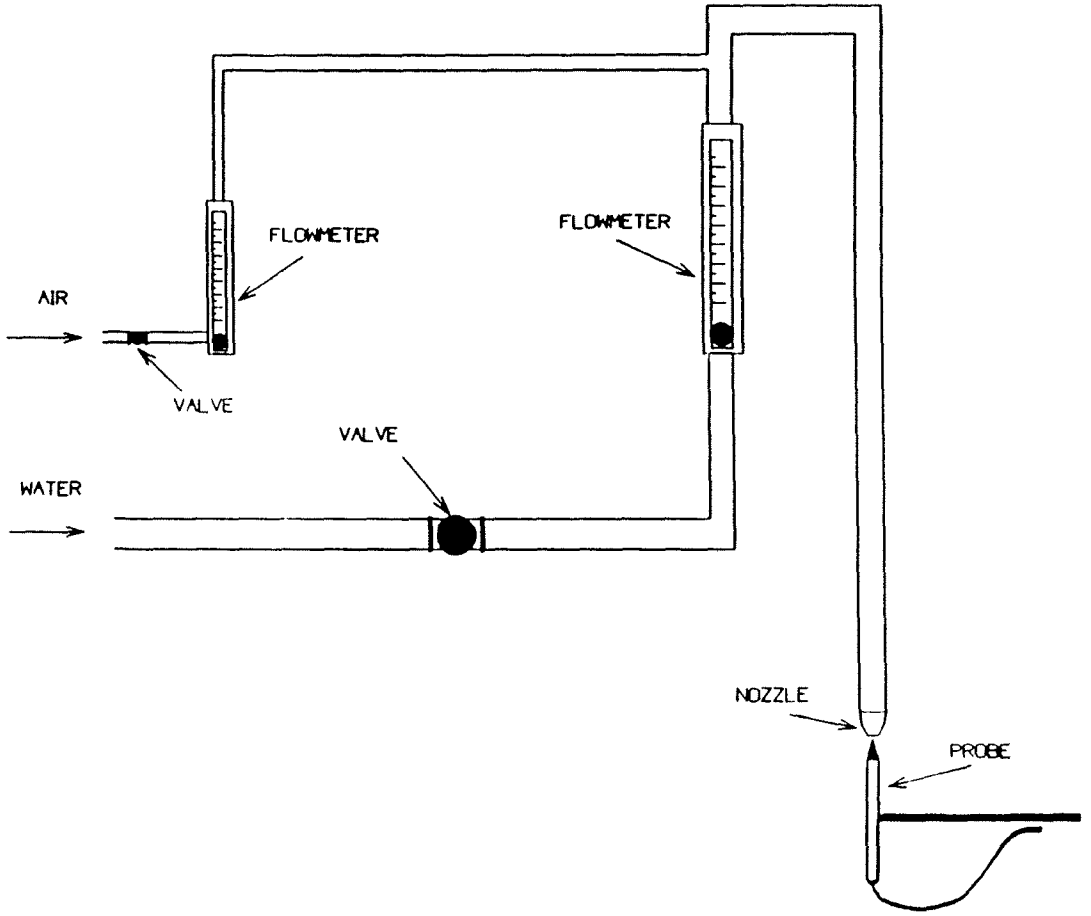

Figure 3.8: Velocity and air concentration probe calibration setup

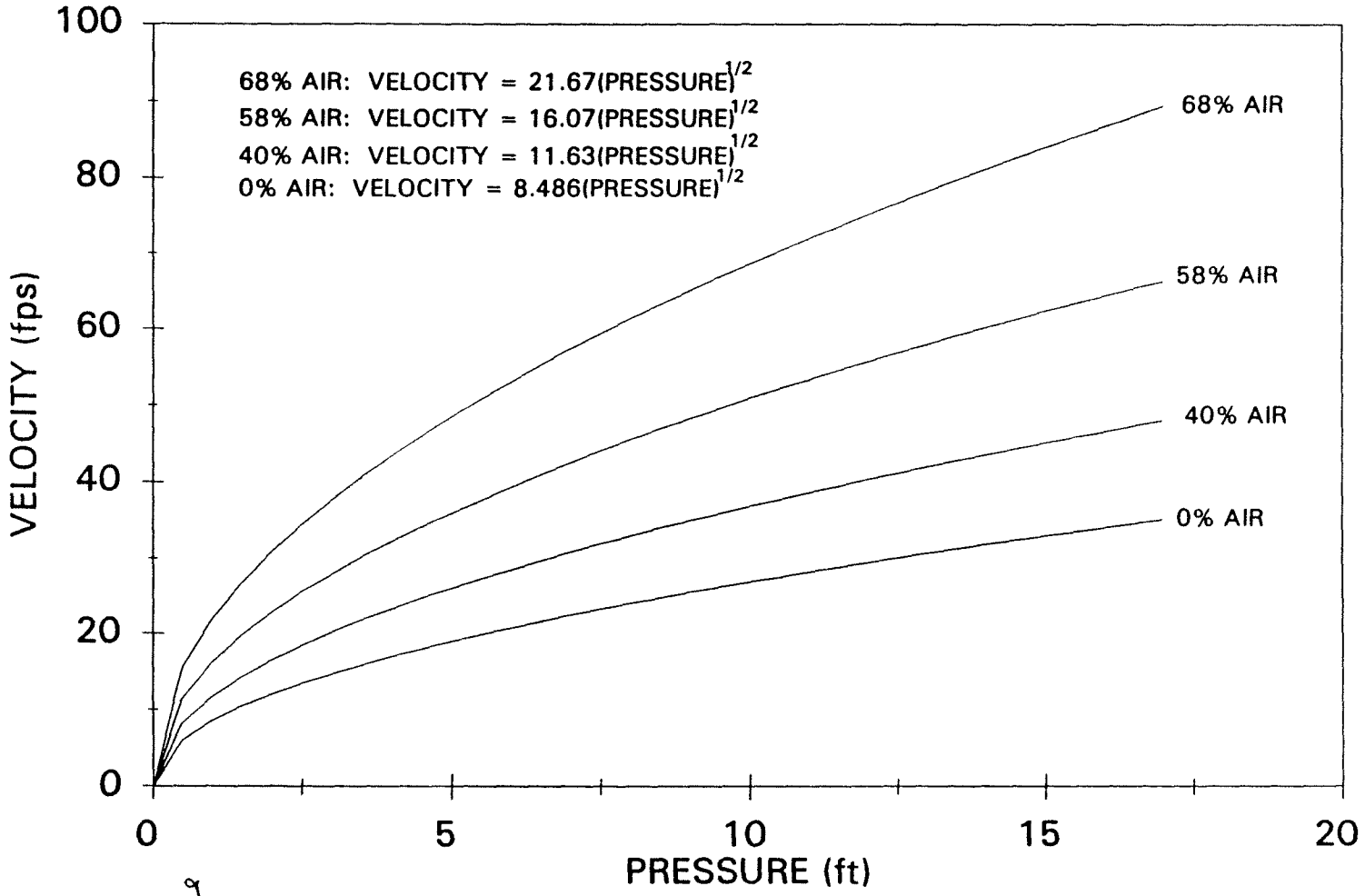

Figure 3.8: Velocity-Pressure relationship at various air concentrations for calibration of the velocity probe.

C, was determined for the four different air concentrations mentioned above. Fitting a curve to the plot of C versus air concentration then allowed C to be determined for any air concentration between 0% and 68%. Extrapolations above 68% air concentration would not have been reliable. This plot follows as Figure 3.10.

Prior to testing, the lines in the pitot tube were flushed to remove any air bubbles which might be present. The probe was then zeroed in a no-water, zero velocity condition. Velocity profiles were then run at stations 2, 3, and 4 for the unit flow rates of 28.2 and 32.2 cfs/ft, and at stations 2 and 3 for the lower three unit flow rates. Velocity measurements were taken throughout the depth of flow starting 0.03 feet up from the floor of the flume, and continuing at approximately 0.1 ft. increments to the surface of the flow. This surface was not well defined for most stations and flow rates, so readings were taken until the probe was only being hit with periodic splashes of water. To avoid wall effects as much as possible, all data were taken at the centerline of the flume only. The profiles obtained from these measurements are shown in the next chapter as Figures 4.1 through 4.5.

AIR CONCENTRATION MEASUREMENTS:

A device based on the same principle as Cain's (1978) single-tip air concentration probe was used to determine the amount of air entrained in the flow. The resistance of water is 1000 times less than that of air. This difference in resistance makes it possible for a probe, consisting of two conductors spaced a small

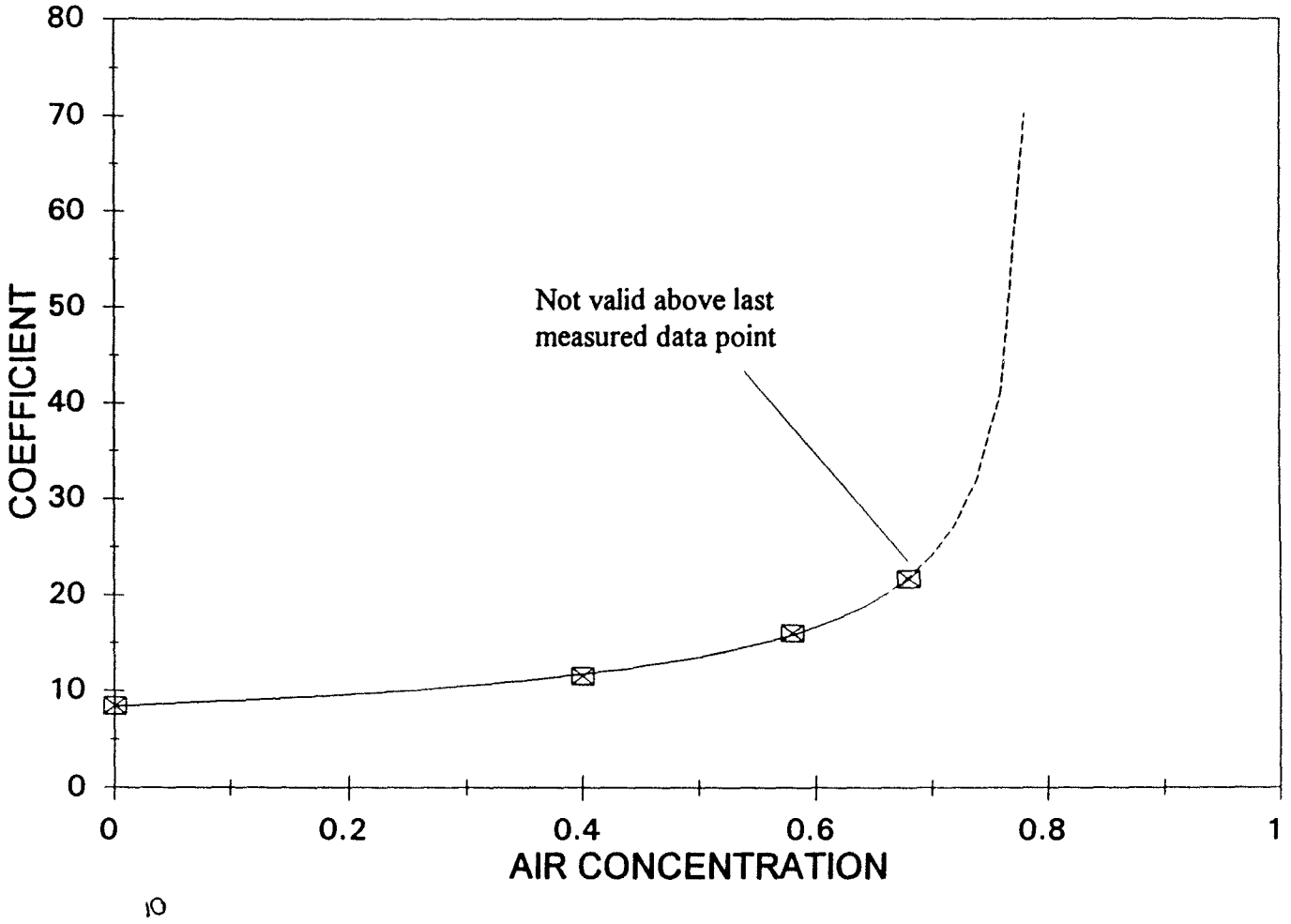

Figure 3.9: Velocity probe coefficient determination plot

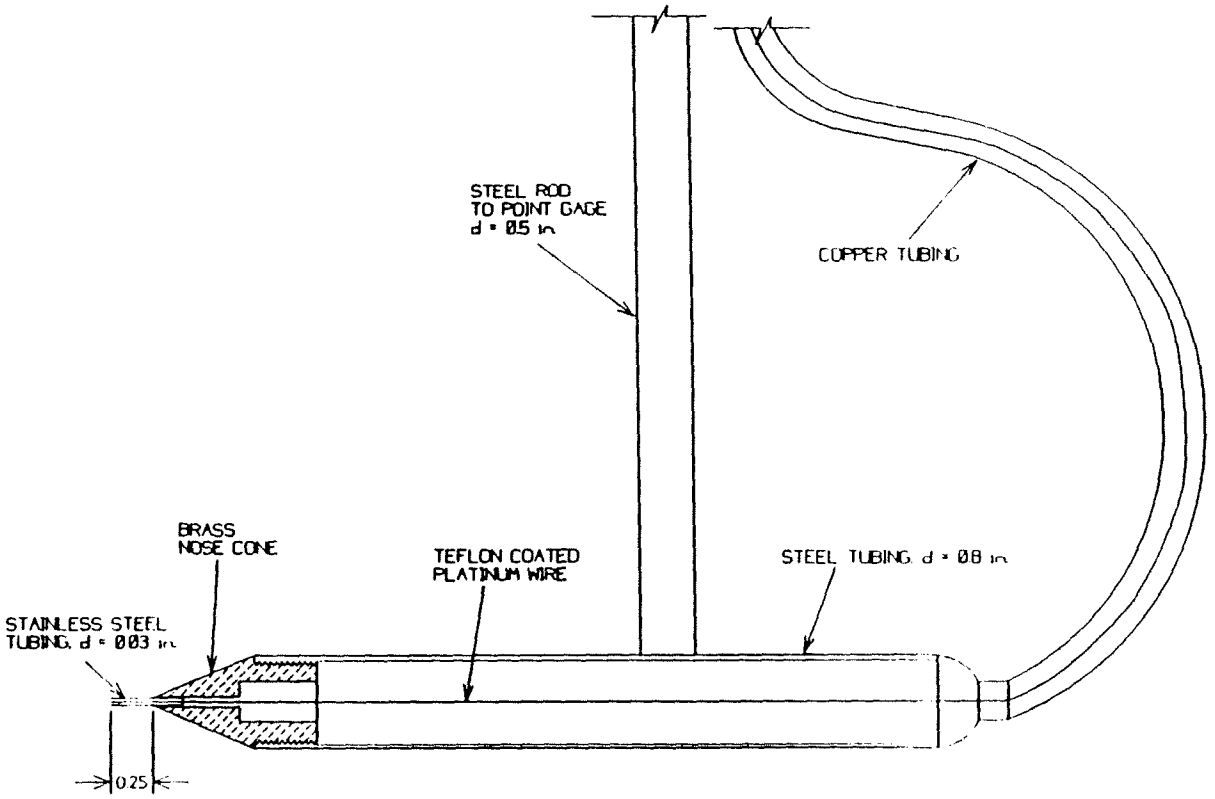

Figure 3.11: Air concentration probe

across the tip to be reversed periodically. The period between polarity reversals could be set by the operator. The electronic circuitry is shown in Figure 3.12.

Another problem that needed to be dealt with was the streamlining of the probe so the most accurate measurements could be obtained. Flow around an object creates what is known as a stagnation point, or a point where the velocity in every direction is zero, at the leading edge of the object. The stagnation point makes fluid and air particles tend to want to go around it. If the stagnation point at the tip of an air probe is too large the probe will never see smaller bubbles, thus making the probe inaccurate. An attempt to minimize this effect was made by extending the platinum wire and stainless steel tubing out beyond the cone of the probe by 0.25 inches (6.4 mm).

The calibration of the probe entailed problems of its own. Because there are very few reliable sampling techniques, calibration of the air concentration probe was quite difficult. Several methods to sample the amount of air in a sample of air-water mixture taken from a flow were tried, and several were abandoned. A sampler much like that of a reservoir sediment sampler was tried first, but data proved too difficult to acquire and too inconsistent to use for a calibration. A straight tube based on the same principle allowed for either an instantaneous measurement or a timed measurement, but friction losses through the tube and stagnation pressures at the leading edge made it too unreliable.

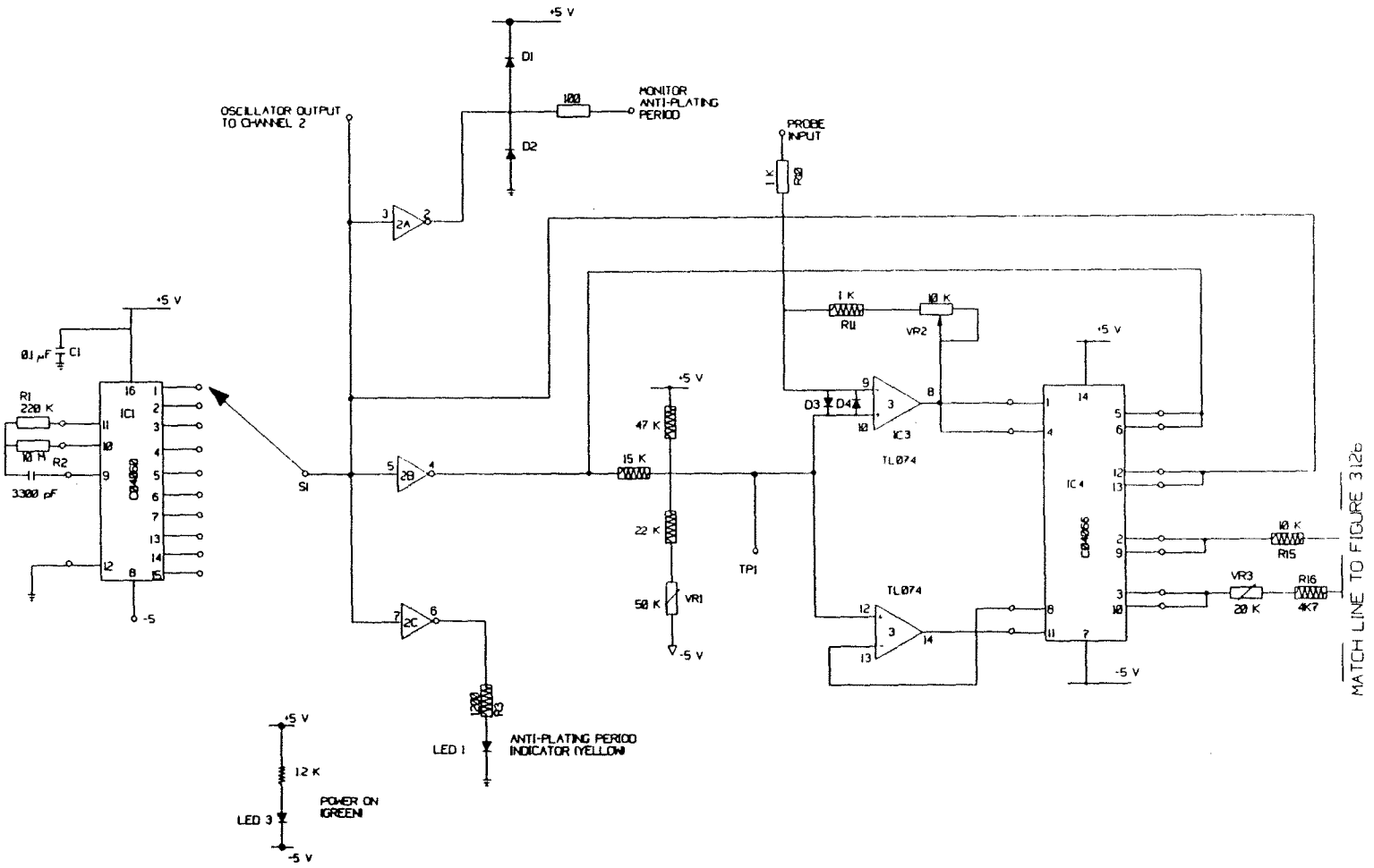

Figure 3.12a: Electronic circuitry for air concentration probe

The calibration procedure that finally proved to be very consistent used the same method applied by Bachmeier (1987/88). A schematic of the calibration setup is shown in Figure 3.8. Two rotameter flow meters were used to measure amounts of water and air before the two components were mixed together. The probe tip was then placed in the center of a jet made from this mixture, approximately 0.04 inches (1 mm) from the jet nozzle. The voltage obtained from this measurement was divided by the maximum voltage to obtain the air concentration. This data was then compared to the known air concentration and is plotted in Figure 3.13. The equation solver "Tablecurve" was used to fit a curve to the data. The equation of this curve, shown below, was then used in a spreadsheet to convert voltage readings to air-concentrations.

$$y = \frac{(-11.99x - 4.02x^2)}{(-2.32 - 31.17x + 17.32x^2)} \qquad (3.2)$$

Where y = known air concentration, and x = the voltage read by the probe divided by the maximum possible voltage.

Prior to each run, the air concentration probe was checked to make sure it was still performing as calibrated. The air concentration data were taken in the same manner as the velocity data. Data were taken for the highest two unit flow rates of 28.2 and 32.2 cfs/ft at Stations 2, 3, and 4. Data were taken only at stations 2 and 3 for the lower three unit flow rates. This was due to the fact that at the time the tests

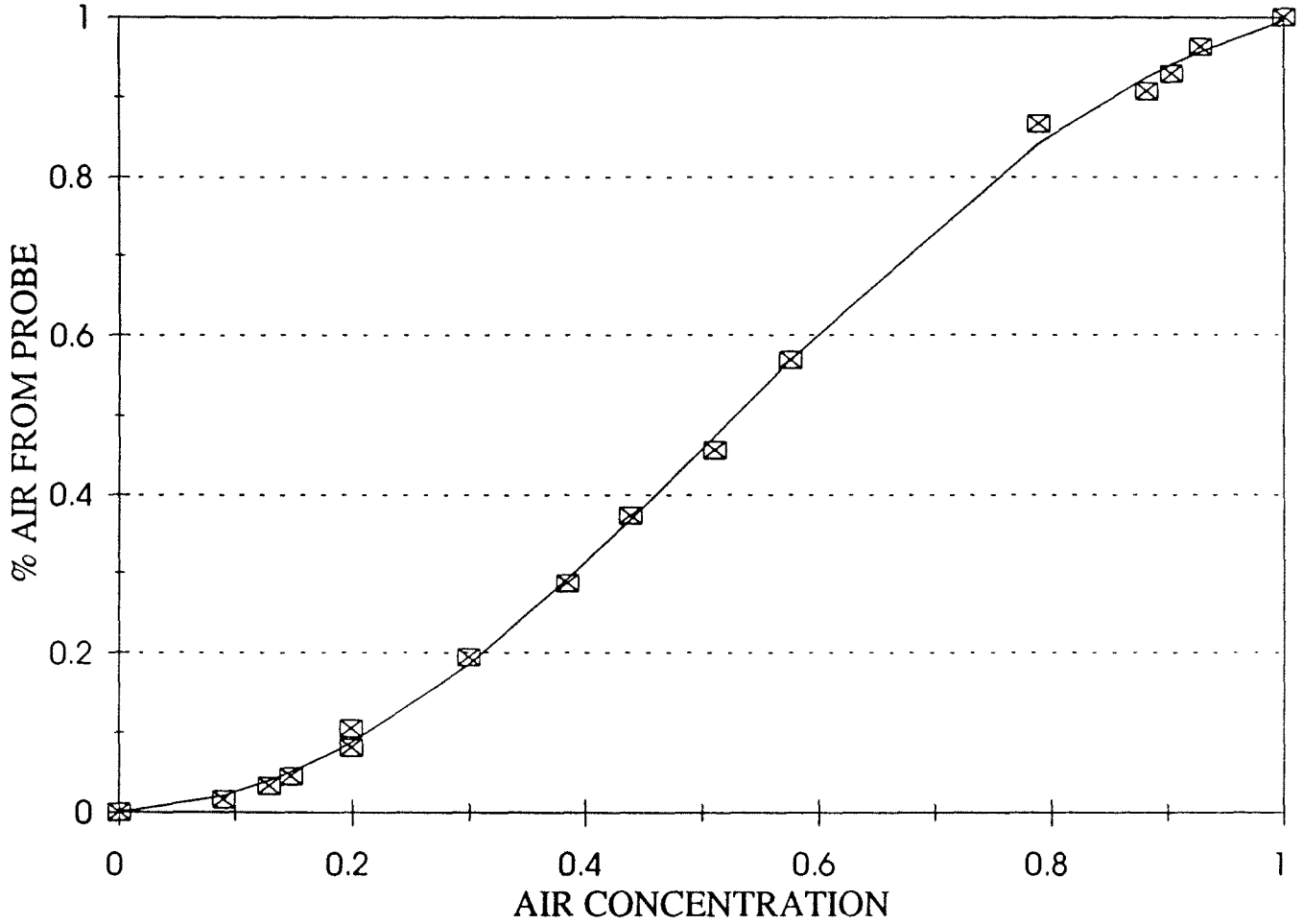

Figure 3.13: Air probe calibration plot

on the lower three unit flow rates were performed, not enough cable was available to allow the probe to reach the first or fourth stations. As with the collection of the velocity data, measurements were only taken at the centerline of the flume. Starting at the base of the flume, measurements were taken at equal increments throughout the depth of flow until an air concentration of at least 90 percent was reached. This increment varied according to the depth of flow. For the low unit flow rates the increment was decreased to 0.05 feet to allow more readings to be taken. For the higher unit flow rates an increment of 0.1 feet was used. The profiles obtained from this data are shown in the next chapter as Figures 4.10 through 4.14.

DEPTH MEASUREMENTS:

Depth measurements were taken by two different methods. The depth of flow up to the point where the air concentration was equal to 90% was measured with the air concentration probe. This was done by simply using the depth corresponding to an air concentration of 90% taken from the air concentration profiles. For this experiment it was assumed that the surface of the flow corresponded to this depth (this will be explained in the next chapter). The second method used to measure the flow depth involved the use of an acoustic based distance measuring instrument (DMI). This instrument measured the distance between itself and the object closest to it using reflections of sound waves. All depth data taken by this instrument were, therefore, the depths of the closest water surface. For unaerated flow this

corresponds to the flow depth. For aerated flow, however, the DMI measures the spray surface of the flow, or the aerated flow depth where the air concentration is approximately 100%.

CHAPTER 4

ANALYSIS OF DATA

SUMMARY

At the commencement of this study it was hoped that the velocity and air concentration data collected during the tests at five unit flow rates would reveal two important parameters:

1. The kinetic energy of the flow at the toe of the spillway. Knowing the energy remaining in the flow at the toe of a spillway permits the proper design of the stilling basin required for that spillway. Thus, it is helpful to know if a terminal velocity is reached.

2. The depth of the entire aerated flow, as well as a method for predicting this depth, given a parameter such as unit flow rate. Knowing the bulked depth of the flow allows for the proper design of spillway sidewalls. These sidewalls must be built high enough to prevent overtopping that could cause abutment or embankment erosion.

This chapter describes the analysis of the data obtained in the current tests and its relation to the above parameters. The tables and figures presented in this chapter are a summary of the most important information. However, all data taken is included in

this paper. Any table, spreadsheet, or figure not shown in this chapter can be found in the Appendices.

DEFINITIONS

To make it easier to understand the following data analysis, it was felt that some items needed to be defined or reiterated.

Uniform Equilibrium Flow:

When describing an aerated flow over a spillway, uniform equilibrium flow implies that an equilibrium is reached between air entrainment and air escaping the fluid. For the flow to be considered uniform, the depth, velocity profiles, and air concentration profiles must remain relatively constant as the flow continues downstream. In 1958, Straub and Anderson described equilibrium flow as "that condition of the flow of the air-water mixture for which the air-concentration distribution was the same at two sections 3.05 meters apart along the channel." It will be shown that uniform equilibrium flow was reached for flow rates up to 28.2 cfs/ft.

Depth:

In this study, depth is always measured as positive in the direction normal to the spillway floor, as shown in Figure 3.6.

Non-dimensional Depth:

When comparing a parameter, such as air concentration, at different depths above the same point on a spillway, it is often helpful to identify depth not in feet or meters, but as a percentage of "total depth." Many figures in this study use this non-dimensional method of identifying depth.

Total depth was enclosed in quotation marks because in actual conditions the uneven splashing involved with turbulent aerated flow makes it impractical to measure total depth precisely. Instead, the common practice is to use a depth related to the point where the air concentration in the flow profile has reached 90 percent, or y_{90}. This practice has been followed in this study.

Flow Bulking:

This parameter refers to the increase in flow depth due to the presence of air entrained in the flow.

Base:

This refers to the toe of the slope at the stilling basin. This does not refer to the floor of the flume.

VELOCITY DATA

Two issues were of particular concern during the analysis of the velocity data:

1. When does the flow achieve a terminal velocity? That is, one must know whether the flow accelerates to a certain velocity and then continues at that velocity to the base, or whether the flow is still accelerating when it reaches the base.

2. How the friction factor changes as the flow rate increases, and proceeds down the slope. To calculate an accurate water surface profile, the friction factor must first be known.

Velocity profiles at each station were created and analyzed. The use of these profiles, in conjunction with the air concentration profiles described in the next section, allowed a friction factor for the spillway surface to be determined. These profiles also showed that a terminal velocity was reached for flow rates up to 28.2 cfs/ft. This section describes the analysis of the velocity profiles.

GENERAL DESCRIPTION OF PROFILES:

Figures 4.1 through 4.5 show the velocity profiles for stations 2 and 3 at flow rates of 3.3, 9.7, and 18.0 cfs/ft, and at stations 2, 3, and 4 at flow rates of 28.2 and 32.2 cfs/ft respectively. These profiles show the complete set of original data, as well as the extensions or contractions to the depth of y_{90}. Where data were taken above y_{90}, points were linearly interpolated to determine the velocity at y_{90}. If data

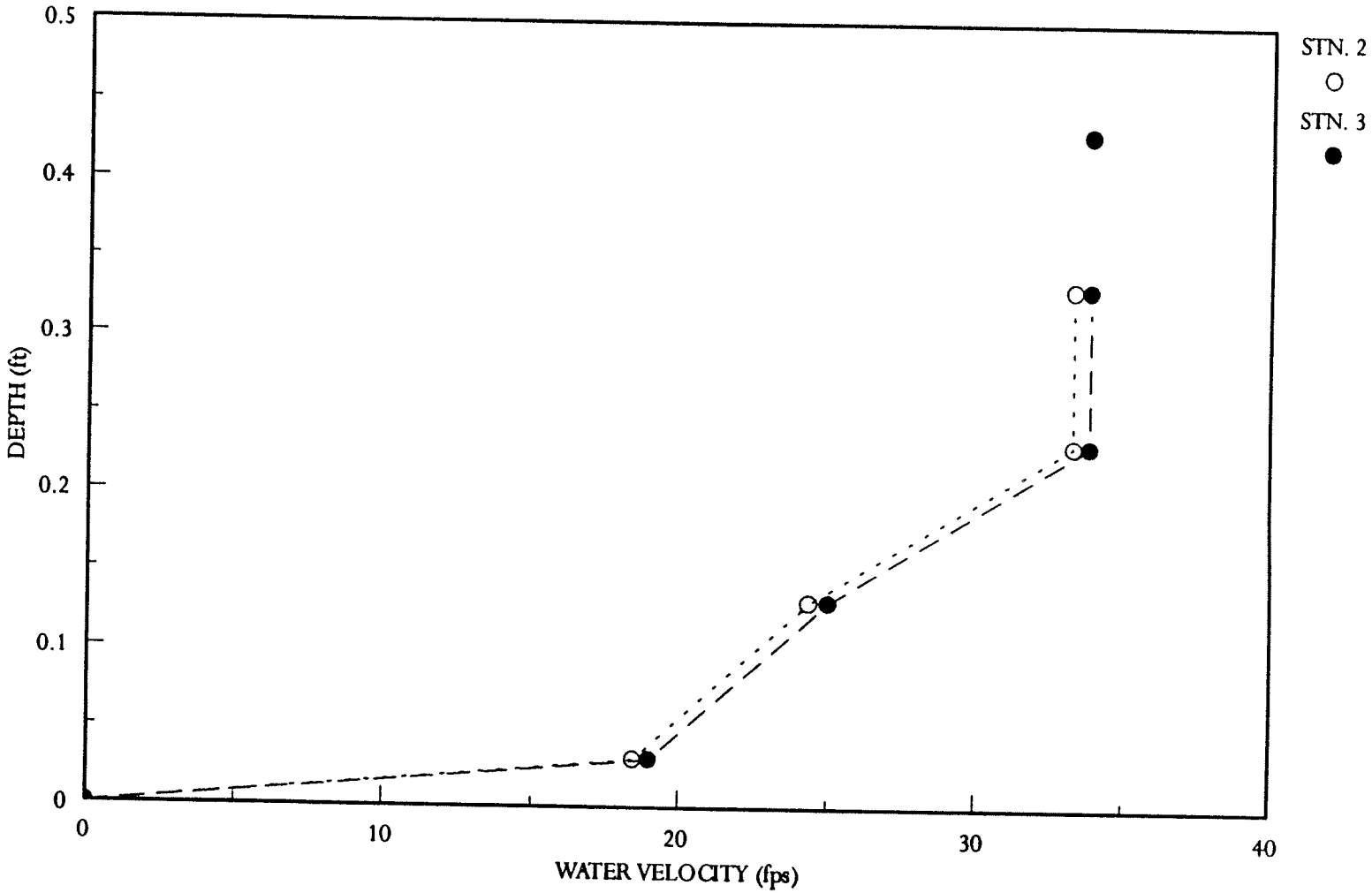

Figure 4.1: Velocity profiles, 3.3 cfs/ft

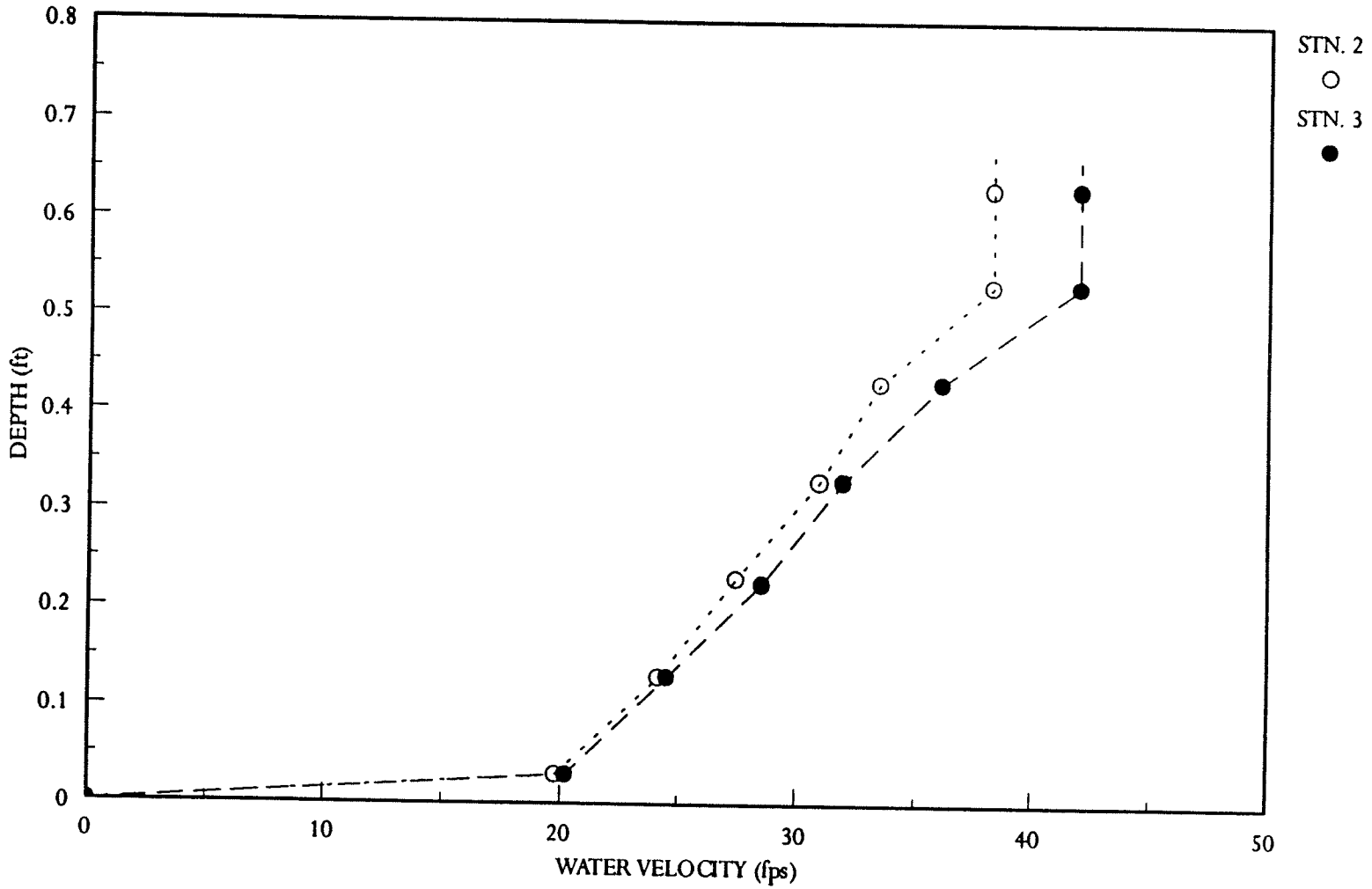

Figure 4.2: Velocity profiles, 9.7 cfs/ft

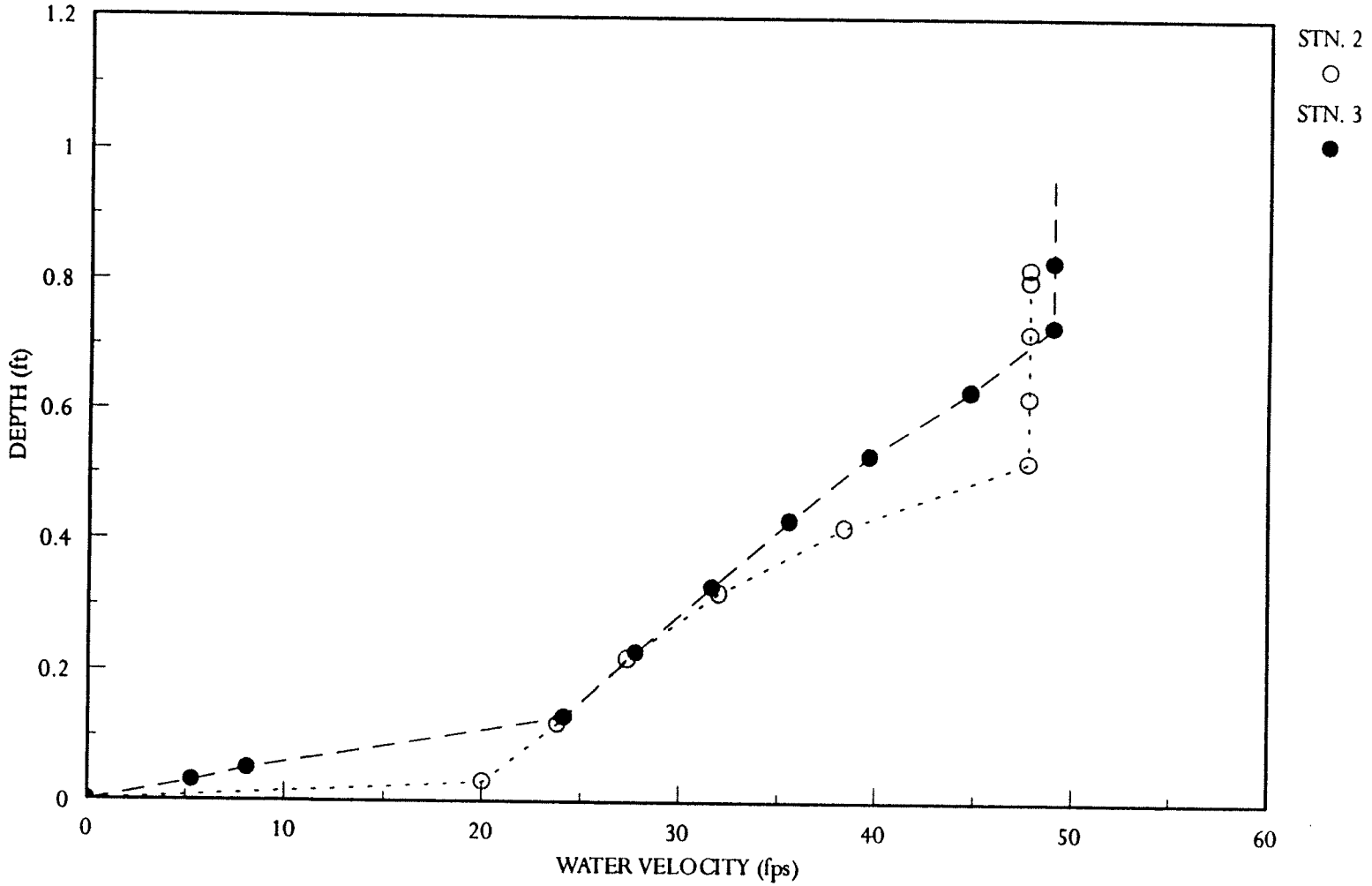

Figure 4.3: Velocity profiles, 18.0 cfs/ft

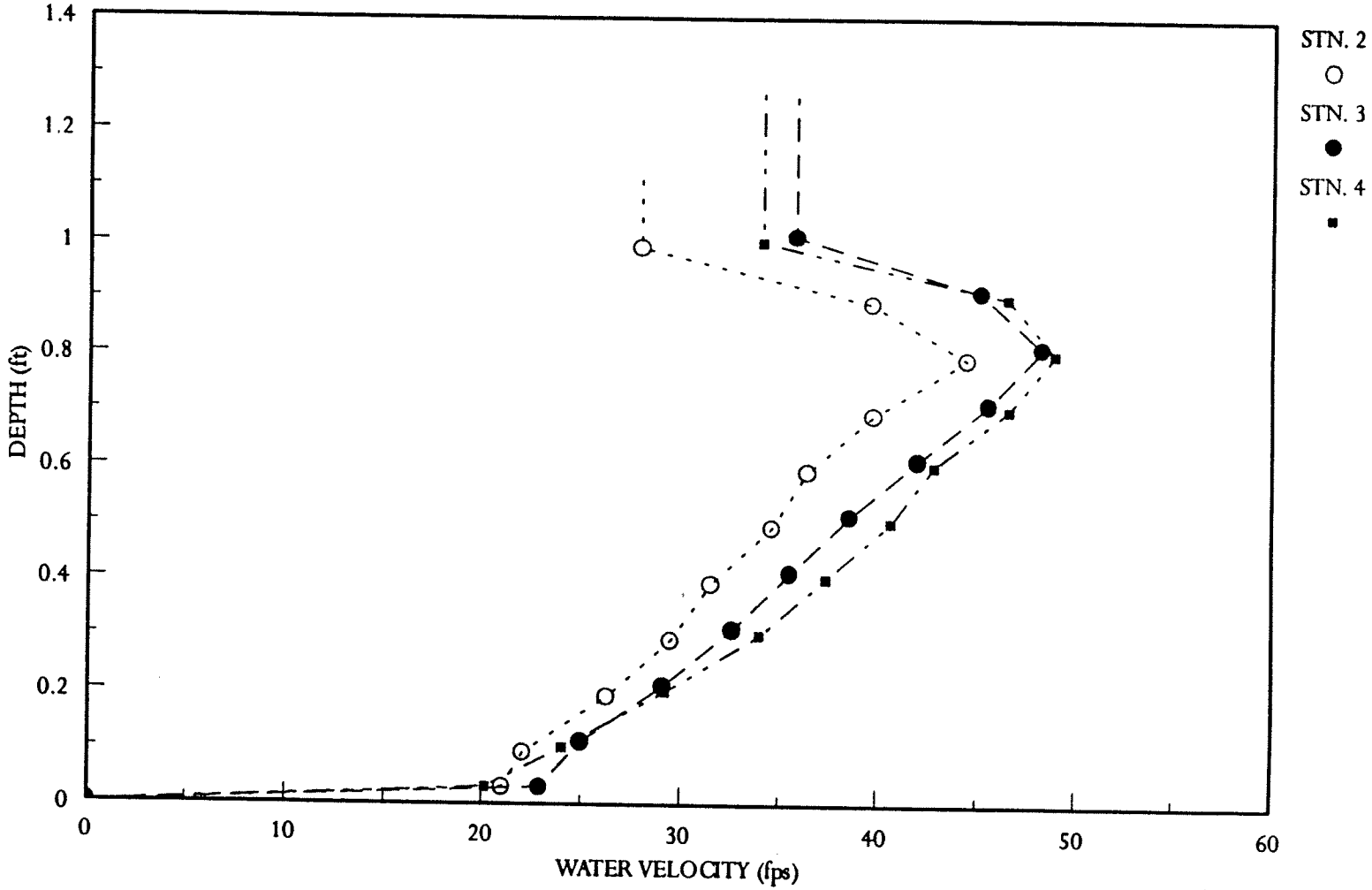

Figure 4.4: Velocity profiles, 28.2 cfs/ft

plotted from Appendix A data velocity vs. depth

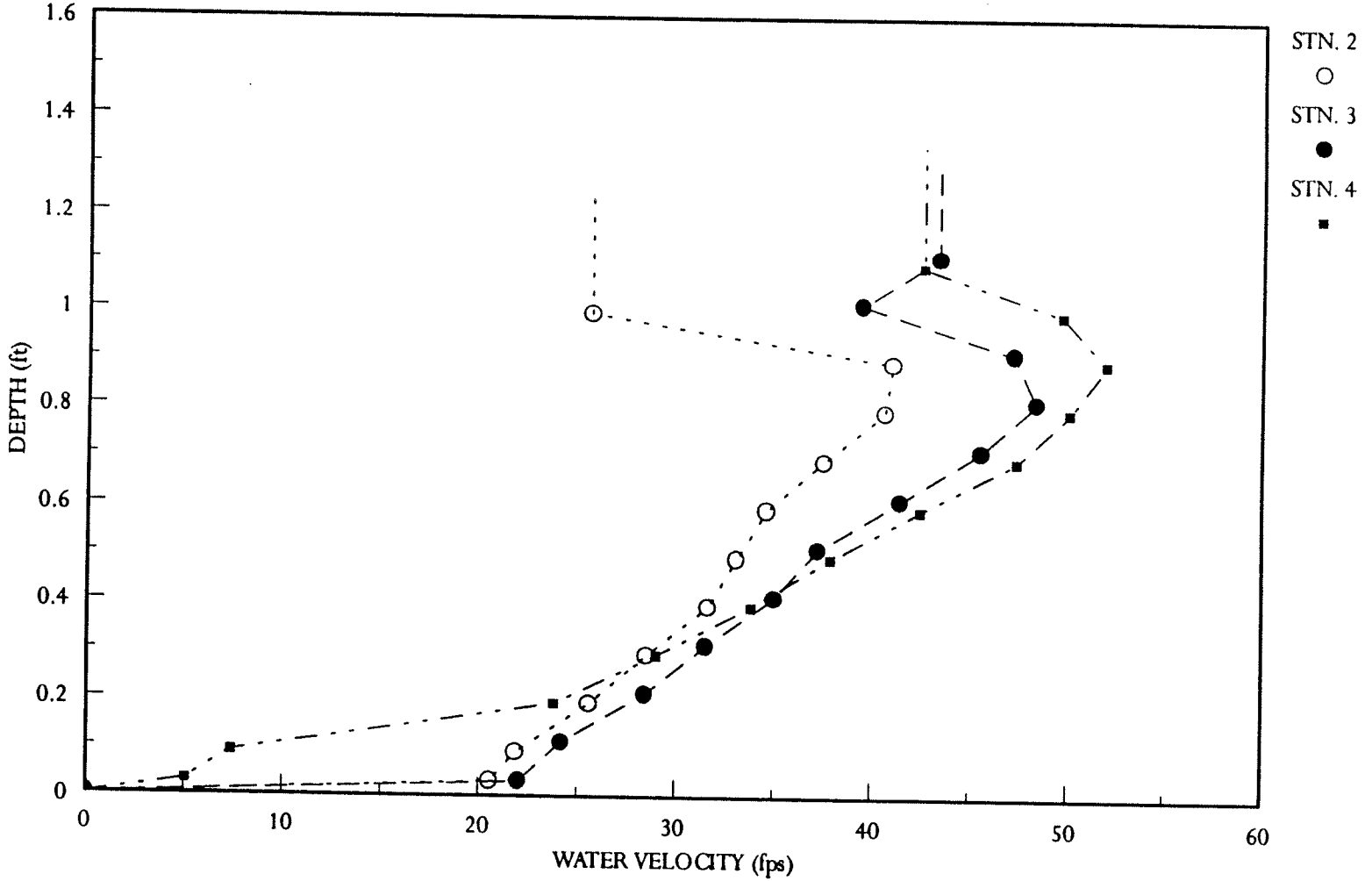

Figure 4.5: Velocity profiles, 32.2 cfs/ft

were not collected to the depth of y_{90}, the profiles were simply extended vertically from the last test data point to the depth of y_{90}. In both cases, the profiles to y_{90} are shown as dotted or dashed lines.

Several characteristics can be noticed from these profiles. The most obvious is the parabolic shape they all display, conforming to the typical velocity profile. Several of the profiles, however, curve sharply back on themselves in the upper portion of the profile. Straub and Anderson (1958) explain this decrease in velocity by, "the presence of a shear caused by the change in momentum that is created by the return of water droplets from the atmosphere after they have been ejected from the main flow." It is believed that this is the major reason for the shape of the curves in this study. However, another possible explanation lies in the physical conditions of the tests themselves. Although the velocity probe was calibrated for aerated flows, it did not always read the true water velocity when it was in the well aerated portions of the flow. This is due to the fact that in this portion of the flow the probe was seeing slugs of water followed by slugs of air, thus apparently giving it periods of high velocity (the water) followed by periods of very low velocity (the air). This explains, also, why many of the profiles extend vertically upward at a certain point. It was felt that because of this "sluggish" flow, the velocity data could not be considered valid above air concentrations of about 65%. The profiles were therefore simply extended straight up after that point.

Figure 4.3 shows something puzzling at 18.0 cfs/ft. At this flow, the velocities at station 2 (except the maximums) are higher than those shown at station 3. Also, the velocities at this flow are higher than velocities for the higher unit flow rates at the same stations. These peculiarities prompted a second running of the tests at this flow in the belief that an error had occurred during testing. The second set of data, however, produced similar results. It is not believed that the data is incorrect. There simply seems to be a localized instability that can not be explained at this time. From video of this test, though, it appears that the data taken at station 2 might have been taken close to the point of inception. Analysis of this region was considered to be out of the scope of this study. The peculiar velocity reversal shown in Figure 4.5 at station 3 was also studied closely, and cannot be explained at this time.

AVERAGE VELOCITIES:

Knowing the shape and magnitude of the velocity profiles at each station allows average water velocities at each station to be calculated. Two methods were used to determine this average. Because the profiles were obtained by taking velocity measurements at equal increments throughout the depth of flow, the profiles were automatically divided into sections of equal depth. An average velocity for each section was determined, and these velocities were averaged to determine the average water velocity for the entire profile. Because all calculations in this study are based on the depth of y_{90}, however, most of the profiles were altered. This meant the depth increments were not always equal. This method, then, could not be used in all cases.

The second method entailed calculating the area behind each profile and dividing by the total depth. This method produced the values shown in Table 4.1. The second method was chosen over the first because it allowed sections of unequal depth to be accounted for.

TERMINAL VELOCITIES:

The availability of an average water velocity at each station allows several observations to be made. One of these is the determination of the presence of a terminal velocity. One item of major concern to stilling basin design is the question of whether a terminal velocity is reached on a particular slope, and if so what that velocity is. A terminal velocity means that an equilibrium has been reached between energy dissipation and the fall. The determination of a terminal velocity allows the data to be applied to embankments higher than the Dam Safety Overtopping Facility. For applications to dams 50 feet or less, the measured flume data can be applied to determine the energy of the flow at the entrance to the tailwater or stilling basin. It also allows the designer to judge the potential cost savings that a rough or stepped spillway may offer as a result of the high energy dissipation.

From the data obtained in the present study it is evident that a terminal velocity was indeed reached for every flow rate tested, except for the highest rate of 32.2 cfs/ft. For the lower two unit flow rates a terminal velocity appears to have

Table 4.1: Maximum and average velocity values

FLOW RATE (cfs/ft)	STATION 2		STATION 3		STATION 4	
	MAX. (fps)	AVG. (fps)	MAX. (fps)	AVG. (fps)	MAX. (fps)	AVG. (fps)
3.3	33	26	34	26	N/A	N/A
9.7	38	30	42	32	N/A	N/A
18.0	48	38	49	36	N/A	N/A
28.2	44	32	48	36	49	37
32.2	41	30	47	37	52	37

been reached by the second station, approximately 57 feet down the slope. For 28.2 cfs/ft, a terminal velocity was reached by station 3, approximately 95 feet down the slope. At the highest unit flow rate of 32.2 cfs/ft, it is not clear that a terminal velocity was reached. The average velocities between the last two stations remained constant, but the maximum velocity at station four was approximately 6% higher than that at station three. Due to the instabilities occurring at 18.0 cfs/ft, it is not clear what the terminal velocity is at this flow. A plot of terminal velocity against unit flow rate, shown in Figure 4.6, shows that for the given slope and block dimensions the terminal velocity appears to level off at approximately 38 fps.

VERIFYING THE DATA:

To check the accuracy of the data, a continuity check was performed. To do this, the average water velocity between each data point of each profile was multiplied by the depth of that increment of the profile, and by the width of the flume. This gave incremental flow rates for each portion of the profiles. For each profile these incremental flow rates were totaled. Theoretically, this total should be equal to the flow rate measured by the staff gages in the head box. The greatest deviation that occurred between this calculation and the known flow rate was approximately 30%. In most cases, however, the deviation was below 15%, and at the higher flow rates the difference was generally well below 10%. This is quite good considering that data was only taken at the center of the flume, and that at some flow rates cascading flow was present, thus making readings less accurate. A continuity check, therefore,

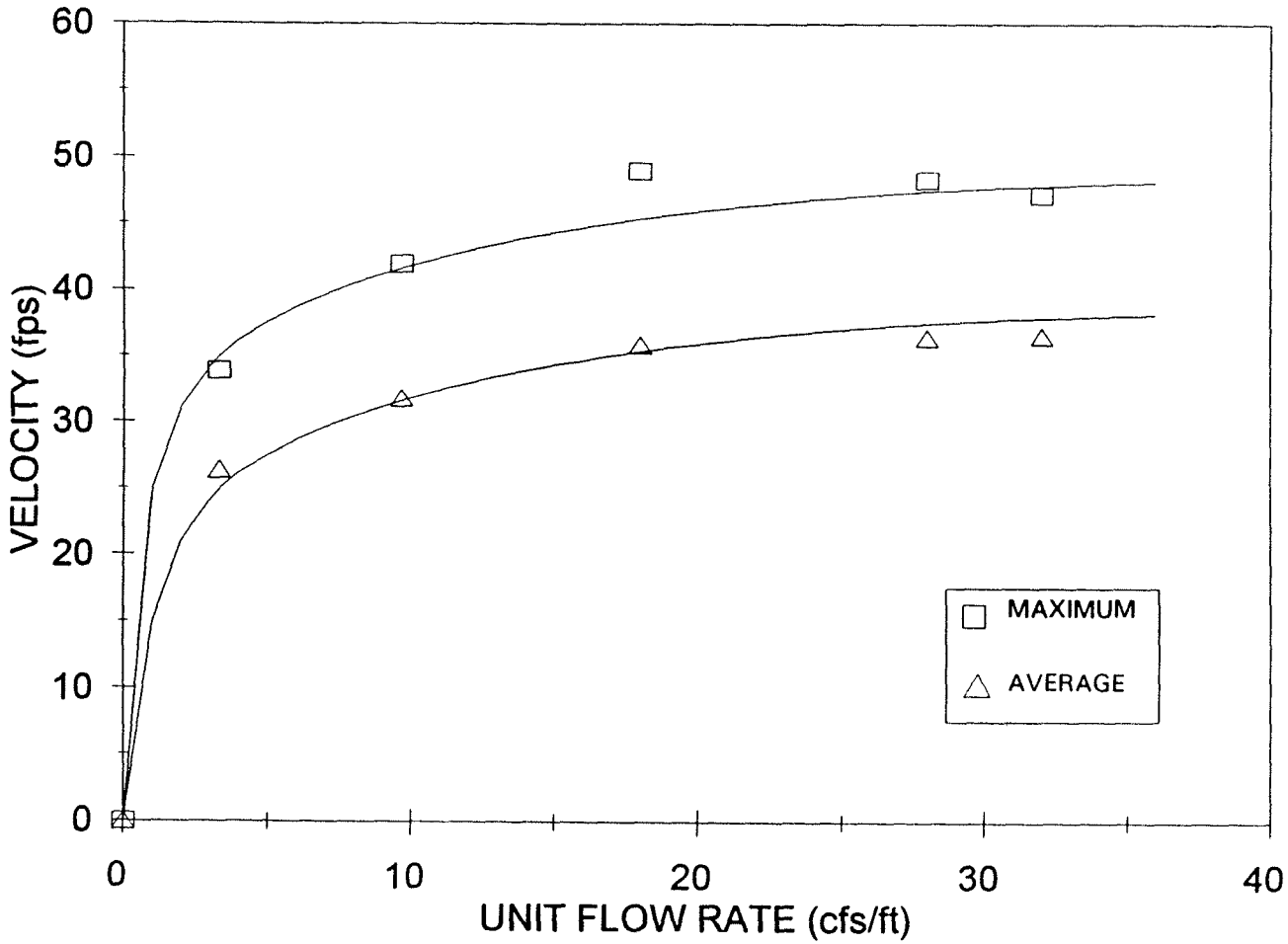

Figure 4.6: Terminal velocities; maximum and average values at Station 3

provides good correlation of both air concentration and velocity data. Tables for these calculations are shown in Appendix 4.

FRICTION FACTOR DETERMINATION:

Average velocities at each station also permit a friction factor to be determined between each of the stations. To accomplish this, equations were required that compensated for gradually varied flow conditions, the change in fluid density between each station, and the steepness of the slope. From the Bernoulli equation, the following equation can be derived:

$$h_L = \left[\rho_1\left(dz + D_1\cos\theta + \frac{V_1^2}{2g}\right) - \rho_2\left(D_2\cos\theta + \frac{V_2^2}{2g}\right)\right]\frac{1}{\rho_{AVG}} \qquad (4.1)$$

where ρ_{AVG} is the average density of the reach, and the subscripts 1 and 2 denote the values at the upstream and downstream ends of the reach, respectively. The rest of the variables are as defined in Figure 4.7. Knowing that the head loss can also be defined by the following equation:

$$h_L = \frac{\tau\, dx}{\rho_{AVG} g D_1} \qquad (4.2)$$

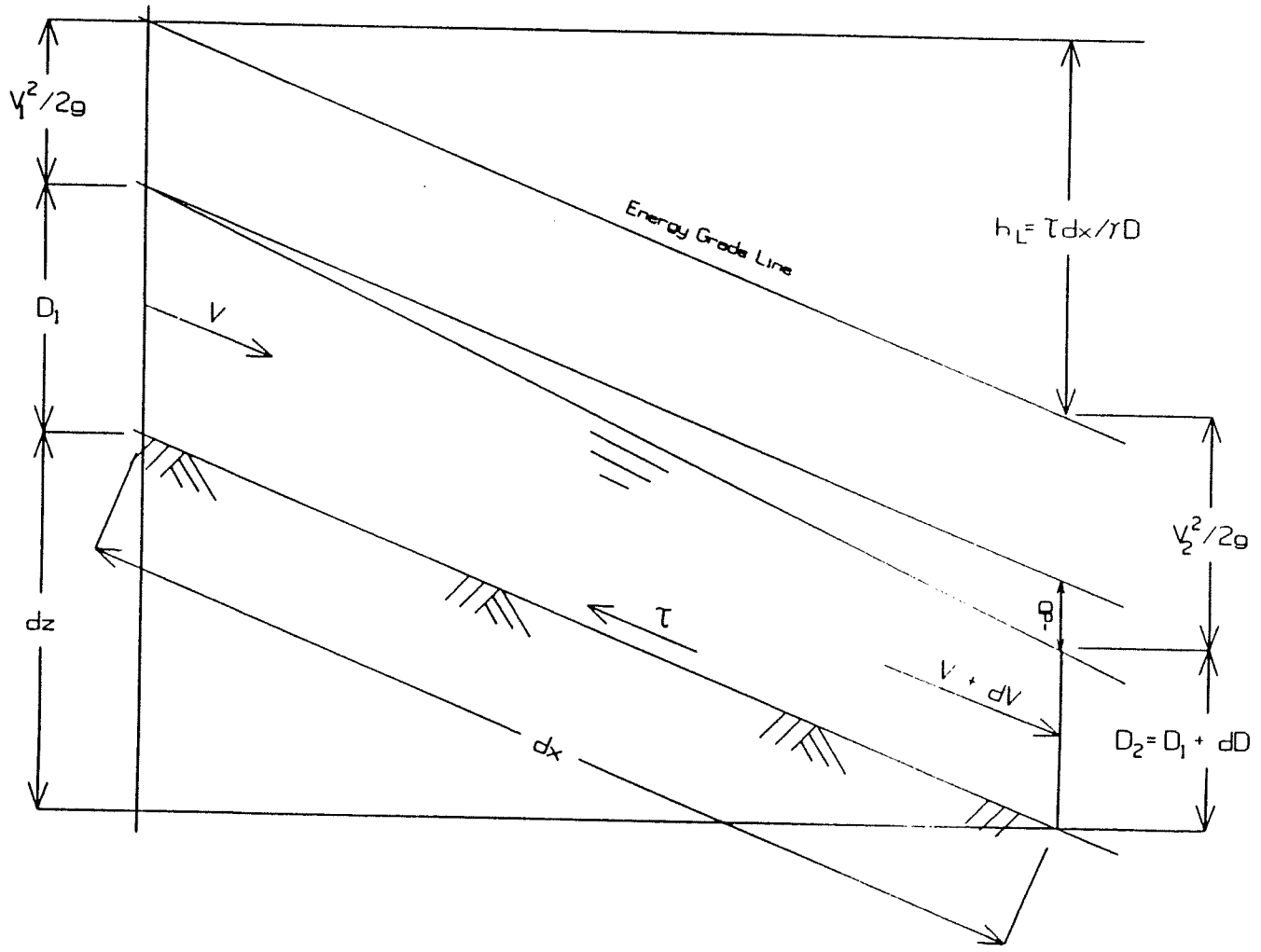

Figure 4.7: Gradually varied flow definition drawing

The average tractive shear, τ, can be found from:

$$\tau = \frac{g D_1}{dx\left[\rho_1\left(dD_1 + D_1\cos\theta + \frac{V_1^2}{2g}\right) - \rho_2\left(D_2\cos\theta + \frac{V_2^2}{2g}\right)\right]} \tag{4.3}$$

The following equation can then be used to determine the friction factor, f.

$$f = \frac{8g\tau}{\rho_{AVG} V_{AVG}^2} \tag{4.4}$$

Table 4.2 displays the friction factors determined for each flow rate and each section of the slope.

Table 4.2: Summary of friction factors at each flow rate

FLOW RATE (cfs)	UNIT FLOW RATE (cfs/ft)	FRICTION FACTORS		
		REACH 1-2	REACH 2-3	REACH 3-4
16.6	3.3	0.45	0.06	N/A
48.5	9.7	0.54	0.09	N/A
90.0	18.0	0.39	0.10	N/A
140.9	28.2	0.68	0.12	0.14
160.9	32.2	0.89	0.11	0.13

Average = 0.11

Velocity data was not available at station 4 for the lower three unit flow rates, therefore, no friction factor computations could be made. Figure 4.8 shows the relationship between the friction factor and the various unit flow rates between the different stations. This figure shows that the values determined for 18.0 cfs/ft were ignored, and a straight line was simply drawn between the values determined for the surrounding flow rates. The instabilities at this flow rate made it impossible to determine an accurate friction factor. Since no velocity data was taken at station 4 for the lower three unit flow rates, it is difficult to tell exactly what the friction factor is between stations 3 and 4 at unit flow rates less than 28.2 cfs/ft. From Figure 4.8, however, it would be reasonable to assume that the values are very close to the friction factors found between stations 2 and 3.

From Figure 4.8 it is evident that for all unit flow rates the friction factor decreases between stations 1 and 3, and then remains relatively constant on the lower portion of the slope where uniform flow has been achieved. The decrease in friction factor with increasing downstream distance can be explained by the relationship between the friction factor and velocity. From the Darcy-Weisbach head loss equation, shown below, it can be seen that the friction factor is inversely related to the square of the flow velocity.

$$f = h_f \frac{D}{L} \frac{2g}{V^2} \tag{4.5}$$

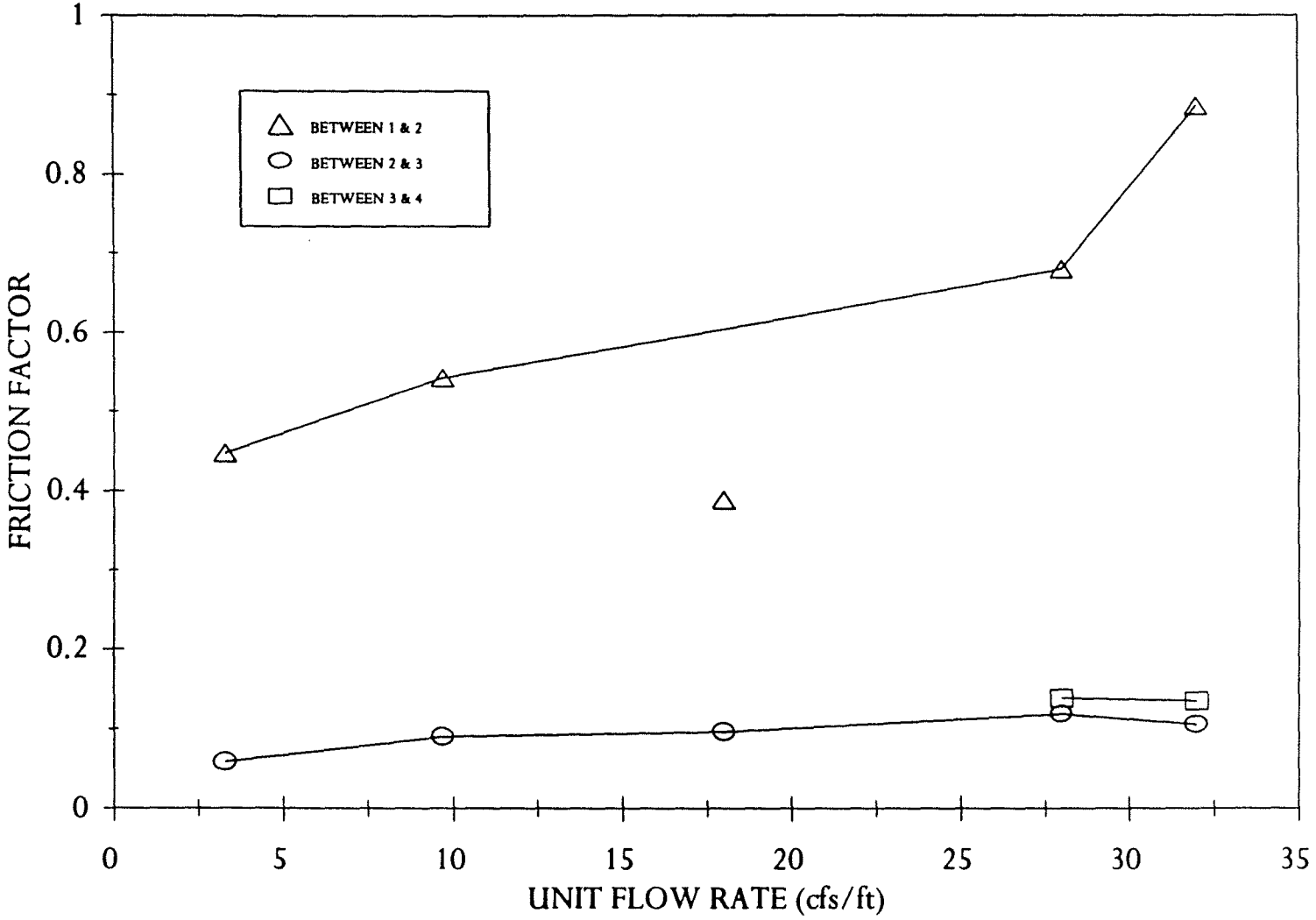

Figure 4.8: Unit flow rate vs. Friction factor

The decrease in friction factor would then be expected because between stations 1 and 2 the velocity is rapidly increasing, while the depth is decreasing. After this point, the depth and velocity remain relatively constant since in all cases except for the highest unit flow rate uniform flow was reached by station 3. This explains why the friction factor between stations 2 and 3 remains approximately constant. Figure 4.8 then shows that if uniform flow has been reached, as with most cases between stations 3 and 4, a constant friction factor value will be achieved that is independent of flow rate.

For the upper portions of the spillway, however, the friction factor increases with increasing flow rate. This is best explained by the higher air concentrations associated with the lower unit flow rates on the upper portions of the spillway (this is shown in the next section). Recalling Straub and Anderson's conclusion that the friction factor decreases with increasing air concentration, this relationship between friction factor and unit flow rate would be expected on this portion of the spillway.

With the friction factors known, it is possible to develop relatively accurate flow profiles by the standard step method. However, the variability of the friction factor, as just described, makes the choice of which friction factor to use in a water surface profile difficult. It was felt that the most accurate choice would be from the region where the friction factor remains the most constant. For this reason the friction factors between stations 2 and 3, and 3 and 4 were averaged. This yielded a

friction factor of 0.11 to use in the water surface profile calculations for the unbulked depth. These profiles are shown in Figure 4.9. These profiles can be compared to actual depths recorded during each test to help determine the amount of flow bulking taking place due to the entrained air. This comparison will be discussed further in the "Air-Concentration" section.

AIR-CONCENTRATION DATA

When studying the air-concentration data, flow bulking was the major issue of concern. Two methods were used for the comparison of bulked and unbulked flow depths, these being:

1. The bulked depth of flow corresponding to y_{90} should be related to an unbulked depth calculated by using the friction factor determined in the previous section.

2. The unbulked flow depth was assumed to be a percentage of the bulked flow depth directly related to the average air concentration.

The rest of this chapter describes the air concentration profiles and discusses the analysis of these issues.

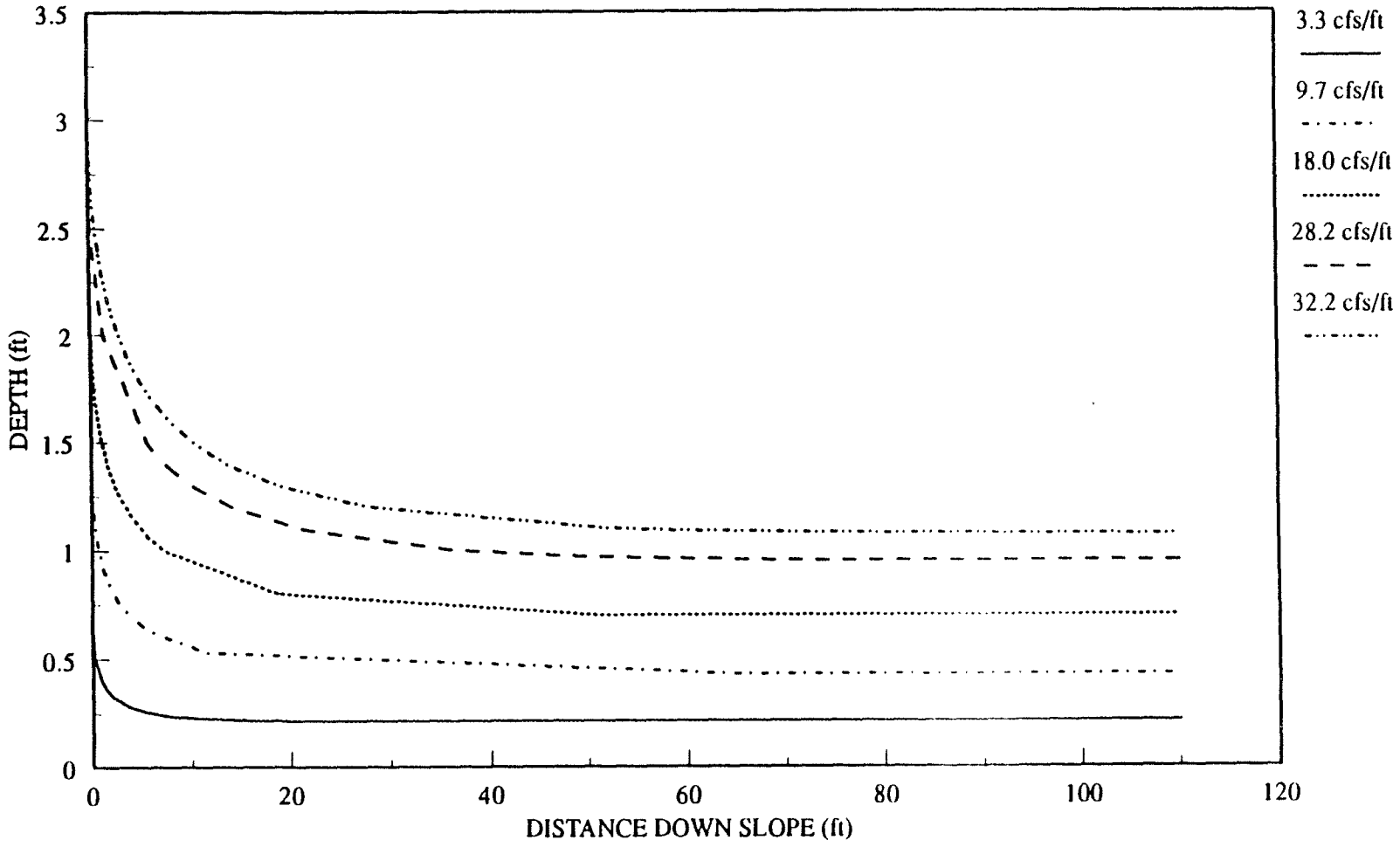

Figure 4.9: Calculated water surface profiles: Unbulked depths based on a friction factor of 0.11

GENERAL DESCRIPTION OF PROFILES

Displayed in Figures 4.10 through 4.14 are the air-concentration profiles obtained from the data collected for the current study. These profiles exhibit the same form as those found by Straub & Anderson. Referring to Figures 4.13, and 4.14, it can be seen that at the most upstream station the profiles start out at the floor of the flume with very low air concentrations, and very low increases in air concentration. Moving farther from the spillway floor, however, the profiles curve over with a dramatic increase in air concentration. Farther downstream at station 3, the increase in air concentration with increasing depth becomes more gradual, and the curves in the profiles become smoother. At the base of the spillway, the profiles for the higher two unit flow rates become practically straight lines, as shown in Figures 4.13 and 4.14. From these figures it is again seen that the profiles are almost identical between the bottom two stations of recorded data for each flow rate, suggesting that uniform equilibrium flow was reached in each case.

These air concentration profiles show the same peculiarity at 18.0 cfs/ft that the velocity profiles did. At this flow, the air concentration at station 2 for a given depth is higher than that at station 3. Once again, no explanation can be offered for this fact.

NORMALIZED PROFILES:

Each air concentration profile was normalized, and the corresponding

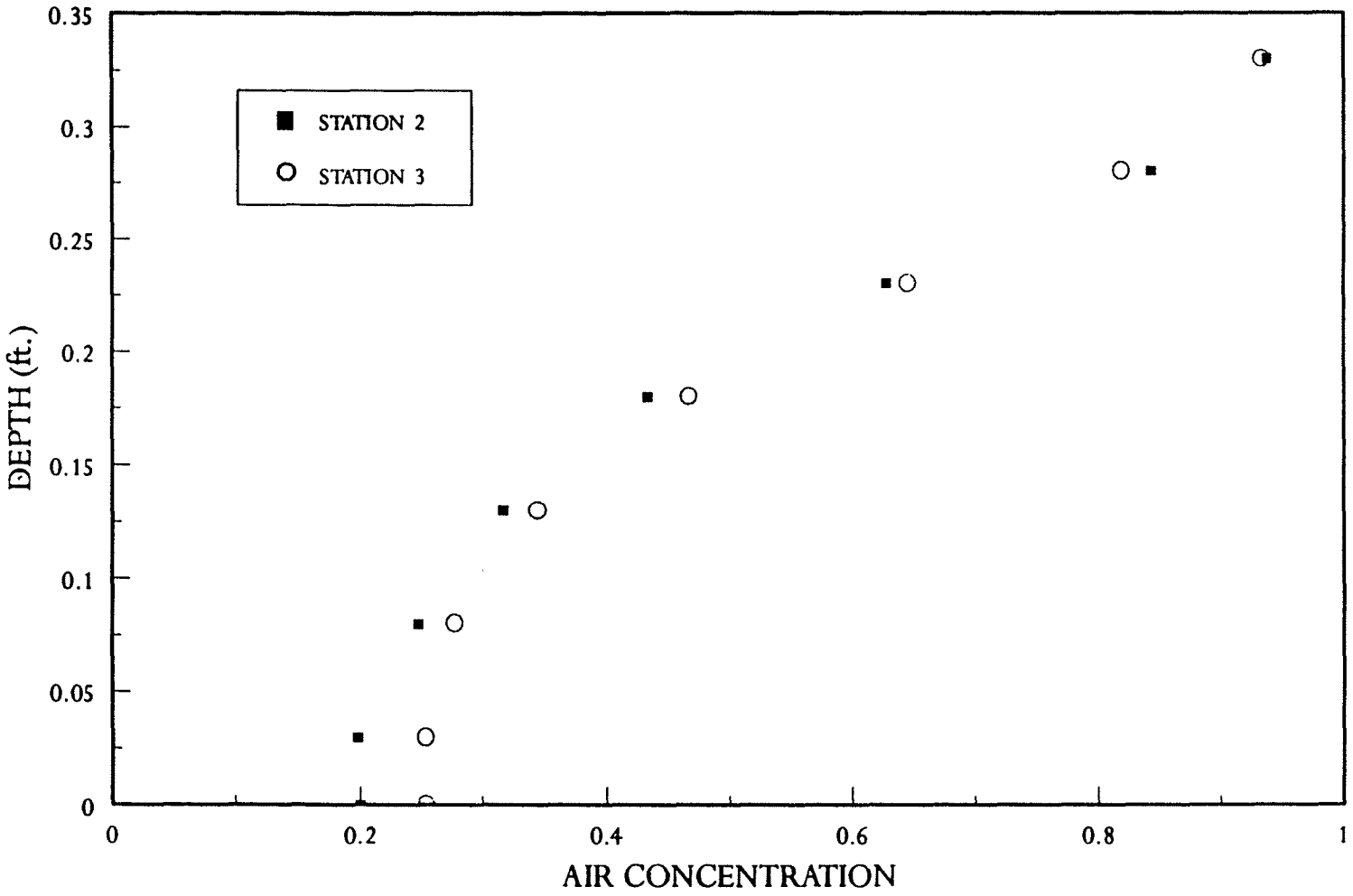

Figure 4.10: Air concentration profiles - 3.32 cfs/ft

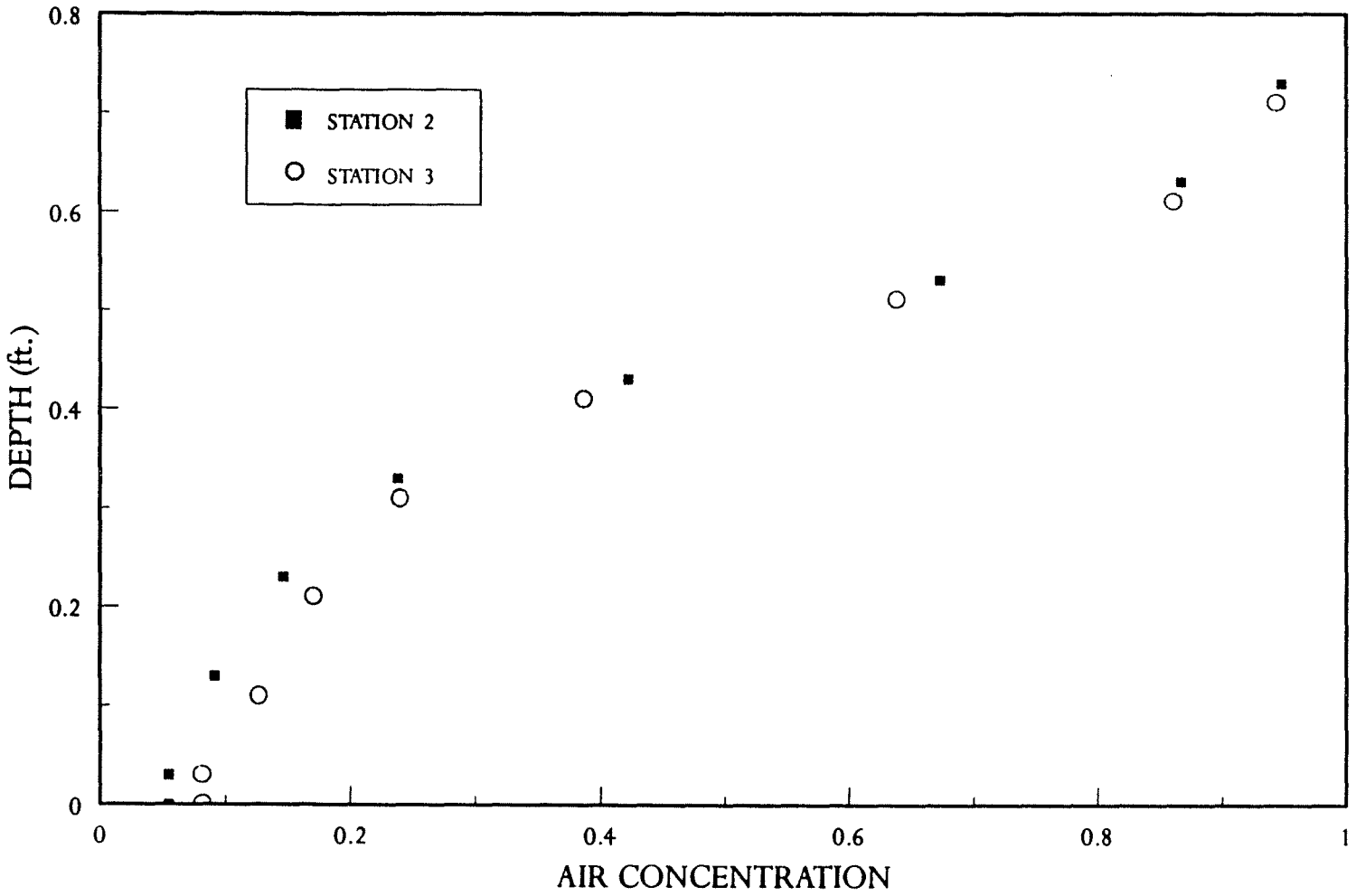

Figure 4.11: Air concentration profiles - 9.7 cfs/ft,

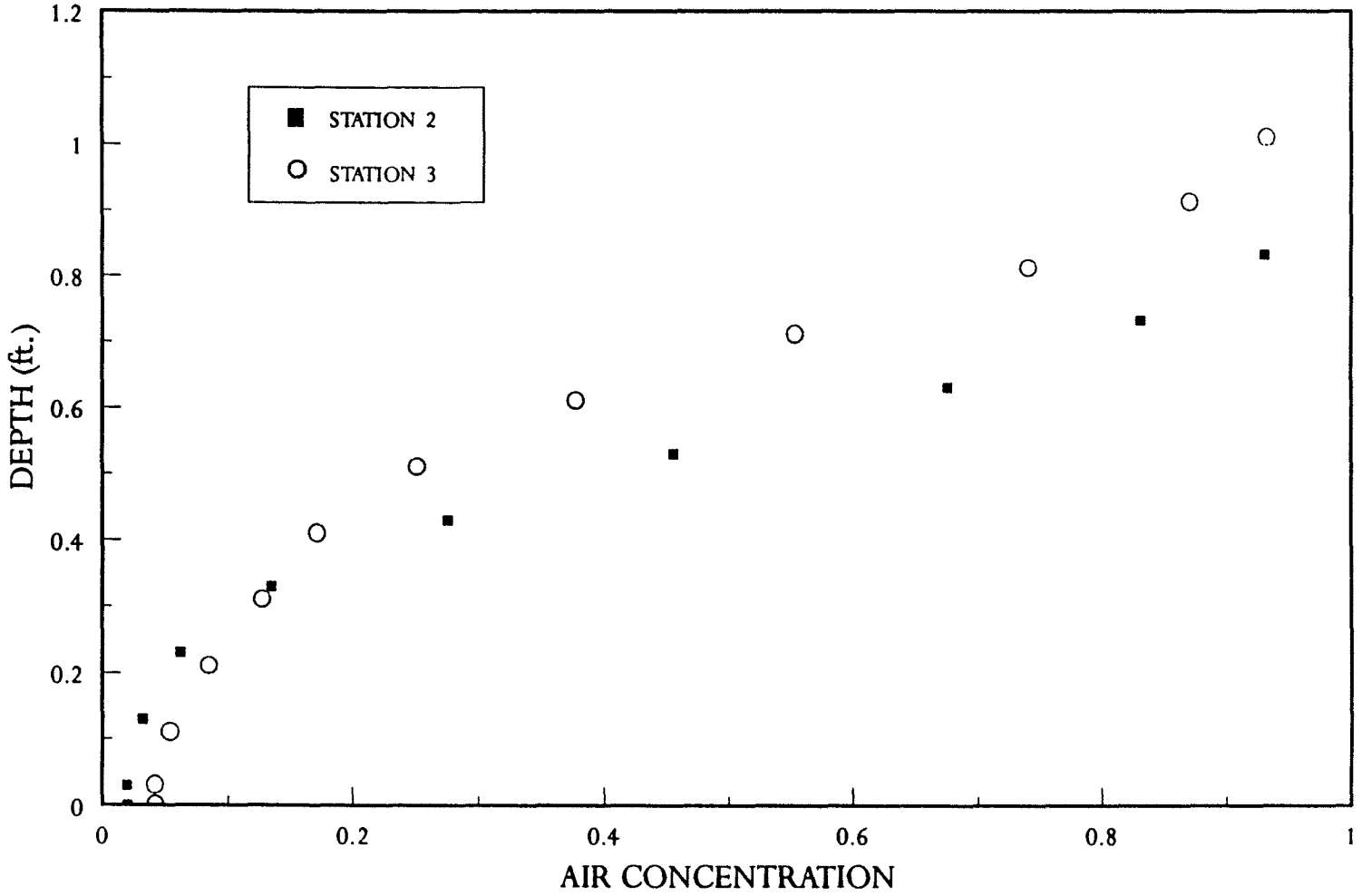

Figure 4.12: Air concentration profiles - 18.0 cfs/ft

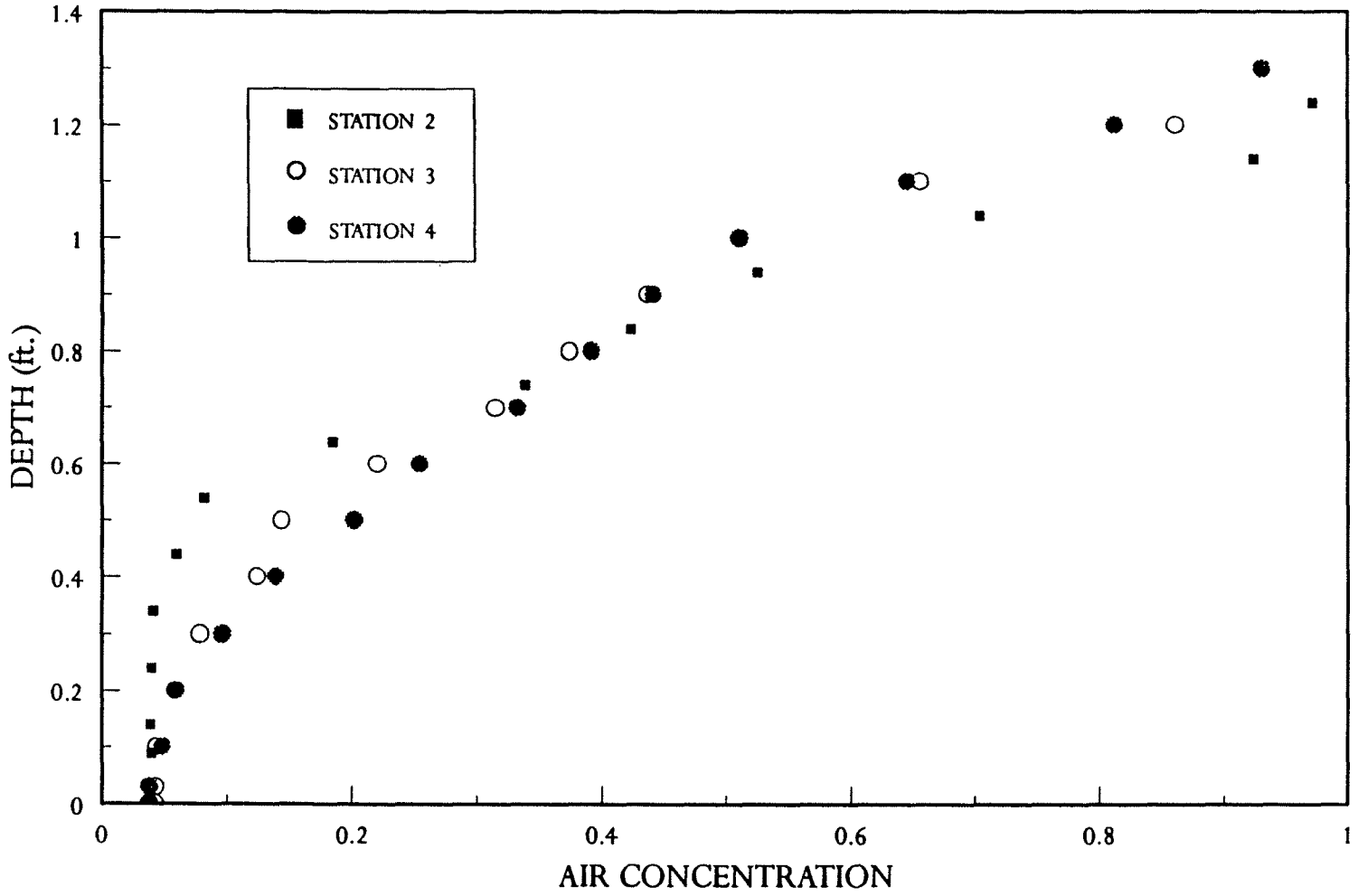

Figure 4.13: Air concentration profiles - 28.2 cfs/ft

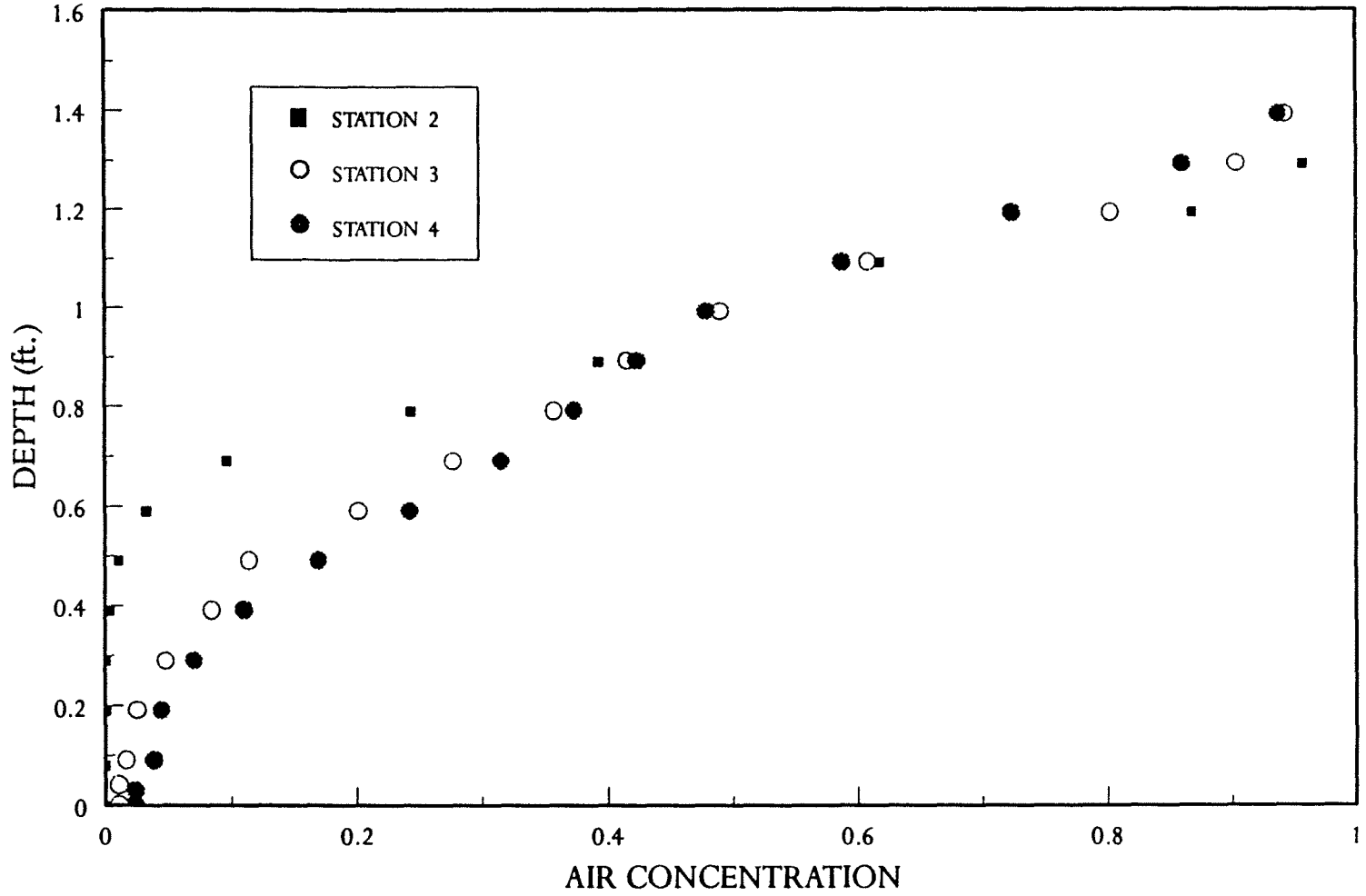

Figure 4.14: Air concentration profiles - 32.2 cfs/ft

normalized profiles are shown in Figures 4.15 through 4.17. The normalization of the profiles was accomplished by dividing each depth reading by the depth of y_{90}. Y_{90} depths were determined from the profiles in Figures 4.10 through 4.14. These depths are summarized in Table 4.3. This is the same method used by previous researchers (Straub & Anderson, 1958). Normalizing the profiles does not allow any quantitative assessments to be made. It is meant merely to be a means of observing the characteristics of profiles from different flow rates. From these figures it is easy to recognize several general trends taking place, one of which is the general shape of the profiles. To add to the previous description, one obvious characteristic visible from these figures is the more gradual increase in air concentration with increasing depth at station 2 as the flow rate is decreased. This means that for a given relative depth, the lower unit flow rates will have higher air concentrations. However, once in the equilibrium flow region, such as at Stations 3 and 4, it can be seen that the shape of the air concentration distributions, except for that of the lowest unit flow rate of 3.3 cfs/ft, become independent of the flow rate. This agrees with Wood's (1983) findings. Based on observations made during testing, the difference in behavior of the profile for the lowest unit flow rate of 3.3 cfs/ft can be attributed to the cascading flow which accompanied this flow rate. A cascading flow is much more turbulent than a skimming flow, so higher air concentrations would be expected near the floor of the spillway.

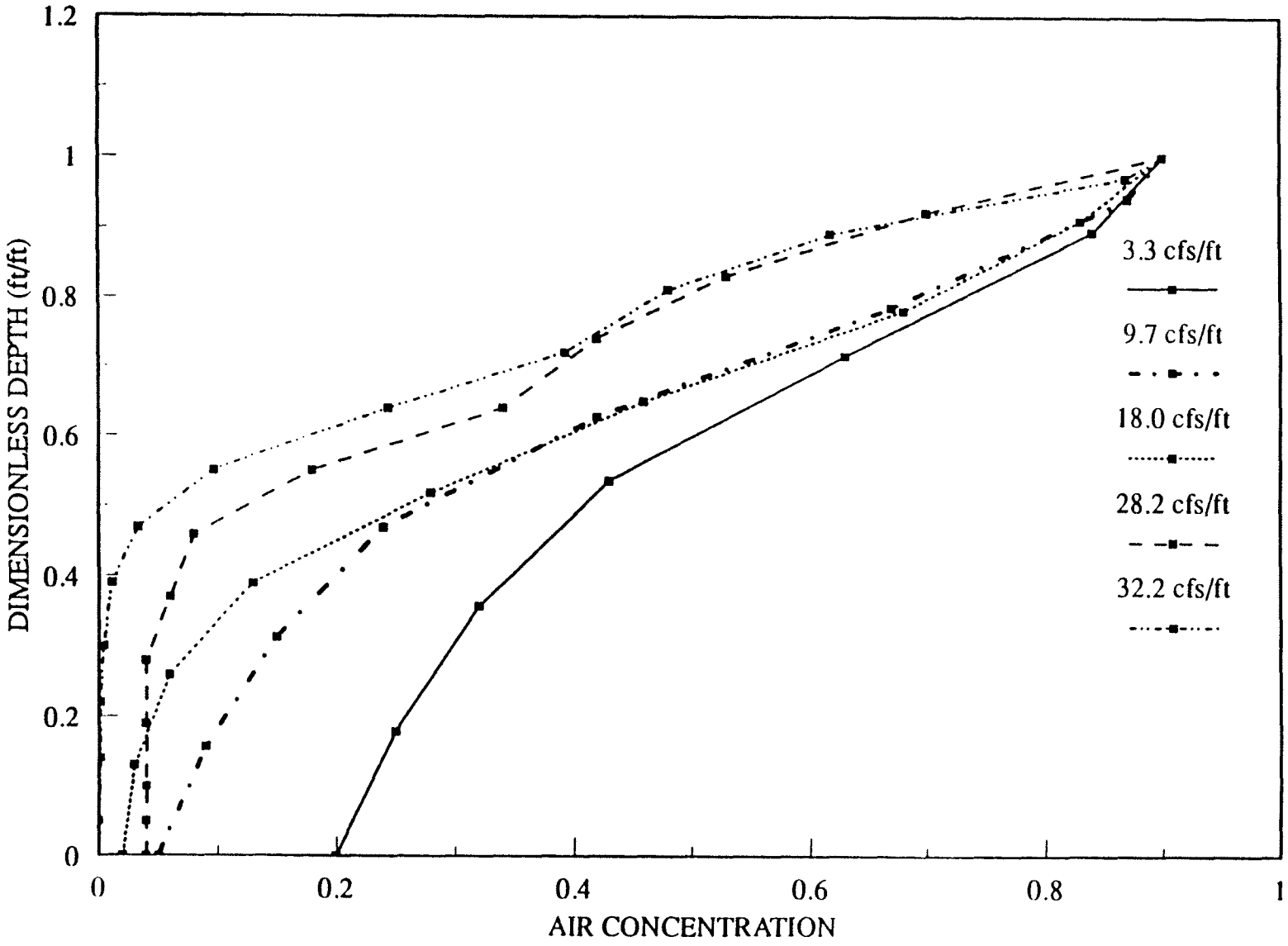

Figure 4.15: Dimensionless air concentration profiles, Station 2, all flow rates

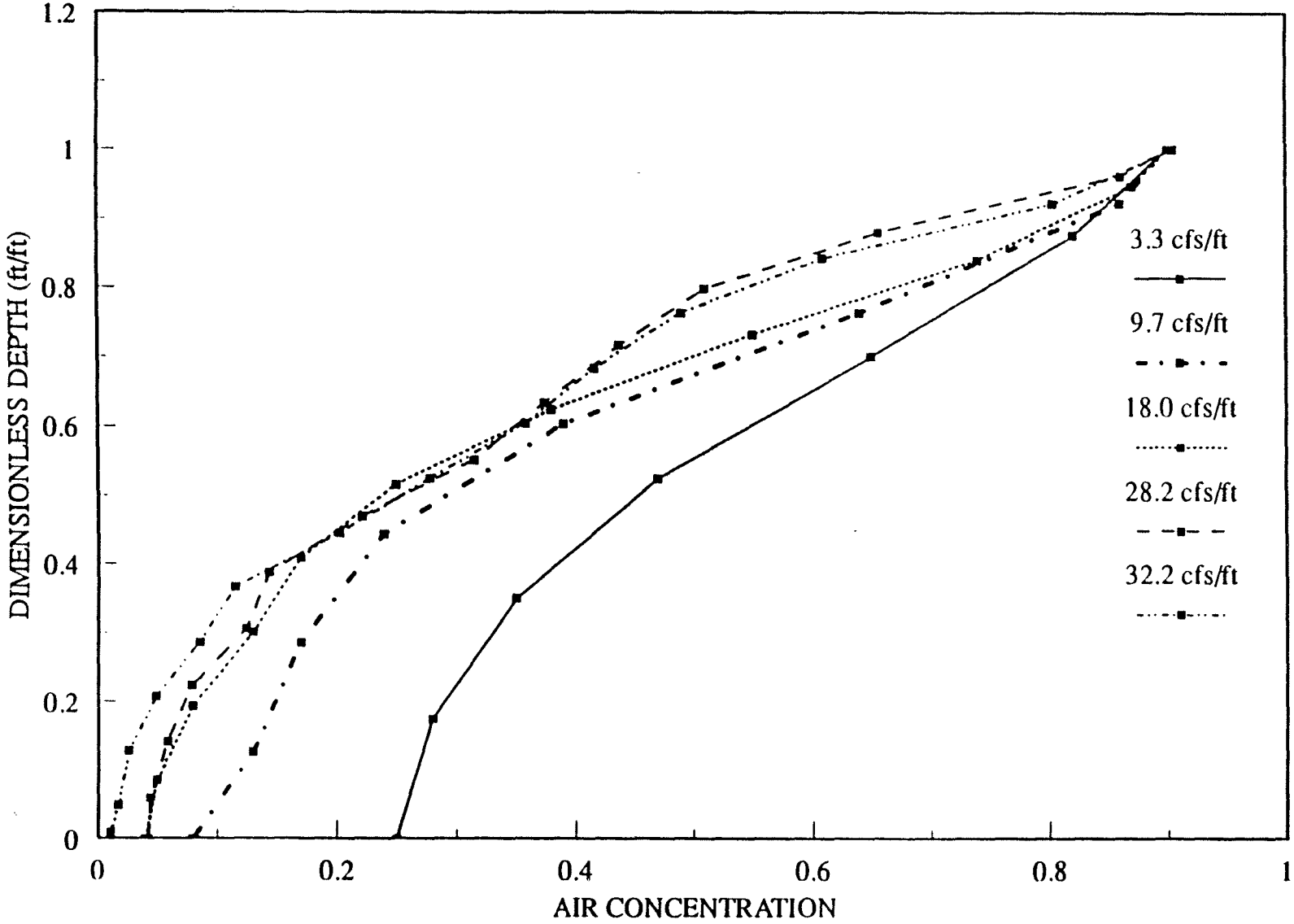

Figure 4.16: Dimensionless air concentration profiles, Station 3, all flow rates

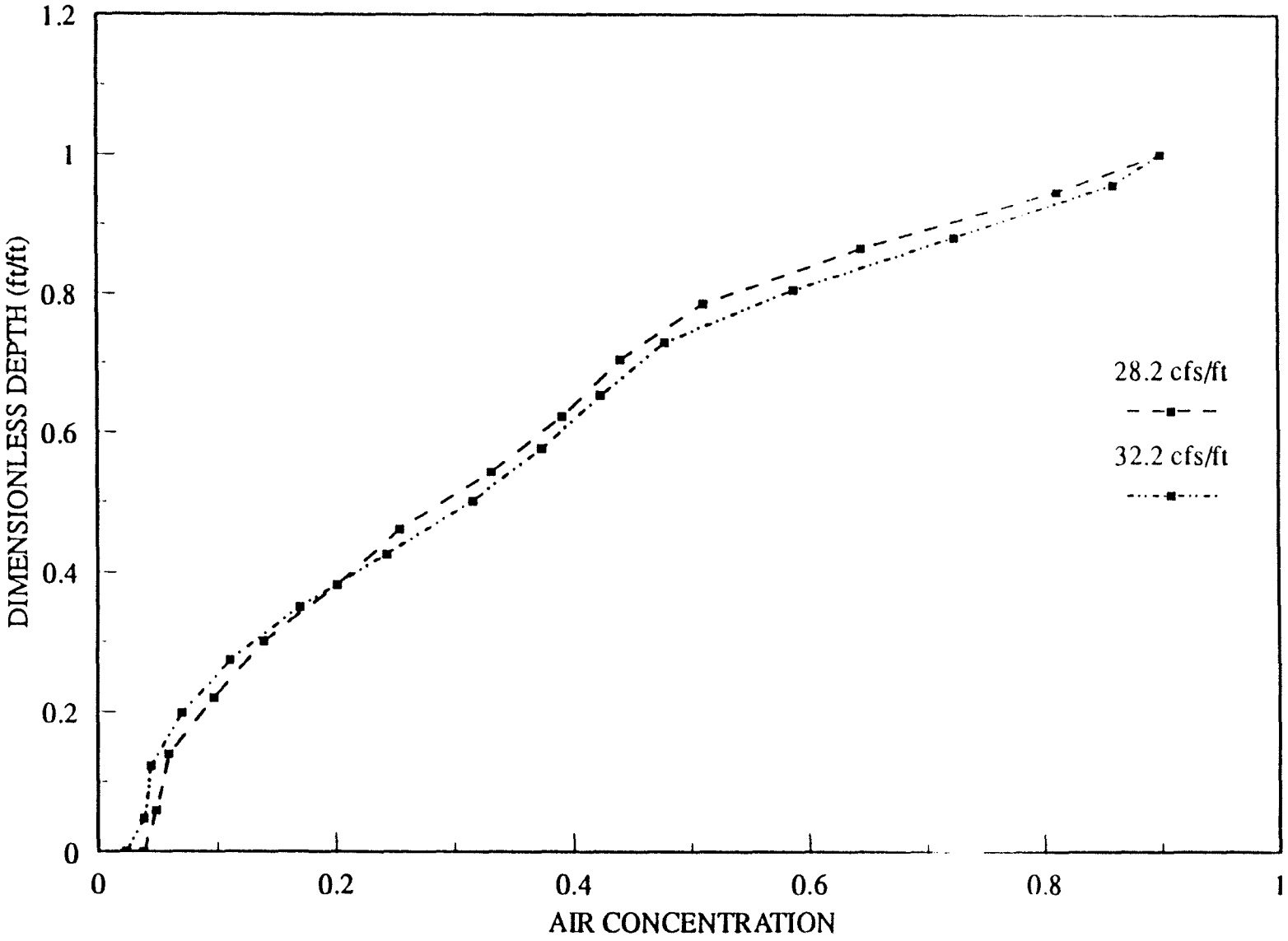

Figure 4.17: Dimensionless air concentration profiles, Station 4, 28.2 & 32.2 cfs/ft

Table 4.3: Y90 depths for each flow rate and station

STATION	UNIT FLOW RATE				
	3.2 cfs/ft	9.7 cfs/ft	18.0 cfs/ft	28.2 cfs/ft	32.2 cfs/ft
	Y90 (ft)				
2	0.31	0.67	0.80	1.13	1.22
3	0.32	0.66	0.96	1.26	1.29
4	N/A	N/A	N/A	1.27	1.34

AVERAGE AIR-CONCENTRATIONS:

For each air concentration profile an average air concentration was determined. To do this, each profile was divided into sections of equal depth. The area of each section was then calculated. These areas were summed up and divided by the total depth, thus giving the average air concentration. Table 4.4 shows the values determined for each flow rate at each station. Figure 4.18 is a plot of the average air concentrations at Station 3 for each flow rate. This figure reveals a very interesting characteristic. As the unit flow rate is increased, the average air concentration decreases asymptotically to a finite value. For the conditions of the present study this value appears to be about 33%. This result is extremely interesting when compared to the conclusion made by Ian Wood stated in Chapter 2. Wood stated that an average air concentration existed for each slope, and was able to create the table shown as Table 2.1 in this thesis. A linear interpolation between values shown in Table 2.1 gives an average air concentration of 36.3% for a slope of 26.5

Table 4.4: Average air concentrations

STATION	UNIT FLOW RATE				
	3.3 cfs/ft	9.7 cfs/ft	18.0 cfs/ft	28.2 cfs/ft	32.2 cfs/ft
	AIR CONCENTRATION				
2	53%	44%	37%	25%	28%
3	54%	46%	40%	31%	30%
4	N/A	N/A	N/A	33%	33%

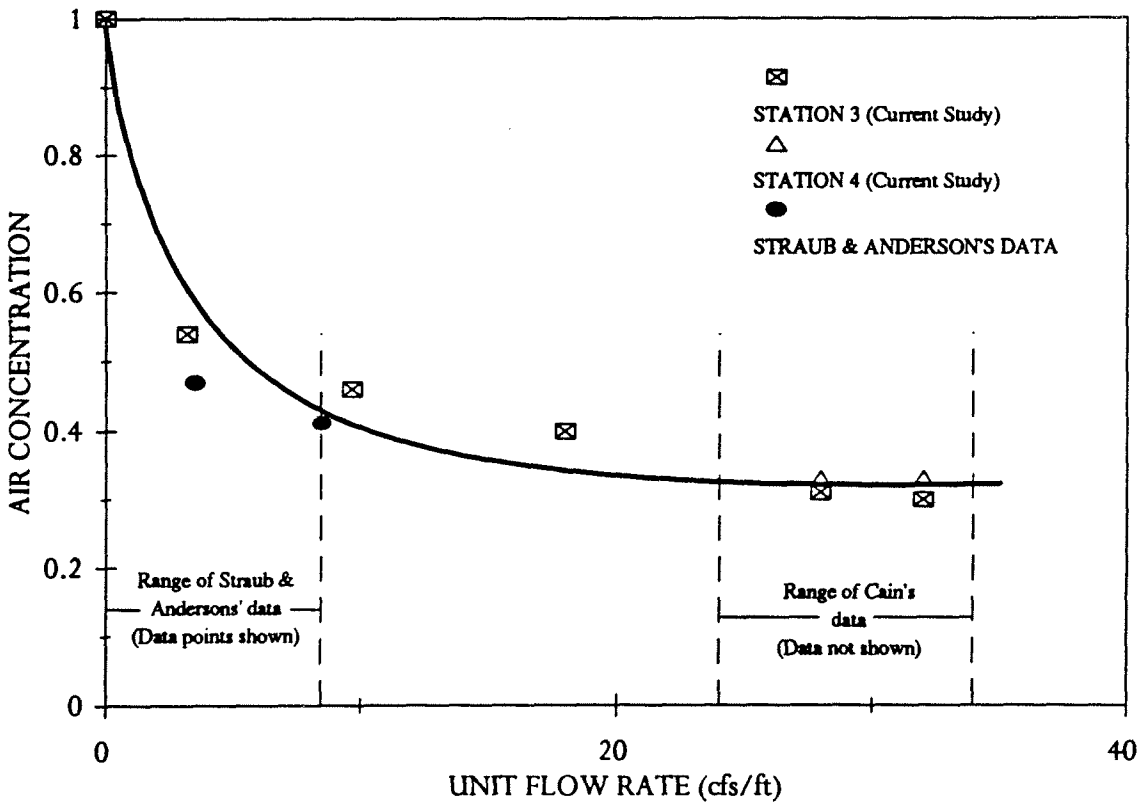

Figure 4.18: Average air concentrations for various flow rates at Stations 3 & 4
Note: Cain's data not shown due to difference in slope which would make comparisons misleading.

degrees, the slope of the CSU flume. The data collected for the current study, then, shows that once the unit flow rate over the stepped block spillway is high enough so that a cascading flow is no longer present (such as with the lowest two flow rates tested for the current study) the air concentration in the flow is no longer affected by the very high roughness of the blocks.

Wood's analysis, as stated in Chapter 2, was based on Straub & Anderson's data. A comparison of the results from the current study to Straub & Anderson's original data, then, should show a good correlation. Looking at their data, it is seen that their tests were limited to a very small range of flows. Their maximum unit flow rate was only 8.5 cfs/ft at the slopes closest to those of this study. Comparing the results of their 3.5 cfs/ft and 8.5 cfs/ft flow rates to the 3.3 cfs/ft and 9.7 cfs/ft flow rates of the current study (the closest comparable flows) again shows remarkable similarities. From Straub & Anderson's original data at 3.5 cfs/ft and 8.5 cfs/ft, average air concentrations at a 26.5 degree slope (by linear interpolation) of 47% and 41%, respectively, are given. The data from the current study at 3.3 cfs/ft and 9.7 cfs/ft gives average air concentrations of 53.5% and 45% respectively. Again, considering the cascading flow at these flow rates in the current study, higher average air concentrations would be expected. Looking at the much higher flow rates tested in the current study, though, shows that the average air concentrations do level out very near those values given by Straub & Anderson, as stated earlier.

Although the flow rates were more comparable to those of the current study, a comparison with the data taken by Cain on the Aviemore Dam spillway is difficult since his data was taken on a very different slope, 45 degrees. Also, Cain's flows never really reached an equilibrium state. His data, taken on a "rough surface", however, shows average air concentrations beginning to level out at about 50%. Once again, it should be noted that the flow had not yet reached equilibrium, where the air concentration would have been greater. With this in mind, a comparison to Wood's results shows good similarities, as at a 45 degree slope Wood predicted an average air concentration of 62%. It does appear, then, that once the flow over a spillway has exceeded a skimming flow, the average air concentration has no dependency on the roughness of the spillway surface. This knowledge is of particular interest when considering the bulking effects of flow over the wedge blocks.

BULKING:

Flow bulking is the phenomenon that occurs when air entrained in the flow causes the flow depth to increase. This becomes an important parameter when designing the height of spillway side-walls. Since flow bulking is a product of entrained air, it is reasonable to assume that the amount of bulking taking place in a given flow is dependent upon the average air concentration of that flow. In fact, if the average air concentration is known, then the flow depth for an unaerated flow should be the aerated flow depth minus the percentage of that depth equalling the average air concentration. For example, if the aerated flow depth was 1 foot, and the

average air concentration was 30%, then the unaerated flow depth would be approximately 70% of the aerated flow depth, or 0.7 feet. This is illustrated in Figure 4.19. This figure shows the relationship between unit flow rate, and flow depth for the bulked and unbulked flow cases at Station 3. Unbulked flow depths are shown for the method described above, as well as for the calculated water surface profile.

Figure 4.19 and Table 4.5 present a very significant result, namely the relationship between the calculated water surface profile (WSP) depths, which are based on the previously determined friction factor of 0.11 and accounts for the roughness of the blocks, and the bulked flow depths measured during the tests. A linear regression analysis was performed for both the bulked depths and the WSP depths for the upper three flow rates where the flow was no longer cascading. The results of these regressions are shown in Figure 4.19 as solid lines. The two lines are practically parallel, separated by approximately 0.25 feet. This suggests that once the flow rate over the blocks is high enough to be a skimming flow, the bulked depth will always be approximately 0.25 feet greater than the calculated WSP depth, if the friction factor calculated in this study is used. With this result, it is then possible to accurately determine the bulked depth of flow for a wide range of flow rates. It should be noted that these values are based on the bulked depth of y_{90}. To account for the flow above y_{90}, a factor of safety should be used.

Table 4.5: Various flow depths at Station 3 (101 ft. down the flume)

FLOW RATE (cfs/ft)	AIR CONCEN. (%)	Y90 (ft)	UNBULKED DEPTH (ft)	CALCULATED WSP DEPTH (ft)
0.0	100.00	0.00	0.00	0.00
3.3	54.00	0.32	0.15	0.22
9.7	46.00	0.66	0.36	0.43
18.0	40.00	0.96	0.58	0.70
28.2	31.00	1.26	0.87	0.95
32.2	30.00	1.29	0.90	1.07

$Y_{90}(1-C_A)$

$d_{wer}(1-C_A)$

$f = 0.11$ entrained air depth

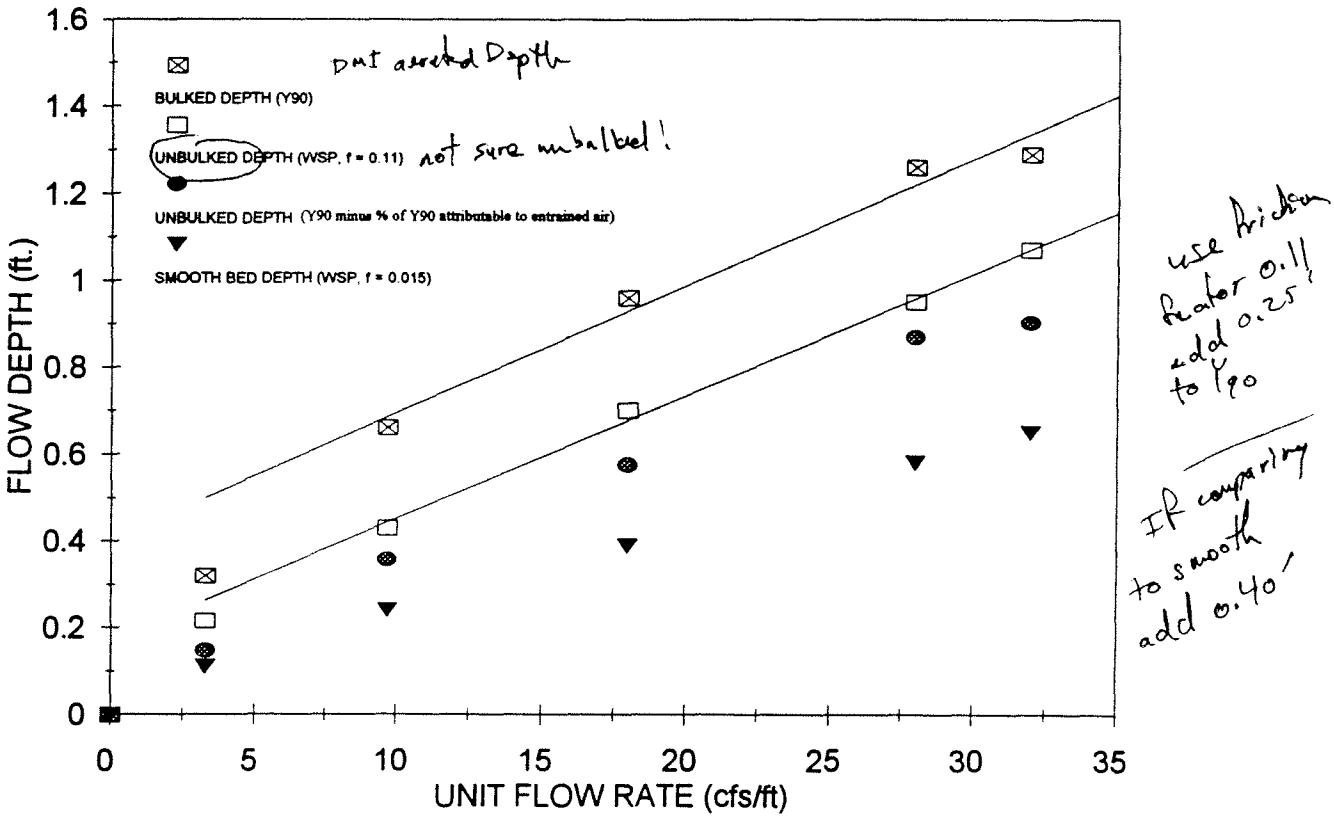

Figure 4.19: Flow bulking effects at Station 3

Shown also in Figure 4.19 are the depths obtained from water surface profiles calculated for a spillway with a smooth surface. These profiles were developed using a friction factor of 0.015, an average value for a smooth concrete surface. This was done to provide a known reference to relate with the bulked flow depths obtained from the test data. A comparison of this type allows a relationship to be made between a water surface profile of a spillway with a known friction factor, and the depth of flow of a spillway covered with the wedge blocks. This gives an indication of the energy dissipation caused by using the stepped block overlay.

It was also hoped that a comparison could be made between the amount of bulking on a wedge-block-covered spillway, and the amount of bulking proposed by the USBR's freeboard equation found in "Design of Small Dams." This would show the amount of increased bulking created by using a wedge-block-covered spillway surface. This equation is:

$$FB = 2 + (0.025)\, Vd^{1/3} \qquad (4.6)$$

where FB is the freeboard in feet, V is the velocity, and d is the depth of unaerated flow in feet. Without doing any calculations it can be seen that this equation has a large factor of safety built in to it, as at a minimum, the freeboard will be at least two feet greater than the WSP depth. For this reason, the results of the present study were compared to only the second half of equation 4.6 (please see Appendix F). This comparison, however, revealed no obvious relationships.

CHAPTER 5
SUMMARY, CONCLUSIONS, AND RECOMMENDATIONS

Over the past several years the increased availability of historical data on precipitation and floods has increased the estimates of the Probable Maximum Flood (PMF). This increase has in turn meant that many embankment dams and their spillways are not capable of retaining or safely passing the PMF. To combat this problem there are essentially three options available, the first two of which are in most cases extremely expensive. The options that exist are; (1) raising the height of the dam, (2) increasing the spillway capacity, and (3) letting the flood waters overtop the dam while using some type of protective overlay on the downstream face of the dam. Due to the expense associated with options 1 and 2, a lot of research has recently been performed on overtopping protection measures. Several types of protective overlays ranging from geotextiles to soil cement have been tested, but, as shown by Slovensky (1993), the aspirating stepped block designs appear to be the most stable. One such design, developed by the United States Bureau of Reclamation (USBR), has been the subject of a series of recent tests. Slovensky demonstrated the stability of this design in tests performed in the fall of 1992. However, in an effort to more fully understand the dynamics of the flow over these blocks, and determine certain design criteria such as the friction factor, flow bulking, and spillway base

energy, another set of tests was performed in the summer and fall of 1993. The aim of these tests was to study the velocity and air-concentration profiles of the flow over the wedge blocks, thus allowing design criteria such as flow bulking and energy remaining in the flow at the toe of the dam to be determined. With this information available, proper design of spillway side-walls and stilling basins can then be carried out.

The study of self-aerated flow is not a new subject. From Chapter 2 it can be seen that as early as 1926 the process of air entrainment was being studied by Ehrenberger. Straub and Anderson took data in 1958 that was reanalyzed by Ian Wood in 1983, and is still referred to today. Even today, Hubert Chanson continues to publish papers on this subject. To date, however, no studies have been performed in self-aerated flow over a surface as rough as the stepped block spillway used for the current study.

Step type surfaces cause the flow to become completely aerated more quickly than does a smooth surface. This was described in Chapter 4. The results discussed in Chapter 4 produced six main conclusions:

1. A terminal velocity was reached for flow rates up through 28.2 cfs/ft. For the block geometry shown in Figures 3.5 and 3.6, and a 2H:1V spillway slope, the average velocities become relatively constant at about 38 fps. At

the highest flow rate of 32.2 cfs/ft, the average velocity stopped increasing after station 3, although the maximum velocity increased by approximately 6%. It is therefore questionable whether a terminal velocity was reached for the flow rate of 32.2 cfs/ft.

2. If the flow is great enough so skimming flow is present, the bulked flow depth determined from the collected data appears to be greater than the unbulked depth determined from the calculated water surface profiles by a constant depth of approximately 0.25 feet.

3. If the flow is great enough so skimming flow is present, the average air concentration of the flow is no longer affected by the very high roughness of the blocks, but is a function of the slope of the spillway. This agrees well with Wood's conclusions that were based on Straub & Anderson's data. For the 2:1 slope used in the present study, this average air concentration is approximately 33%.

4. Air-concentration profiles for a stepped block spillway assume the same general form as those published by Straub and Anderson in 1958 for a smooth spillway.

5. The data taken appears to agree with Ian Wood's finding that once in the

uniform flow region, the shape of the air concentration profile is independent of unit discharge.

6. Due to the tumbling and cascading of the flow, the friction factor is higher at the top of the spillway. As the flow proceeds down the spillway, it accelerates and begins to skim over the blocks, and the air concentration increases. This causes the friction factor to decrease. When uniform flow is reached, the friction factor stops decreasing, and becomes independent of flow rate. For the current tests, this friction factor was 0.106.

Each one of these conclusions advance our knowledge of how a stepped-block spillway affects self-aerated flows. In light of these conclusions, stepped blocks continue to appear an attractive alternative for dam protection in the presence of overtopping flow. Future research in this area could profitably examine the effects of localized instabilities associated with the point of inception.

REFERENCES

1. Bachmeier, G., (1987/88), "Setup, Calibration and Use of a Measuring Probe for Determination of the Air Concentration in a Spillway Chute," Dissertation, Institute for Hydromechanics of Karlsruhe University, (translated from German).

2. Cain, P., (1978), "Measurements within Self-Aerated Flow on a Large Spillway," Thesis, Department of Civil Engineering, University of Canterbury, Christchurch, New Zealand.

3. Cain, P., and Wood, I.R., (1981), "Instrumentation for Aerated Flow on Spillways," ASCE, Journal of the Hydraulics Division, Vol. 107, No. HY11, 1407-1424.

4. Cain, P., and Wood, I.R., (1981), "Measurements of Self-Aerated Flow on a Spillway," ASCE, Journal of the Hydraulics Division, Vol. 107, No. HY11, 1425-1444.

5. Chanson, H., (1989), "Flow Downstream of an Aerator - Aerator Spacing," Journal of Hydraulic Research, Vol. 27, No. 4.

6. Chanson, H., (1992), "Drag Reduction in Self-Aerated Flows. Analogy with Dilute Polymer Solutions and Sediment Laden Flows," Research Report CE141, Dept. of Civil Engineering, University of Queensland, Australia.

7. Chanson, H., (1993), "Self-Aerated Flows on Chutes and Spillways," ASCE, Journal of Hydraulic Engineering, Vol. 119, No. 2.

8. Ervine, D.A. and Falvey, H.T., (1987), "Behavior of Turbulent Water Jets in the Atmosphere and in Plunge Pools," Proceedings of the Institution of Civil Engineers, Vol. 83, Part 2, 295-314.

9. Falvey, H.T., (1979), "Mean Air Concentration of Self-Aerated Flows," ASCE, Journal of the Hydraulics Division, Vol. 105, No. HY1, 91-95.

10. Halbronn, G., and Cohen de Lara, G., (1953), "Air Entrainment in Steeply Sloping Flumes," Proceedings, Minnesota International Hydraulics Convention, Minneapolis, Minn., 455-466.

11. Hino, M., (1961), "On the Mechanism of Self-Aerated Flow on Steep Slope Channels. Applications of the Statistical Theory of Turbulence," Proceedings, 9th IAHR Congress, Dubrovnick, Yugoslavia, 123-132.

12. Killen, J.M., (1968), "The Surface Characteristics of Self-Aerated Flow in Steep Channels," Thesis, University of Minnesota.

13. Lai, K.K., (1971), "Studies of Air Entrainment on Steep Open Channels," Thesis, University of South Wales, Sydney, Australia.

14. Lamb, O.P., and Killen, J.M., (1950), "An Electrical Method for Measuring Air Concentration in Flowing Air-Water Mixtures," Technical Paper No. 2, Series B, University of Minnesota, St. Anthony Falls Hydraulic Laboratory, Minneapolis, Minn.

15. Marie, J.L., (1987), "A Simple Analytical Formulation for Microbubble Drag Reduction," PhysicoChemical Hydrodynamics, Vol. 8, No. 2, 213-220.

16. Michels, V. and Lovely, M., (1953), "Some Prototype Observations of Air Entrained Flow," Proceedings, 5th IAHR Congress, 403-414.

17. Rao, N.S. and Rajaratnam, N., (1961), " On the Inception of Air-Entrainment in Open Channel Flows," Proceedings, 9th IAHR Congress, Dubrovnick, Yugoslavia, 9-12.

18. Slovensky, G.G., (1993), "Near-Prototype Testing of Wedge-Block Overtopping Protection," Thesis, Colorado State University, USA.

19. Straub, L.G. and Anderson, A.G., (1958), "Experiments on Self-Aerated Flow in Open Channels," ASCE, Journal of the Hydraulics Division, Vol. 84, No. HY7, paper 1890.

20. Straub, L.G., Killen, J.M. and Lamb, O.P., (1954), "Velocity Measurement of Air-Water Mixtures," ASCE Transactions, Vol. 119, 207-220.

21. Straub, L.G., and Lamb, O.P., (1956), "Studies of Air Entrainment in Open Channel Flows," ASCE Transactions, Vol. 121, 30-44.

22. U.S. Bureau of Reclamation, (1977), Design of Small Dams, 2nd edition, 393.

23. U.S. Bureau of Reclamation, (1988), Overtopping Flow on Low Embankment Dams - Summary Report of Model Tests, 3-5.

24. Volkart, P., (1980), "The Mechanism of Air Bubble Entrainment in Self-Aerated Flow," International Journal of Multiphase Flow, Vol. 6, 411-423.

25. Viparelli, M., (1957), "Fast Water Flow in Steep Channels," Proceedings, 7th IAHR Congress, D39.1-D39.12.

26. Wood, I.R., (1983), "Uniform Region of Self-Aerated Flow," ASCE, Journal of Hydraulic Engineering, Vol. 109, No. 3, 447-461.

27. Wood, I.R., (1985), "Air-Water Flows," Proceedings, 21st IAHR Congress, Vol 6., Melbourne, Australia, 19-23.

APPENDIX A

VELOCITY DATA

Table A1: Column definitions for tables found in Appendix A

POINT DEPTH CALCULATIONS:

COLUMN NUMBER	COLUMN TITLE	FORMULA DESCRIPTION
1	POINT GAGE READING	Direct reading from point gage on velocity probe.
2	DEPTH	Column 1 subtracted from the zero reading for the probe at that station.
3	VOLTAGE	Voltage read directly from the voltmeter.
4	AVERAGE VOLTAGE	Average of the values found in column 3 for the depth given in column 2.
5	AVERAGE PRESSURE	Pressure found using the voltage in column 4 in the following equation: -1.9255165+(4.786125373*voltage)
6	PRESSURE CORRECTED FOR ZERO	Pressure from column 5 corrected for the pressure found when the velocity probe was in 100% air.
7	AIR CONCENTRATION	Air concentration at the depth given in column 2 taken directly from the air concentration spreadsheets.
8	CORRECTION COEFFICIENT	Velocity probe correction coefficient determined during calibration of the probe. Can be determined from the following equation: (71.67149 - 8.085219*(air conc.)) / (1 - 1.265099*(air conc.))
9	VELOCITY	Velocity at the depth given in column 2 determined from the following equation: (correction coefficient)*((corrected pressure)^(1/2))
10	STANDARD DEVIATION	The standard deviation of the voltage readings found in column 3, given by the voltmeter.
10	DIMENSIONLESS DEPTH	For tables to Y90 only: The depth from column 2 divided by the depth of Y90.
11	DIMENSIONLESS VELOCITY	For tables to Y90 only: The velocity in column 9 divided by the velocity at a depth of Y90.

Table A1 (continued): Column definitions for tables found in Appendix A

CALCULATION OF AVERAGES:

COLUMN NUMBER	COLUMN TITLE	FORMULA DESCRIPTION
1	AREA	Portion of the profile being looked at.
2	DEPTH	Depth from the floor of the flume to the top of the portion being looked at.
3	AVERAGE VELOCITY	The average velocity of the portion of the profile being looked at. The number titled "AVERAGE" at the base of this column is the overall average of this column.
4	UNIT FLOW RATE	The product of the previous 2 columns. The sum of this column is the area of the region to the left of the curves shown in Figures 4.1 through 4.5. The number titled "AVERAGE VELOCITY" at the bas of this column is this sum divided by the total depth of the profile. This gives the average velocity.

Table A2: Velocity data, Station 2, 3.3 cfs/ft

POINT DEPTH CALCULATIONS												
POINT GAGE READING (ft.)	DEPTH (ft.)	VOLTAGE (volts)	AVERAGE VOLTAGE (volts)	AVERAGE PRESSURE HEAD (ft)	PRESSURE CORRECTED FOR ZERO (ft)	AIR CONCENTRATION	CORRECTION COEFFICIENT	VELOCITY (fps)	DIMENSIONLESS DEPTH	DIMENSIONLESS VELOCITY	STANDARD DEVIATION	NOTES
6.685	0.000					0.00		0.000	0.00	0.00		
6.655	0.030	1.180 1.218	1.199	3.811	3.638	0.20	9.684	18.472	0.09	0.55	0.062 0.055	
6.555	0.130	1.506 1.507	1.506	5.284	5.111	0.32	10.774	24.356	0.41	0.73	0.071 0.072	
6.455	0.230	1.174 1.117	1.145	3.556	3.383	0.63	18.110	33.311	0.73	1.00	0.065 0.060	Mostly air
***	0.317					0.90	NOT VALID	33.311	1.00	1.00		
6.355	0.330	0.597 0.589	0.593	0.912	0.739	0.94	NOT VALID	33.311			0.024 0.025	
AIR		0.399 0.478	0.438	0.173	0.000						0.043 0.002	Zero with probe in air

AVERAGE VELOCITY			
AREA	DEPTH (ft.)	AVERAGE VELOCITY (fps)	UNIT FLOW RATE (sq.ft./sec)
A1	0.03	9.24	0.28
A2	0.10	21.41	2.14
A3	0.10	28.83	2.88
A4	0.10	33.31	3.33

AVERAGE VELOCITY (TO DEPTH OF Y90 ONLY)			
AREA	DEPTH (ft.)	AVERAGE VELOCITY (fps)	UNIT FLOW RATE (sq.ft./sec)
A1	0.03	9.24	0.28
A2	0.10	21.41	2.14
A3	0.10	28.83	2.88
A4	0.09	33.31	2.90

AVERAGE VELOCITY
25.87

*** Actual data was not taken for this point. Values at the depth of Y90 were determined from the graphs.

Table A3: Velocity data, Station 3, 3.3 cfs/ft

POINT DEPTH CALCULATIONS												
POINT GAGE READING (ft.)	DEPTH (ft.)	VOLTAGE (volts)	AVERAGE VOLTAGE (volts)	AVERAGE PRESSURE HEAD (ft)	PRESSURE CORRECTED FOR ZERO (ft)	AIR CONCENTRATION	CORRECTION COEFFICIENT	VELOCITY (fps)	DIMENSIONLESS DEPTH	DIMENSIONLESS VELOCITY	STANDARD DEVIATION	NOTES
6.731	0.000					0.000		0.000	0.00	0.00		
6.701	0.030	1.189 1.274	1.232	3.969	3.549	0.250	10.093	19.014	0.09	0.56	0.119 0.100	
6.601	0.130	1.546 1.550	1.548	5.484	5.064	0.350	11.115	25.013	0.41	0.74	0.129 0.118	
6.501	0.230	1.129 1.134	1.131	3.488	3.068	0.650	19.334	33.866	0.73	1.00	0.131 0.127	
***	0.316					0.900	NOT VALID	33.866	1.00	1.00		
6.401	0.330	0.590 0.540	0.565	0.779	0.359	0.930	NOT VALID	33.866			0.058 0.059	Mostly air
6.301	0.430	0.565 0.517	0.541	0.662	0.242	0.960	NOT VALID	33.866			0.016 0.030	
AIR		0.491 0.489	0.490	0.420							0.005 0.001	Zero with probe in air

AVERAGE VELOCITY			
AREA	DEPTH (ft.)	AVERAGE VELOCITY (fps)	UNIT FLOW RATE (sq.ft./sec)
A1	0.03	9.51	0.29
A2	0.10	22.01	2.20
A3	0.10	29.44	2.94
A4	0.10	33.87	3.39

AVERAGE VELOCITY (TO DEPTH OF Y90 ONLY)			
AREA	DEPTH (ft.)	AVERAGE VELOCITY (fps)	UNIT FLOW RATE (sq.ft./sec)
A1	0.03	9.51	0.29
A2	0.10	22.01	2.20
A3	0.10	29.44	2.94
A4	0.09	33.87	2.91

AVERAGE VELOCITY
26.40

*** Actual data were not taken for this point. Values at the depth of Y90 were determined from the graphs.

Table A4: Velocity data, Station 2, 9.7 cfs/ft

POINT DEPTH CALCULATIONS												
POINT GAGE READING (ft.)	DEPTH (ft.)	VOLTAGE (volts)	AVERAGE VOLTAGE (volts)	AVERAGE PRESSURE HEAD (ft)	PRESSURE CORRECTED FOR ZERO (ft)	AIR CONCENTRATION	CORRECTION COEFFICIENT	VELOCITY (fps)	DIMENSIONLESS DEPTH	DIMENSIONLESS VELOCITY	STANDARD DEVIATION	NOTES
6.685	0.000					0.000		0.000	0.000	0.000		
6.655	0.030	1.508 1.492	1.500	5.252	5.148	0.050	8.722	19.791	0.045	0.517	0.108 0.102	
6.555	0.130	1.942 1.954	1.948	7.396	7.291	0.090	8.948	24.161	0.195	0.631	0.148 0.158	
6.455	0.230	2.243 2.226	2.235	8.769	8.665	0.150	9.325	27.450	0.344	0.717	0.189 0.197	
6.355	0.330	2.445 2.396	2.420	9.657	9.553	0.240	10.007	30.928	0.494	0.808	0.191 0.198	
6.255	0.430	2.029 2.028	2.029	7.783	7.679	0.420	12.070	33.447	0.644	0.874	0.197 0.188	
6.155	0.530	1.127 1.128	1.128	3.472	3.367	0.670	20.852	38.263	0.793	1.000	0.136 0.135	Mostly air
6.055	0.630	0.650 0.662	0.656	1.213	1.108	0.870	NOT VALID	38.263	0.943	1.000	0.067 0.066	
***	0.668					0.900	NOT VALID	38.263	1.000	1.000		
AIR		0.423 0.425	0.424	0.104	0.000						0.002 0.004	Zero with probe in air

AVERAGE VELOCITY			
AREA	DEPTH (ft.)	AVERAGE VELOCITY (fps)	UNIT FLOW RATE (sq.ft./sec.)
A1	0.03	9.90	0.30
A2	0.10	21.98	2.20
A3	0.10	25.81	2.58
A4	0.10	29.19	2.92
A5	0.10	32.19	3.22
A6	0.10	35.86	3.59
A7	0.10	38.26	3.83

AVERAGE VELOCITY (TO DEPTH OF Y90)			
AREA	DEPTH (ft.)	AVERAGE VELOCITY (fps)	UNIT FLOW RATE (sq.ft./sec.)
A1	0.03	19.79	0.30
A2	0.10	21.98	2.20
A3	0.10	25.81	2.58
A4	0.10	29.19	2.92
A5	0.10	32.19	3.22
A6	0.10	35.86	3.59
A7	0.10	38.26	3.83
A8	0.04	38.26	1.45

AVERAGE VELOCITY
30.06

*** Actual data was not taken for this point. Values at the depth of Y90 were determined from the graphs.

Table A5: Velocity data, Station 3, 9.7 cfs/ft

POINT DEPTH CALCULATIONS												
POINT GAGE READING (ft.)	DEPTH (ft.)	VOLTAGE (volts)	AVERAGE VOLTAGE (volts)	AVERAGE PRESSURE HEAD (ft)	PRESSURE CORRECTED FOR ZERO (ft)	AIR CONCENTRATION	CORRECTION COEFFICIENT	VELOCITY (fps)	DIMENSIONLESS DEPTH	DIMENSIONLESS VELOCITY	STANDARD DEVIATION	NOTES
6.730	0.000					0.000		0.000	0.00	0.00		
6.700	0.030	1.435 1.440	1.437	4.954	5.164	0.080	8.889	20.200	0.05	0.48	0.082 0.080	
6.600	0.130	1.848 1.842	1.845	6.904	7.114	0.130	9.194	24.521	0.20	0.58	0.137 0.135	
6.505	0.225	2.240 2.278	2.259	8.885	9.095	0.170	9.464	28.540	0.34	0.68	0.169 0.140	
6.400	0.330	2.507 2.457	2.482	9.954	10.164	0.240	10.007	31.902	0.50	0.76	0.169 0.172	
6.300	0.430	2.371 2.371	2.371	9.422	9.632	0.390	11.630	36.092	0.65	0.86	0.153 0.199	
6.200	0.530	1.442 1.378	1.410	4.824	5.034	0.640	18.691	41.936	0.80	1.00	0.141 0.149	Mostly air
6.100	0.630	0.736 0.717	0.726	1.551	1.761	0.860	NOT VALID	41.936	0.95	1.00	0.077 0.075	
***	0.660					0.900		41.936	1.00	1.00		
AIR		0.357 0.360	0.358	-0.210	0.000						0.004	Zero with probe in air

AVERAGE VELOCITY			
AREA	DEPTH (ft.)	AVERAGE VELOCITY (fps)	UNIT FLOW RATE (sq.ft./sec.)
A1	0.03	20.20	0.30
A2	0.10	22.36	2.24
A3	0.10	26.53	2.52
A4	0.10	30.22	3.17
A5	0.10	34.00	3.40
A6	0.10	39.01	3.90
A7	0.10	41.94	4.19

AVERAGE VELOCITY (TO DEPTH OF Y90)			
AREA	DEPTH (ft.)	AVERAGE VELOCITY (fps)	UNIT FLOW RATE (sq.ft./sec.)
A1	0.03	10.10	0.30
A2	0.10	22.36	2.24
A3	0.10	26.53	2.52
A4	0.10	30.22	3.17
A5	0.10	34.00	3.40
A6	0.10	39.01	3.90
A7	0.10	41.94	4.19
A8	0.03	41.94	1.26

AVERAGE VELOCITY
31.80

*** Actual data was not taken for this point. Values at the depth of Y90 were determined from the graphs.

Table A6: Velocity data, Station 2, 18 cfs/ft

POINT DEPTH CALCULATIONS												
POINT GAGE READING (ft.)	DEPTH (ft.)	VOLTAGE (volts)	AVERAGE VOLTAGE (volts)	AVERAGE PRESSURE HEAD (ft)	PRESSURE CORRECTED FOR ZERO (ft)	AIR CONCENTRATION	CORRECTION COEFFICIENT	VELOCITY (fps)	DIMENSIONLESS DEPTH	DIMENSIONLESS VELOCITY	STANDARD DEVIATION	NOTES
6.69	0.00					0.00		0.00	0.00	0.00		
6.66	0.03	1.63 1.57	1.60	5.73	5.48	0.02	8.57	20.05	0.04	0.41	0.074	
6.57	0.12	2.02 2.09	2.05	7.90	7.65	0.03	8.62	23.83	0.15	0.50	0.139 0.151	
6.47	0.22	2.50 2.48	2.49	9.99	9.74	0.06	8.78	27.39	0.28	0.57	0.174 0.185	
6.37	0.32	3.02 2.96	2.99	12.38	12.13	0.13	9.19	32.02	0.40	0.67	0.242 0.243	
6.27	0.42	3.31 3.34	3.32	13.98	13.73	0.28	10.37	38.42	0.53	0.80	0.250 0.296	
6.17	0.52	3.34 3.44	3.39	14.29	14.04	0.46	12.75	47.77	0.65	1.00	0.259 0.281	
6.07	0.62	2.56 2.67	2.62	10.60	10.35	0.68	NOT VALID	47.77	0.78	1.00	0.222 0.222	Foam
5.97	0.72	1.32 1.42	1.37	4.63	4.38	0.83	NOT VALID	47.77	0.90	1.00	0.166 0.194	Above foam
***	0.80					0.90	NOT VALID	47.77	1.00	1.00		
5.87	0.82	0.82 0.80	0.81	1.95	1.70	0.93	NOT VALID	47.77			0.103 0.111	Top only spray
AIR		0.45	0.45	0.25	0.00						0.091	Velocity = 0 fps, probe in 100% air

AVERAGE VELOCITY			
AREA	DEPTH (ft.)	AVERAGE VELOCITY (fps)	UNIT FLOW RATE (sq.ft./sec.)
A1	0.03	10.03	0.30
A2	0.09	21.94	1.97
A3	0.10	25.61	2.56
A4	0.10	29.71	2.97
A5	0.10	35.22	3.52
A6	0.10	43.10	4.31
A7	0.10	47.77	4.78
A8	0.10	47.77	4.78
A9	0.10	47.77	4.78

AVERAGE VELOCITY (TO DEPTH OF Y90)			
AREA	DEPTH (ft.)	AVERAGE VELOCITY (fps)	UNIT FLOW RATE (sq.ft./sec.)
A1	0.03	9.91	0.65
A2	0.09	21.82	2.31
A3	0.10	25.61	2.97
A4	0.10	29.71	3.52
A5	0.10	35.22	4.31
A6	0.10	43.10	4.78
A7	0.10	47.77	4.78
A8	0.10	47.77	4.78
A9	0.08	47.77	1.91

AVERAGE VELOCITY
37.51

*** Actual data was not taken for this point. Values at the depth of Y90 were determined from the graphs.

Table A7: Velocity data, Station 3, 18 cfs/ft

POINT DEPTH CALCULATIONS												
POINT GAGE READING (ft.)	DEPTH (ft.)	VOLTAGE (volts)	AVERAGE VOLTAGE (volts)	AVERAGE PRESSURE HEAD (ft)	PRESSURE CORRECTED FOR ZERO (ft)	AIR CONCENTRATION	CORRECTION COEFFICIENT	VELOCITY (fps)	DIMENSIONLESS DEPTH	DIMENSIONLESS VELOCITY	STANDARD DEVIATION	NOTES
6.73	0.00					0.00		0.00	0.00	0.00		
6.70	0.03	0.36 0.36	0.36	-0.11	0.36	0.04	8.67	5.32	0.03	0.11	0.024 0.021	Zero at step
6.68	0.05	0.48 0.48	0.48	0.36	0.87	0.04	8.68	8.12	0.05	0.17	0.064 0.044	
6.60	0.13	1.90 1.88	1.89	7.13	7.62	0.06	8.75	24.17	0.14	0.49	0.241 0.273	
6.50	0.23	2.31 2.33	2.32	9.17	9.66	0.09	8.95	27.81	0.24	0.57	0.274 0.311	
6.40	0.33	2.78 2.73	2.75	11.25	11.74	0.14	9.25	31.68	0.34	0.65	0.397 0.340	
6.30	0.43	3.21 3.17	3.19	13.33	13.82	0.19	9.58	35.61	0.45	0.73	0.425 0.401	
6.20	0.53	3.40 3.37	3.38	14.27	14.76	0.26	10.33	39.69	0.55	0.81	0.428 0.417	
6.10	0.63	3.22 3.22	3.22	13.48	13.97	0.41	11.98	44.77	0.66	0.91	0.411 0.455	Foam
6.00	0.73	2.24 2.20	2.22	8.60	9.18	0.59	16.16	48.97	0.76	1.00	0.395 0.458	Foam/Air
5.90	0.83	1.14 1.17	1.16	3.61	4.10	0.77	NOT VALID	48.97	0.86	1.00	0.289 0.347	Air?
***	0.96					0.90	NOT VALID	48.97	1.00	1.00		
AIR		0.32 0.28	0.30	-0.49	0.00							Outside flume

AVERAGE VELOCITY			
AREA	DEPTH (ft.)	AVERAGE VELOCITY (fps)	UNIT FLOW RATE (sq.ft./sec.)
A1	0.03	5.32	0.08
A2	0.02	6.72	0.13
A3	0.08	16.14	1.29
A4	0.10	25.99	2.60
A5	0.10	29.75	2.97
A6	0.10	33.64	3.36
A7	0.10	37.65	3.76
A8	0.10	42.23	4.22
A9	0.10	46.87	4.69
A10	0.10	48.97	4.90

AVERAGE VELOCITY (TO DEPTH OF Y90)			
AREA	DEPTH (ft.)	AVERAGE VELOCITY (fps)	UNIT FLOW RATE (sq.ft./sec.)
A1	0.03	5.32	0.08
A2	0.05	6.72	0.13
A3	0.13	16.14	1.29
A4	0.23	25.99	2.60
A5	0.33	29.75	2.97
A6	0.43	33.64	3.36
A7	0.53	37.65	3.76
A8	0.63	42.23	4.22
A9	0.73	46.87	4.69
A10	0.83	48.97	4.90
A11	0.96	48.97	6.37

AVERAGE VELOCITY
35.81

*** Actual data was not taken for this point. Values at the depth of Y90 were determined from the graphs.

Table A8: Velocity data, Station 2, 28.2 cfs/ft

POINT DEPTH CALCULATIONS											
POINT GAGE READING (ft.)	DEPTH (ft.)	VOLTAGE (volts)	AVERAGE VOLTAGE (volts)	AVERAGE PRESSURE HEAD (ft)	PRESSURE CORRECTED FOR ZERO (ft)	AIR CONCENTRATION	CORRECTION COEFFICIENT	VELOCITY (fps)	DIMENSIONLESS DEPTH	DIMENSIONLESS VELOCITY	STANDARD DEVIATION
6.79	0.00					0.00		0.00	0.00	0.00	
6.76	0.03	-0.68	-0.70	-5.26	5.88	0.04	8.67	21.02	0.03	0.75	0.15
		-0.72									0.16
6.70	0.09	-0.81	-0.82	-5.86	6.48	0.04	8.67	22.06	0.08	0.79	0.17
		-0.83									0.14
6.60	0.19	-1.37	-1.39	-8.56	9.18	0.04	8.67	26.27	0.17	0.94	0.27
		-1.40									0.22
6.50	0.29	-1.79	-1.89	-10.95	11.57	0.04	8.67	29.49	0.25	1.06	0.33
		-1.98									0.30
6.40	0.39	-2.15	-2.23	-12.61	13.23	0.04	8.67	31.53	0.34	1.13	0.39
		-2.32									0.38
6.30	0.49	-2.70	-2.72	-14.94	15.56	0.06	8.78	34.62	0.43	1.24	0.38
		-2.73									0.38
6.20	0.59	-3.01	-2.98	-16.18	16.81	0.08	8.89	36.44	0.52	1.31	0.29
		-2.94									0.34
6.10	0.69	-3.09	-3.10	-16.76	17.39	0.18	9.54	39.76	0.61	1.42	0.25
		-3.11									0.27
6.00	0.79	-2.87	-2.88	-15.72	16.34	0.34	11.00	44.46	0.70	1.59	0.36
		-2.90									0.28
5.90	0.89	-1.72	-1.73	-10.19	10.81	0.42	12.07	39.68	0.79	1.42	0.34
		-1.73									0.31
5.80	0.99	-0.27	-0.26	-3.18	3.81	0.53	14.30	27.91	0.87	1.00	0.18
		-0.26									0.19
***	1.13					0.90	NOT VALID	27.91	1.00	1.00	
5.70	OUT OF WATER										

AVERAGE VELOCITY			
AREA	DEPTH OF AREA (ft)	AVERAGE VELOCITY (fps)	UNIT FLOW RATE (sq.ft./sec.)
A1	0.03	10.51	0.32
A2	0.06	21.54	1.25
A3	0.10	24.17	2.42
A4	0.10	27.88	2.79
A5	0.10	30.51	3.05
A6	0.10	33.08	3.31
A7	0.10	35.53	3.55
A8	0.10	38.10	3.81
A9	0.10	42.11	4.21
A10	0.10	42.07	4.21
A11	0.10	33.80	3.38

AVERAGE VELOCITY (TO DEPTH OF Y90)			
AREA	DEPTH OF AREA (ft)	AVERAGE VELOCITY (fps)	UNIT FLOW RATE (sq.ft./sec.)
A1	0.03	10.51	0.32
A2	0.06	21.54	1.25
A3	0.10	24.17	2.42
A4	0.10	27.88	2.79
A5	0.10	30.51	3.05
A6	0.10	33.08	3.31
A7	0.10	35.53	3.55
A8	0.10	38.10	3.81
A9	0.10	42.11	4.21
A10	0.10	42.07	4.21
A11	0.10	33.80	3.38
A12	0.14	27.91	3.99

AVERAGE VELOCITY
32.08

*** Actual data was not taken for this point. Values at the depth of Y90 were determined from the graphs.

Table A9: Velocity data, Station 3, 28.2 cfs/ft

POINT DEPTH CALCULATIONS											
POINT GAGE READING (ft.)	DEPTH (ft.)	VOLTAGE (volts)	AVERAGE VOLTAGE (volts)	AVERAGE PRESSURE HEAD (ft)	PRESSURE CORRECTED FOR ZERO (ft)	AIR CONCENTRATION	CORRECTION COEFFICIENT	VELOCITY (fps)	DIMENSIONLESS DEPTH	DIMENSIONLESS VELOCITY	STANDARD DEVIATION
6.81	0.00					0.00		0.00	0.00	0.00	
6.78	0.03	-0.93 -0.92	-0.93	-6.36	7.00	0.04	8.67	22.94	0.02	0.64	0.09 0.10
6.70	0.11	-1.19 -1.21	-1.20	-7.66	8.30	0.04	8.67	24.97	0.09	0.70	0.15 0.15
6.60	0.21	-1.79 -1.73	-1.76	-10.37	11.01	0.06	8.78	29.12	0.17	0.81	0.21 0.21
6.50	0.31	-2.26 -2.30	-2.28	-12.83	13.47	0.08	8.89	32.63	0.25	0.91	0.27 0.23
6.40	0.41	-2.59 -2.68	-2.63	-14.52	15.16	0.12	9.13	35.55	0.33	0.99	0.30 0.28
6.30	0.51	-3.01 -3.17	-3.09	-16.72	17.36	0.14	9.26	38.58	0.41	1.08	0.23 0.17
6.20	0.61	-3.27 -3.27	-3.27	-17.59	18.23	0.22	9.84	42.02	0.49	1.17	0.14 0.15
6.10	0.71	-3.27 -3.28	-3.28	-17.60	18.24	0.31	10.67	45.56	0.57	1.27	0.17 0.17
6.00	0.81	-3.23 -3.25	-3.24	-17.42	18.06	0.37	11.36	48.28	0.65	1.35	0.18 0.20
5.90	0.91	-2.34 -2.13	-2.24	-12.82	13.26	0.44	12.39	45.14	0.73	1.26	0.21 0.23
5.80	1.01	-0.93 -0.81	-0.87	-6.09	6.73	0.51	13.80	35.79	0.80	1.00	0.16 0.15
***	1.26					0.90		35.79	1.00	1.00	
5.70	OUT OF WATER										

AVERAGE VELOCITY			
AREA	DEPTH OF AREA (ft)	AVERAGE VELOCITY (fps)	UNIT FLOW RATE (sq.ft./sec.)
A1	0.03	11.47	0.34
A2	0.08	23.95	2.01
A3	0.10	27.04	2.70
A4	0.10	30.87	3.09
A5	0.10	34.09	3.41
A6	0.10	37.06	3.71
A7	0.10	40.30	4.03
A8	0.10	43.79	4.38
A9	0.10	46.92	4.69
A10	0.10	46.71	4.67
A11	0.10	40.46	4.05

AVERAGE VELOCITY (TO DEPTH OF Y90)			
AREA	DEPTH OF AREA (ft)	AVERAGE VELOCITY (fps)	UNIT FLOW RATE (sq.ft./sec.)
A1	0.03	22.94	0.34
A2	0.08	23.95	2.01
A3	0.10	27.04	2.70
A4	0.10	30.87	3.09
A5	0.10	34.09	3.41
A6	0.10	37.06	3.71
A7	0.10	40.30	4.03
A8	0.10	43.79	4.38
A9	0.10	46.92	4.69
A10	0.10	46.71	4.67
A11	0.10	40.46	4.05
A12	0.25	35.79	8.80

AVERAGE VELOCITY
36.42

*** Actual data was not taken for this point. Values at the depth of Y90 were determined from the graphs.

Table A10: Velocity data, Station 4, 28.2 cfs/ft

POINT DEPTH CALCULATIONS

POINT GAGE READING (ft.)	DEPTH (ft.)	VOLTAGE (volts)	AVERAGE VOLTAGE (volts)	AVERAGE PRESSURE HEAD (ft)	PRESSURE CORRECTED FOR ZERO (ft)	AIR CONCENTRATION	CORRECTION COEFFICIENT	VELOCITY (fps)	DIMENSIONLESS DEPTH	DIMENSIONLESS VELOCITY	STANDARD DEVIATION
6.80	0.00					0.00		0.00	0.00	0.00	
6.77	0.03	-0.64 -0.64 -0.61	-0.63	-4.94	5.41	0.04	8.67	20.16	0.02	0.59	0.10 0.10 0.10
6.70	0.10	-1.03 -1.09 -1.14	-1.09	-7.13	7.60	0.05	8.72	24.04	0.08	0.71	0.17 0.15 0.15
6.60	0.20	-1.83 -1.79 -1.83	-1.82	-10.63	11.09	0.06	8.78	29.23	0.15	0.86	0.21 0.24 0.22
6.50	0.30	-2.44 -2.55 -2.45	-2.48	-13.79	14.26	0.10	9.01	34.01	0.23	1.00	0.23 0.24 0.29
6.40	0.40	-2.90 -2.85 -2.98	-2.91	-15.85	16.32	0.14	9.26	37.40	0.31	1.10	0.22 0.25 0.19
6.30	0.50	-3.20 -3.18 -3.18	-3.19	-17.18	17.64	0.20	9.68	40.68	0.39	1.19	0.07 0.11 0.14
6.20	0.60	-3.25 -3.31 -3.24	-3.27	-17.56	18.03	0.25	10.09	42.85	0.47	1.26	0.08 0.04 0.09
6.10	0.70	-3.31 -3.33 -3.35	-3.33	-17.66	18.33	0.33	10.68	46.59	0.55	1.37	0.09 0.08 0.07
6.00	0.80	-3.22 -3.18 -3.20	-3.20	-17.24	17.71	0.39	11.63	48.94	0.62	1.44	0.14 0.15 0.15
5.90	0.90	-3.19 -2.09 -2.05	-2.44	-13.62	14.09	0.44	12.39	46.52	0.70	1.36	0.21 0.25 0.23
5.80	1.00	-0.80 -0.73 -0.80	-0.78	-5.64	6.11	0.51	13.80	34.09	0.78	1.00	0.18 0.17 0.16
***	1.28					0.90	NOT VALID	34.09	1.00	1.00	
5.70	OUT OF WATER										

AVERAGE VELOCITY

AREA	DEPTH OF AREA (ft)	AVERAGE VELOCITY (fps)	UNIT FLOW RATE (sq ft /sec)
A1	0.03	10.08	0.30
A2	0.07	22.10	1.50
A3	0.10	26.64	2.66
A4	0.10	31.62	3.16
A5	0.10	35.71	3.57
A6	0.10	39.04	3.90
A7	0.10	41.76	4.18
A8	0.10	44.72	4.47
A9	0.10	47.77	4.78
A10	0.10	47.73	4.77
A11	0.10	40.31	4.03

AVERAGE VELOCITY (TO DEPTH OF Y90)

AREA	DEPTH OF AREA (ft)	AVERAGE VELOCITY (fps)	UNIT FLOW RATE (sq ft /sec)
A1	0.03	10.08	0.30
A2	0.07	22.10	1.50
A3	0.10	26.64	2.66
A4	0.10	31.62	3.16
A5	0.10	35.71	3.57
A6	0.10	39.04	3.90
A7	0.10	41.76	4.18
A8	0.10	44.72	4.47
A9	0.10	47.77	4.78
A10	0.10	47.73	4.77
A11	0.10	40.31	4.03
A12	0.28	34.09	9.55

AVERAGE VELOCITY
36.68

*** Actual data was not taken for this point. Values at the depth of Y90 were determined from the graphs.

Table A11: Velocity data, Station 2, 32.2 cfs/ft

POINT DEPTH CALCULATIONS											
POINT GAGE READING (ft.)	DEPTH (ft.)	VOLTAGE (volts)	AVERAGE VOLTAGE (volts)	AVERAGE PRESSURE HEAD (ft)	PRESSURE CORRECTED FOR ZERO (ft)	AIR CONCENTRATION	CORRECTION COEFFICIENT	VELOCITY (fps)	DIMENSIONLESS DEPTH	DIMENSIONLESS VELOCITY	STANDARD DEVIATION
6.79	0.00					0.00		0.00	0.00	0.00	
6.76	0.03	-0.69 -0.64	-0.66	-5.11	5.91	0.00	8.47	20.58	0.02	0.80	0.12 0.12
6.70	0.09	-0.81 -0.83	-0.82	-5.86	6.67	0.00	8.47	21.86	0.07	0.85	0.14 0.14
6.60	0.19	-1.37 -1.32	-1.34	-8.35	9.15	0.00	8.47	25.61	0.15	1.00	0.20 0.27
6.50	0.29	-1.80 -1.81	-1.80	-10.56	11.36	0.00	8.47	28.54	0.24	1.11	0.32 0.29
6.40	0.39	-2.31 -2.40	-2.36	-13.21	14.01	0.00	8.47	31.69	0.32	1.24	0.41 0.41
6.30	0.49	-2.68 -2.51	-2.59	-14.34	15.15	0.01	8.52	33.14	0.40	1.29	0.42 0.38
6.20	0.59	-2.87 -2.75	-2.81	-15.37	16.17	0.03	8.62	34.65	0.48	1.35	0.33 0.35
6.10	0.69	-3.02 -3.09	-3.06	-16.56	17.36	0.10	9.01	37.53	0.56	1.47	0.31 0.18
6.00	0.79	-2.87 -2.89	-2.88	-15.70	16.50	0.24	10.01	40.65	0.64	1.59	0.28 0.30
5.90	0.89	-2.12 -1.94	-2.03	-11.65	12.45	0.39	11.63	41.04	0.73	1.60	0.30 0.28
5.80	0.99	-0.25 -0.20	-0.22	-2.99	3.80	0.48	13.14	25.60	0.81	1.00	0.20 0.40
***	1.23					0.90	NOT VALID	25.60	1.00	1.00	

AVERAGE VELOCITY			
AREA	DEPTH OF AREA (ft)	AVERAGE VELOCITY (fps)	UNIT FLOW RATE (sq.ft./sec.)
A1	0.03	20.58	0.31
A2	0.06	21.22	1.25
A3	0.10	23.73	2.37
A4	0.10	27.07	2.71
A5	0.10	30.11	3.01
A6	0.10	32.41	3.24
A7	0.10	33.89	3.39
A8	0.10	36.09	3.61
A9	0.10	39.09	3.91
A10	0.10	40.85	4.08
A11	0.10	33.32	3.33

AVERAGE VELOCITY (TO DEPTH OF Y90)			
AREA	DEPTH OF AREA (ft)	AVERAGE VELOCITY (fps)	UNIT FLOW RATE (sq.ft./sec.)
A1	0.03	10.29	0.31
A2	0.06	21.22	1.25
A3	0.10	23.73	2.37
A4	0.10	27.07	2.71
A5	0.10	30.11	3.01
A6	0.10	32.41	3.24
A7	0.10	33.89	3.39
A8	0.10	36.09	3.61
A9	0.10	39.09	3.91
A10	0.10	40.85	4.08
A11	0.10	33.32	3.33
A12	0.24	25.60	6.04

AVERAGE VELOCITY
30.42

*** Actual data was not taken for this point. Values at the depth of Y90 were determined from the graphs.

Table A12: Velocity data, Station 3, 32.2 cfs/ft

POINT DEPTH CALCULATIONS											
POINT GAGE READING (ft.)	DEPTH (ft.)	VOLTAGE (volts)	AVERAGE VOLTAGE (volts)	AVERAGE PRESSURE HEAD (ft)	PRESSURE CORRECTED FOR ZERO (ft)	AIR CONCENTRATION	CORRECTION COEFFICIENT	VELOCITY (fps)	DIMENSIONLESS DEPTH	DIMENSIONLESS VELOCITY	STANDARD DEVIATION
6.81	0.00					0.00		0.00	0.00	0.00	
6.78	0.03	-0.88 -0.87	-0.87	-8.10	6.68	0.01	8.52	22.01	0.02	0.56	0.15 0.13
6.70	0.11	-1.12 -1.13	-1.12	-7.30	7.89	0.02	8.55	24.01	0.09	0.61	0.19 0.20
6.60	0.21	-1.69 -1.76	-1.73	-10.19	10.77	0.03	8.60	28.21	0.16	0.71	0.26 0.27
6.50	0.31	-2.21 -2.14	-2.18	-12.35	12.93	0.05	8.72	31.35	0.24	0.79	0.30 0.25
6.40	0.41	-2.74 -2.54	-2.64	-14.56	15.14	0.09	8.92	34.71	0.32	0.88	0.29 0.34
6.30	0.51	-2.97 -2.95	-2.96	-16.08	16.67	0.11	9.10	37.14	0.40	0.94	0.25 0.28
6.20	0.61	-3.16 -3.20	-3.18	-17.16	17.74	0.20	9.70	40.86	0.47	1.03	0.26 0.18
6.10	0.71	-3.30 -3.29	-3.29	-17.68	18.27	0.28	10.35	44.24	0.55	1.12	0.17 0.17
6.00	0.81	-3.14 -3.21	-3.17	-17.12	17.70	0.36	11.21	47.16	0.63	1.19	0.25 0.21
5.90	0.91	-2.53 -2.49	-2.51	-13.93	14.51	0.42	12.01	45.75	0.71	1.16	0.29 0.27
5.80	1.01	-1.09 -1.16	-1.13	-7.32	7.90	0.49	13.36	37.53	0.78	0.95	0.21 0.26
5.70	1.11	-0.23 -0.98	-0.60	-4.81	5.39	0.61	17.05	39.57	0.86	1.00	0.14 1.39
***	1.29					0.90	NOT VALID	39.57	1.00	1.00	

AVERAGE VELOCITY			
AREA	DEPTH OF AREA (ft)	AVERAGE VELOCITY (fps)	UNIT FLOW RATE (sq.ft./sec.)
A1	0.03	22.01	0.33
A2	0.08	23.01	1.86
A3	0.10	26.11	2.61
A4	0.10	29.78	2.98
A5	0.10	33.03	3.30
A6	0.10	35.93	3.59
A7	0.10	39.00	3.90
A8	0.10	42.55	4.26
A9	0.10	45.70	4.57
A10	0.10	46.45	4.65
A11	0.10	41.64	4.16
A12	0.10	38.55	3.86

AVERAGE VELOCITY (TO DEPTH OF Y90)			
AREA	DEPTH OF AREA (ft)	AVERAGE VELOCITY (fps)	UNIT FLOW RATE (sq.ft./sec.)
A1	0.03	11.00	0.33
A2	0.08	23.01	1.86
A3	0.10	26.11	2.61
A4	0.10	29.78	2.98
A5	0.10	33.03	3.30
A6	0.10	35.93	3.59
A7	0.10	39.00	3.90
A8	0.10	42.55	4.26
A9	0.10	45.70	4.57
A10	0.10	46.45	4.65
A11	0.10	41.64	4.16
A12	0.10	38.55	3.86
A13	0.18	39.57	7.16

AVERAGE VELOCITY
36.56

*** Actual data was not taken for this point. Values at the depth of Y90 were determined from the graphs.

Table A13: Velocity data, Station 4, 32.2 cfs/ft

POINT DEPTH CALCULATIONS										
POINT GAGE READING (ft.)	DEPTH (ft.)	VOLTAGE (volts)	AVERAGE PRESSURE HEAD (ft)	PRESSURE CORRECTED FOR ZERO (ft)	AIR CONCENTRATION	CORRECTION COEFFICIENT	VELOCITY (fps)	DIMENSIONLESS DEPTH	DIMENSIONLESS VELOCITY	STANDARD DEVIATION (fps)
6.79	0.00				0.00		0.00	0.00	0.00	
6.76	0.03	0.67	1.28	0.35	0.02	8.57	5.06	0.02	0.12	0.15
6.70	0.09	0.75	1.66	0.73	0.04	8.67	7.39	0.07	0.17	0.19
6.60	0.19	2.17	8.48	7.54	0.04	8.67	23.80	0.14	0.56	0.26
6.50	0.29	2.86	11.75	10.81	0.07	8.83	29.04	0.22	0.68	0.30
6.40	0.39	3.52	14.90	13.96	0.11	9.07	33.88	0.29	0.80	0.29
6.30	0.49	3.95	16.97	16.04	0.17	9.46	37.90	0.37	0.89	0.25
6.20	0.59	4.37	18.97	18.04	0.24	10.01	42.50	0.44	1.00	0.26
6.10	0.69	4.64	20.29	19.35	0.32	10.77	47.40	0.52	1.11	0.17
6.00	0.79	4.66	20.38	19.44	0.37	11.36	50.10	0.59	1.18	0.25
5.90	0.89	4.47	19.47	18.54	0.42	12.07	51.97	0.66	1.22	0.29
5.80	0.99	3.59	15.24	14.30	0.48	13.14	49.69	0.74	1.17	0.21
5.70	1.09	2.04	7.82	6.88	0.59	16.24	42.61	0.81	1.00	0.14
***	1.34				0.90	NOT VALID	42.61	1.00	1.00	

AVERAGE VELOCITY			
AREA	DEPTH OF AREA (ft)	AVERAGE VELOCITY (fps)	UNIT FLOW RATE (sq.ft./sec.)
A1	0.03	2.53	0.08
A2	0.06	6.22	0.39
A3	0.10	15.59	1.56
A4	0.10	26.42	2.64
A5	0.10	31.46	3.15
A6	0.10	35.89	3.59
A7	0.10	40.20	4.02
A8	0.10	44.95	4.49
A9	0.10	48.75	4.87
A10	0.10	51.04	5.10
A11	0.10	50.83	5.08
A12	0.10	46.15	4.61

AVERAGE VELOCTIY (TO DEPTH OF Y90)			
AREA	DEPTH OF AREA (ft)	AVERAGE VELOCITY (fps)	UNIT FLOW RATE (sq.ft./sec.)
A1	0.03	2.53	0.08
A2	0.06	6.22	0.39
A3	0.10	15.59	1.56
A4	0.10	26.42	2.64
A5	0.10	31.46	3.15
A6	0.10	35.89	3.59
A7	0.10	40.20	4.02
A8	0.10	44.95	4.49
A9	0.10	48.75	4.87
A10	0.10	51.04	5.10
A11	0.10	50.83	5.08
A12	0.10	46.15	4.61
A13	0.25	42.61	10.65

AVERAGE VELOCITY
37.44

*** Actual data was not taken for this point. Values at the depth of Y90 were determined from the graphs.

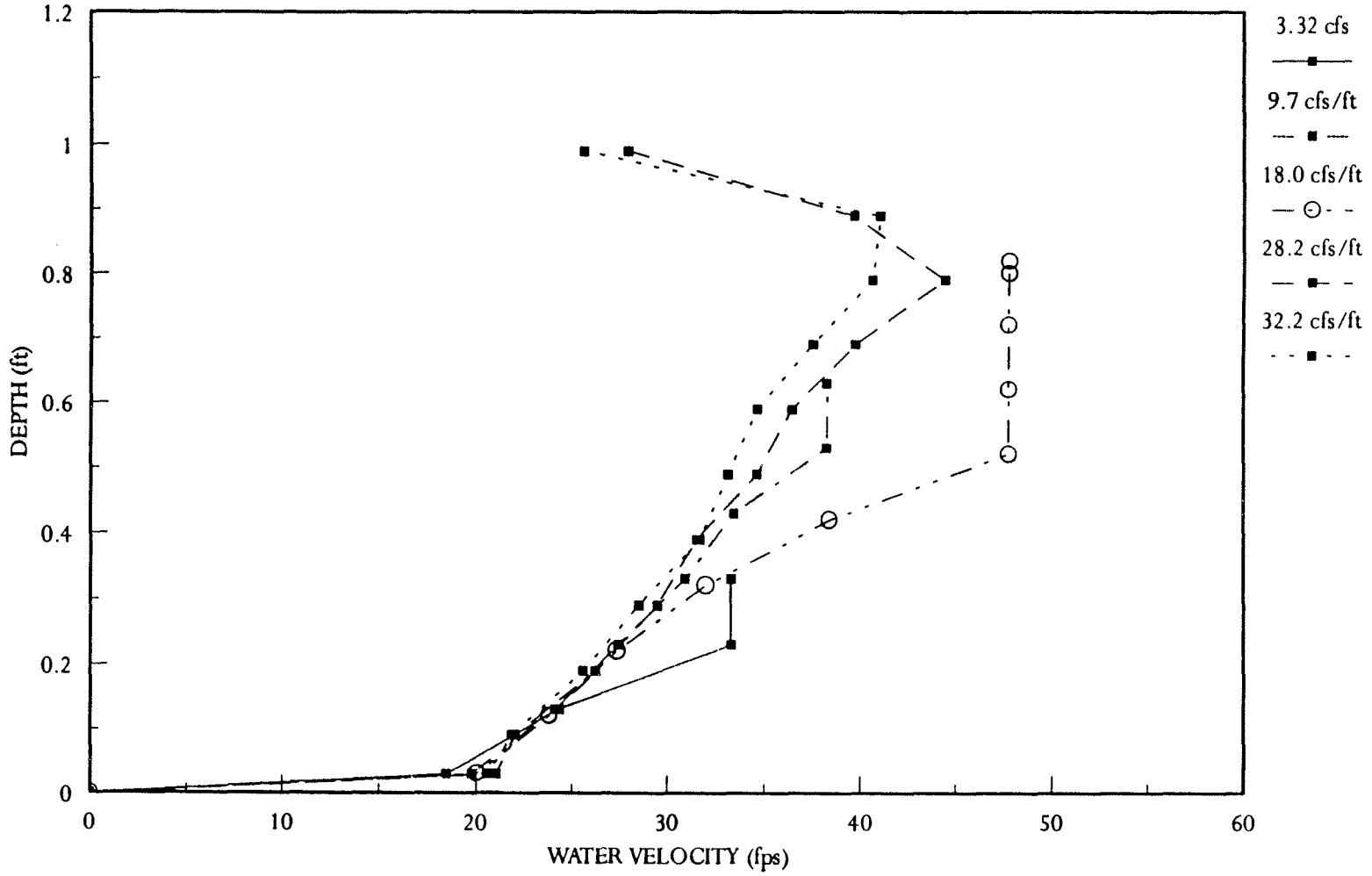

Figure A1: Velocity profiles at Station 2, all flow rates

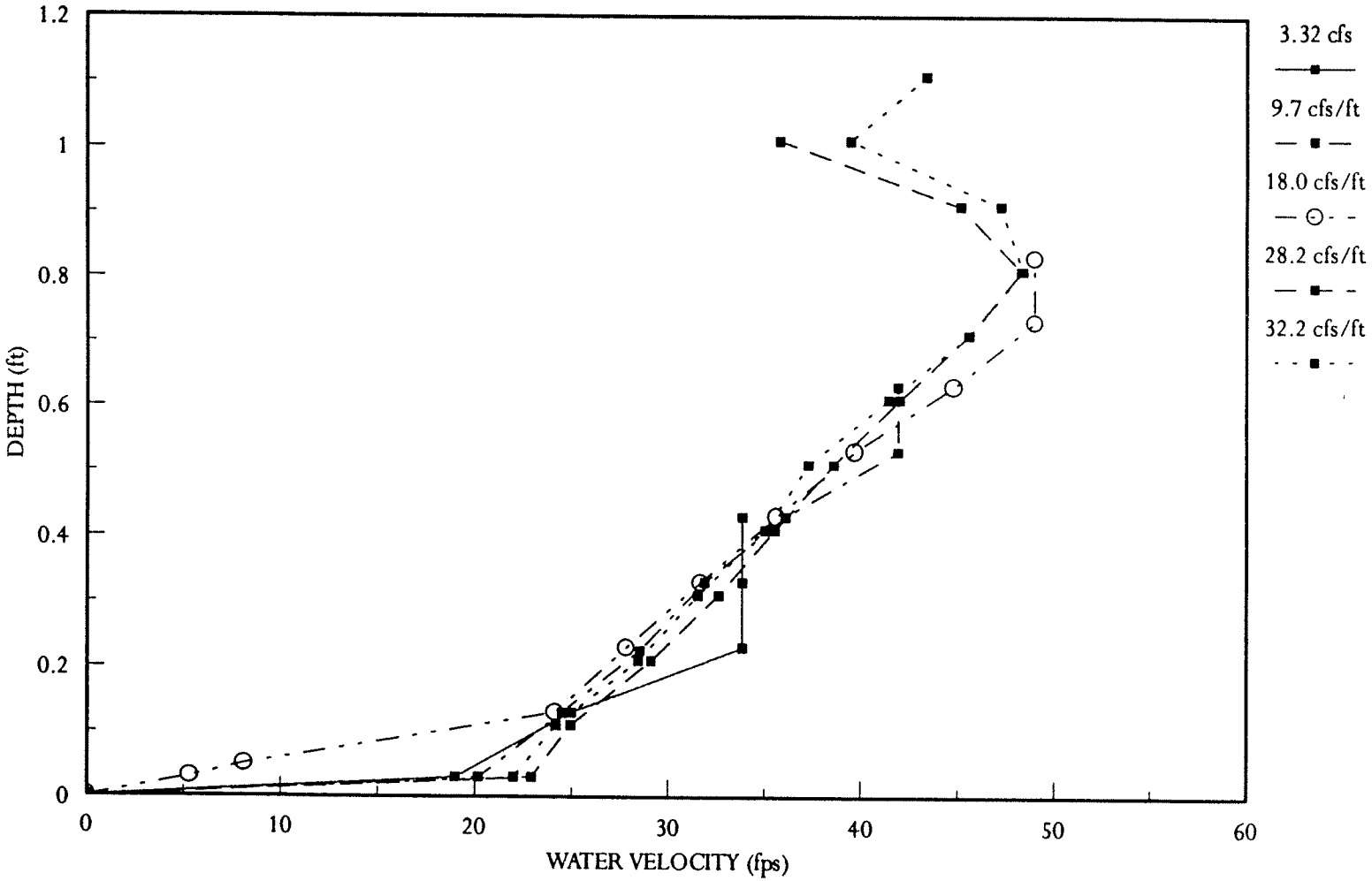

Figure A2: Velocity profiles at Station 3, all flow rates

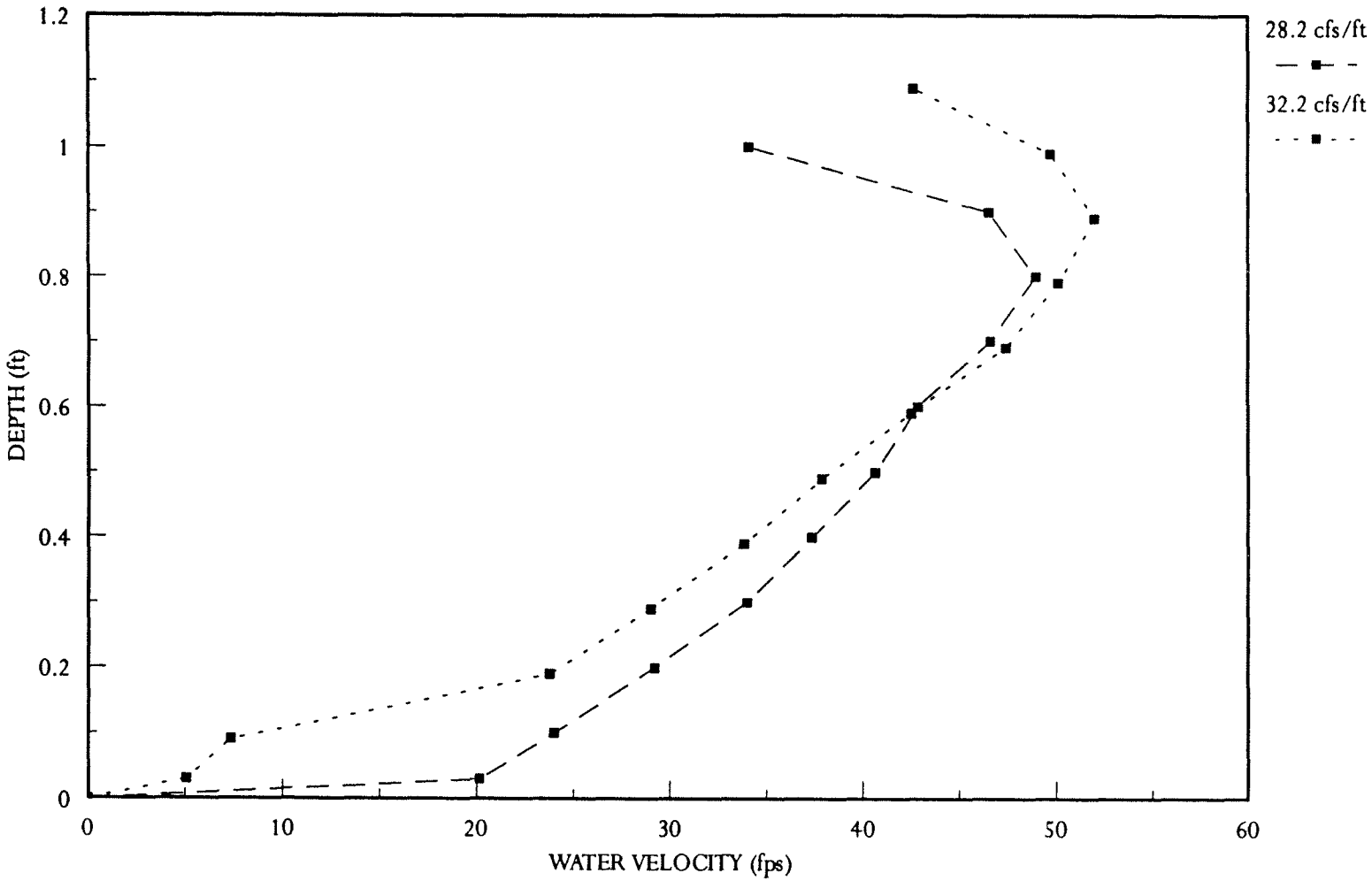

Figure A3: Velocity profiles at Station 4, 28.2 & 32.2 cfs/ft

APPENDIX B

FRICTION FACTOR DATA

Table B1: Column descriptions for friction factor calculations

A: Tested flow rate
B: Tested flow rate divided by the width of the flume, 5 ft.
C: Vertical depth at the upstream end of the reach in question (using y90)
D: Vertical depth at the downstream end of the reach in question; also equal to (D + dD) (using y90)
E: Change in vertical depth between upstream & downstream ends of the reach in question
F: Slope distance between the upstream and downstream ends of the reach
G: Change in depth divided by the slope distance of the reach
H: Change in bed elevation divided by the slope distance
I: Velocity at upstream end of the reach (fps)
J: Velocity at downstream end of the reach (fps)
K: Air concentration at the upstream end of the reach
L: Density at the upstream end of the reach
M: Air concentration at the downstream end of the reach
N: Density at the downstream end of the reach
O: Bed shear stress (see equation below)
P: friction factor (see equation below)

The following formulas are in terms of the column letters described above:

TAU = gC/F[L(HF + Ccos@ + I^2/2g) - N(Dcos@ + J^2/2G)]

$$\tau = \frac{gD}{dx\left[\rho_1\left(dD+D\cos(\alpha)+\frac{V_1^2}{2g}\right)-\rho_2\left(y_2\cos(\alpha)+\frac{V_2^2}{2g}\right)\right]}$$

where: @ = angle of the flume

f = 8gTau/[((L + N)/2)(((I + J)/2)^2)]

$$f = \frac{8g\tau}{\left[\left(\frac{\rho_1+\rho_2}{2}\right)\left(\frac{V_1+V_2}{2}\right)^2\right]}$$

Table B2: Friction factor calculations

cos(@) = 0.89

FLOW RATE (cfs)	UNIT FLOW RATE (cfs/ft)	D (y1) (ft)	y2 (ft)	- dD (ft)	dx (ft)	dD/dX	dZ/dX	V1 (fps)	V2 (fps)	AIR CONCENTRATION @ UPSTRM. STATION	DENSITY AT UPSTREAM STATION (pcf)	AIR CONCENTRATION @ DWNSTRM. STATION	DENSITY AT DOWNSTREAM STATION (pcf)	TAU (psf)	f
BETWEEN STATIONS 1 & 2															
16.6	3.3	0.70	0.32	0.38	55.59	-0.01	0.50	4.75	25.9	0.00	1.94	0.53	0.91	18.67	0.45
48.5	9.7	1.43	0.67	0.76	55.59	-0.01	0.50	6.78	30.1	0.00	1.94	0.44	1.08	34.77	0.54
90.0	18.0	2.16	0.80	1.36	55.59	-0.02	0.50	8.34	37.5	0.00	1.94	0.37	1.22	40.25	0.39
140.9	28.2	2.91	1.10	1.81	55.59	-0.03	0.50	9.68	32.1	0.00	1.94	0.25	1.45	62.64	0.68
160.9	32.2	3.18	1.20	1.99	55.59	-0.04	0.50	10.12	30.4	0.00	1.94	0.28	1.39	75.69	0.89
BETWEEN STATIONS 2 & 3															
16.6	3.3	0.31	0.35	-0.04	36.54	-0.00	0.50	25.9	26.4	0.53	0.91	0.54	0.90	4.53	**0.06**
48.5	9.7	0.71	0.74	-0.02	36.54	-0.00	0.50	30.1	31.8	0.44	1.08	0.46	1.06	11.52	**0.09**
90.0	18.0	0.86	1.07	-0.21	36.54	-0.01	0.50	37.5	35.8	0.37	1.22	0.39	1.17	19.33	**0.10**
140.9	28.2	1.23	1.38	-0.14	36.54	-0.00	0.50	32.1	36.4	0.25	1.45	0.31	1.34	24.07	**0.12**
160.9	32.2	1.34	1.41	-0.07	36.54	-0.00	0.50	30.4	36.6	0.28	1.39	0.30	1.35	20.25	**0.11**
BETWEEN STATIONS 3 & 4															
140.9	28.2	1.38	1.40	-0.02	17.45	0.00	0.50	36.4	36.7	0.31	1.34	0.33	1.30	30.42	**0.14**
160.9	32.2	1.41	1.47	-0.06	17.45	0.00	0.50	36.6	37.4	0.30	1.35	0.33	1.30	30.49	**0.13**
A	B	C	D	E	F	G	H	I	J	K	L	M	N	O	P

AVERAGE FRICTION FACTOR: **0.11**
(Average of shaded values)

APPENDIX C

AIR CONCENTRATION DATA

TABLE C1: Column definitions for tables found in Appendix C

POINT DEPTH CALCULATIONS:

COLUMN NUMBER	COLUMN TITLE	FORMULA DESCRIPTION
1	POINT GAGE	Direct reading from point gage on air concentration probe.
2	DEPTH	Column 1 subtracted from the zero reading for the probe at that station.
3	VOLTAGE	Voltage read directly from the volt meter.
4	AVERAGE VOLTAGE	Average of the values found in column 3 for the depth given in column 2.
5	PROBE AIR CONCENTRATION	The average voltage from column 4 divided by the maximum possible voltage from a 100% air reading of 500 volts.
6	AIR CONCENTRATION	Actual air concentration. Column 5 corrected by the calibration using the equation (1 - 1.2E+25*X - 4E + 24*X^2) / (-2.3E+24 - 3.1E+25*X + 1.7E+25*X^2) where X is the value from column 5, and E+__ stands for "times 10 to the __ power.
7	DIMENSIONLESS DEPTH	The depth from column 2 divided by the maximum depth.

TABLE C1 (continued): Column definitions for tables found in Appendix C

CALCULATION OF AVERAGES:

COLUMN NUMBER	COLUMN TITLE	FORMULA DESCRIPTION
1	REGION	Portion of profile being looked at.
2	DEPTH OF REGION	Depth of the particular region being looked at.
3	AVERAGE AIR CONCENTRATION	Average air concentration for the region indicated in column 1.
4	DEPTH X AVG. AIR CONC.	The product of the previous two columns. The sum of this column is the area of the region to the left of the curves shown in Figures 4.10 through 4.21. The number titled "average air concentrati beneath this column is this sum divided by the total depth of the profile.

Table C2.1: Air concentration data, Station 2, 3.3 cfs/ft

POINT DEPTH CALCULATIONS						
POINT GAGE (ft.)	DEPTH (ft.)	VOLTAGE (VOLTS*100)	AVERAGE VOLTAGE (VOLTS*100)	PROBE AIR CONCENTRATION	AIR CONCENTRATION	DIMENSIONLESS DEPTH (ft./ft.)
8.34	0.00			0.07	0.20	0.00
8.31	0.03	36.831 36.612 34.854	36.099	0.072	0.198	0.097
8.26	0.08	53.338 55.118 58.164	55.540	0.111	0.248	0.258
8.21	0.13	100.300 93.165 89.580	94.348	0.189	0.317	0.419
8.16	0.18	181.880 185.314 184.360	183.851	0.368	0.433	0.581
8.11	0.23	327.266 328.838 330.577	328.894	0.658	0.628	0.742
8.06	0.28	440.748 444.734 443.245	442.909	0.886	0.843	0.903
***	0.31				0.900	1.000
8.01	0.33	483.389 479.012 480.989	481.130	0.962	0.938	

CALCULATION OF AVERAGES			
REGION	DEPTH OF REGION (ft.)	AVERAGE AIR CONCENTRATION	DEPTH X AVG. AIR CON.
A1	0.03	0.198	0.010
A2	0.05	0.223	0.011
A3	0.05	0.282	0.018
A4	0.05	0.375	0.019
A5	0.05	0.530	0.027
A6	0.05	0.736	0.037
A7	0.05	0.890	0.045

CALCULATION OF AVERAGES (TO Y90 ONLY)			
REGION	DEPTH OF REGION (ft.)	AVERAGE AIR CONCENTRATION	DEPTH X AVG. AIR CON.
A1	0.03	0.198	0.010
A2	0.05	0.223	0.011
A3	0.05	0.282	0.018
A4	0.05	0.375	0.019
A5	0.05	0.530	0.027
A6	0.05	0.736	0.037
A7(to Y90 only)	0.03	0.872	0.044

AVERAGE AIR CONCENTRATION = 0.530

*** Actual data was not taken at this point. Values at the depth of Y90 were determined from the graphs.

Table C2.2: Air concentration data, Station 3, 3.3 cfs/ft

POINT DEPTH CALCULATIONS						
POINT GAGE (ft.)	DEPTH (ft.)	VOLTAGE (VOLTS*100)	AVERAGE VOLTAGE (VOLTS*100)	PROBE AIR CONCENTRATION	AIR CONCENTRATION	DIMENSIONLESS DEPTH (ft./ft.)
8.38	0.00			0.116	0.254	0.000
8.35	0.03	60.439 56.843 57.258	58.179	0.116	0.254	0.095
8.30	0.08	70.180 70.334 71.665	70.726	0.141	0.278	0.254
8.25	0.13	111.096 114.522 117.356	114.325	0.229	0.345	0.413
8.20	0.18	216.394 216.171 201.448	212.004	0.424	0.467	0.571
8.15	0.23	337.122 344.483 339.031	340.212	0.680	0.646	0.730
8.10	0.28	431.320 435.212 430.556	432.363	0.865	0.819	0.889
***	0.32				0.900	1.000
8.05	0.33	478.367 481.892 479.342	479.867	0.960	0.934	

CALCULATION OF AVERAGES			
REGION	DEPTH OF REGION (ft.)	AVERAGE AIR CONCENTRATION	DEPTH X AVG. AIR CON.
A1	0.03	0.254	0.013
A2	0.05	0.266	0.013
A3	0.05	0.312	0.016
A4	0.05	0.406	0.020
A5	0.05	0.557	0.028
A6	0.05	0.733	0.037
A7	0.05	0.877	0.044

CALCULATION OF AVERAGES (TO Y90 ONLY)			
REGION	DEPTH OF REGION (ft.)	AVERAGE AIR CONCENTRATION	DEPTH X AVG. AIR CON.
A1	0.03	0.254	0.013
A2	0.05	0.266	0.013
A3	0.05	0.312	0.016
A4	0.05	0.406	0.020
A5	0.05	0.557	0.028
A6	0.05	0.733	0.037
A7	0.04	0.860	0.043

AVERAGE AIR CONCENTRATION = 0.538

*** Actual data was not taken at this point. Values at the depth of Y90 were determined from the graphs.

Table C3.1: Air concentration data, Station 2, 9.7 cfs/ft

POINT DEPTH CALCULATIONS						
POINT GAGE (ft.)	DEPTH (ft.)	VOLTAGE (VOLTS*100)	AVERAGE VOLTAGE (VOLTS*100)	PROBE AIR CONCENTRATION	AIR CONCENTRATION	DIMENSIONLESS DEPTH (ft./ft.)
8.34	0.00			0.012	0.055	0.000
8.31	0.03	6.171 5.685 6.686	6.181	0.012	0.055	0.045
8.21	0.13	12.124 10.795 11.588	11.502	0.023	0.092	0.194
8.11	0.23	22.023 23.097 21.607	22.242	0.044	0.147	0.343
8.01	0.33	53.020 49.947 50.109	51.025	0.102	0.238	0.492
7.91	0.43	173.798 171.244 179.708	174.917	0.350	0.422	0.641
7.81	0.53	364.662 354.449 351.154	356.755	0.714	0.673	0.790
7.71	0.63	448.334 454.988 456.543	453.288	0.907	0.867	0.939
***	0.67				0.900	1.000
7.61	0.73	484.365 485.793 484.678	484.945	0.970	0.948	

CALCULATION OF AVERAGES			
REGION	DEPTH OF REGION (ft.)	AVERAGE AIR CONCENTRATION	DEPTH X AVG. AIR CON.
A1	0.03	0.055	0.005
A2	0.10	0.073	0.007
A3	0.10	0.119	0.012
A4	0.10	0.192	0.019
A5	0.10	0.330	0.033
A6	0.10	0.548	0.055
A7	0.10	0.770	0.077
A8	0.10	0.908	0.091

CALCULATION OF AVERAGES (TO Y90 ONLY)			
REGION	DEPTH OF REGION (ft.)	AVERAGE AIR CONCENTRATION	DEPTH X AVG. AIR CON.
A1	0.03	0.055	0.005
A2	0.10	0.073	0.007
A3	0.10	0.119	0.012
A4	0.10	0.192	0.019
A5	0.10	0.330	0.033
A6	0.10	0.548	0.055
A7	0.10	0.770	0.077
A8	0.04	0.884	0.088

AVERAGE AIR CONCENTRATION = 0.443

*** Actual data was not taken at this point. Values at the depth of Y90 were determined from the graphs.

Table C3.2: Air concentration data, Station 3, 9.7 cfs/ft

POINT DEPTH CALCULATIONS						
POINT GAGE (ft.)	DEPTH (ft.)	VOLTAGE (VOLTS*100)	AVERAGE VOLTAGE (VOLTS*100)	PROBE AIR CONCENTRATION	AIR CONCENTRATION	DIMENSIONLESS DEPTH (ft./ft.)
8.36	0.00			0.020	0.082	0.000
8.33	0.03	9.665 9.980 10.320	9.988	0.020	0.082	0.046
8.25	0.11	20.610 16.817 16.201	17.876	0.036	0.127	0.167
8.15	0.21	25.175 31.044 28.524	28.248	0.056	0.171	0.320
8.05	0.31	54.226 48.395 53.743	52.121	0.104	0.240	0.472
7.95	0.41	145.725 146.651 147.956	146.777	0.294	0.387	0.624
7.85	0.51	336.773 330.955 340.521	336.083	0.672	0.639	0.776
7.75	0.61	450.289 449.035 452.270	450.531	0.901	0.861	0.928
***	0.66				0.900	1.000
7.65	0.71	482.041 484.581 484.047	483.556	0.967	0.944	

CALCULATION OF AVERAGES			
REGION	DEPTH OF REGION (ft.)	AVERAGE AIR CONCENTRATION	DEPTH X AVG. AIR CON.
A1	0.03	0.082	0.008
A2	0.08	0.105	0.010
A3	0.10	0.149	0.015
A4	0.10	0.206	0.021
A5	0.10	0.314	0.031
A6	0.10	0.513	0.051
A7	0.10	0.750	0.075
A8	0.10	0.902	0.090

CALCULATION OF AVERAGES (TO Y90 ONLY)			
REGION	DEPTH OF REGION (ft.)	AVERAGE AIR CONCENTRATION	DEPTH X AVG. AIR CON
A1	0.03	0.082	0.008
A2	0.08	0.105	0.010
A3	0.10	0.149	0.015
A4	0.10	0.206	0.021
A5	0.10	0.314	0.031
A6	0.10	0.513	0.051
A7	0.10	0.750	0.075
A8	0.05	0.880	0.088

AVERAGE AIR CONCENTRATION = 0.456

*** Actual data was not taken at this point. Values at the depth of Y90 were determined from the graphs.

Table C4.1: Air concentration data, Station 2, 18.0 cfs/ft

POINT DEPTH CALCULATIONS						
POINT GAGE (ft.)	DEPTH (ft.)	VOLTAGE (VOLTS*100)	AVERAGE VOLTAGE (VOLTS*100)	PROBE AIR CONCENTRATION	AIR CONCENTRATION	DIMENSIONLESS DEPTH (ft./ft.)
8.34	0.00			0.004	0.020	0.000
8.31	0.03	2.029 1.862 2.183	2.025	0.004	0.020	0.038
8.21	0.13	3.220 3.860 3.203	3.428	0.007	0.032	0.163
8.11	0.23	6.593 8.586 6.206	7.160	0.014	0.062	0.288
8.01	0.33	22.441 18.634 17.467	19.514	0.039	0.135	0.413
7.91	0.43	65.822 70.960 71.024	69.275	0.139	0.276	0.538
7.81	0.53	205.975 206.018 196.721	202.905	0.406	0.456	0.663
7.71	0.63	364.757 360.359 350.094	358.403	0.717	0.676	0.788
7.61	0.73	435.478 427.712 450.048	437.746	0.875	0.831	0.914
***	0.80				0.900	1.000
7.51	0.83	484.361 473.211 478.512	478.695	0.957	0.931	

CALCULATION OF AVERAGES			
REGION	DEPTH OF REGION (ft.)	AVERAGE AIR CONCENTRATION	DEPTH X AVG. AIR CON
A1	0.03	0.020	0.002
A2	0.10	0.026	0.003
A3	0.10	0.047	0.005
A4	0.10	0.099	0.010
A5	0.10	0.205	0.021
A6	0.10	0.366	0.037
A7	0.10	0.566	0.057
A8	0.10	0.754	0.075
A9	0.10	0.881	0.088

CALCULATION OF AVERAGES (TO Y90 ONLY)			
REGION	DEPTH OF REGION (ft.)	AVERAGE AIR CONCENTRATION	DEPTH X AVG. AIR CON
A1	0.03	0.020	0.002
A2	0.10	0.026	0.003
A3	0.10	0.047	0.005
A4	0.10	0.099	0.010
A5	0.10	0.205	0.021
A6	0.10	0.366	0.037
A7	0.10	0.566	0.057
A8	0.10	0.754	0.075
A9	0.07	0.866	0.087

AVERAGE AIR CONCENTRATION = 0.370

*** Actual data was not taken at this point. Values at the depth of Y90 were determined from the graphs.

Table C4.2: Air concentration data, Station 3, 18.0 cfs/ft

POINT DEPTH CALCULATIONS						
POINT GAGE (ft.)	DEPTH (ft.)	VOLTAGE (VOLTS*100)	AVERAGE VOLTAGE (VOLTS*100)	PROBE AIR CONCENTRATION	AIR CONCENTRATION	DIMENSIONLESS DEPTH (ft./ft.)
8.36	0.00			0.009	0.042	0.000
8.33	0.03	4.394 4.268 5.042	4.568	0.009	0.042	0.031
8.25	0.11	6.145 5.945 5.998	5.996	0.012	0.054	0.115
8.15	0.21	11.853 10.361 8.886	10.373	0.021	0.085	0.219
8.05	0.31	16.623 19.227 18.373	18.074	0.036	0.128	0.324
7.95	0.41	25.805 28.578 30.575	28.319	0.057	0.172	0.428
7.85	0.51	55.066 54.781 62.978	57.615	0.115	0.252	0.533
7.75	0.61	142.149 135.185 141.065	139.466	0.279	0.378	0.637
7.65	0.71	282.214 270.254 283.785	278.751	0.558	0.554	0.742
7.55	0.81	389.955 392.266 399.772	393.998	0.788	0.741	0.846
7.45	0.91	451.533 460.086 452.527	454.715	0.909	0.871	0.951
***	0.96				0.900	1.000
7.35	1.01	477.961 479.793 480.156	479.303	0.959	0.933	

CALCULATION OF AVERAGES			
AREA	DEPTH OF AREA (ft.)	AVERAGE AIR CONCENTRATION	DEPTH X AVG. AIR CON.
A1	0.03	0.042	0.005
A2	0.08	0.048	0.005
A3	0.10	0.069	0.008
A4	0.10	0.106	0.012
A5	0.10	0.150	0.015
A6	0.10	0.212	0.021
A7	0.10	0.315	0.032
A8	0.10	0.466	0.047
A9	0.10	0.647	0.065
A10	0.10	0.806	0.081
A11	0.10	0.902	0.090

CALCULATION OF AVERAGES (TO Y90 ONLY)			
AREA	DEPTH OF AREA (ft.)	AVERAGE AIR CONCENTRATION	DEPTH X AVG. AIR CON.
A1	0.03	0.042	0.005
A2	0.08	0.048	0.005
A3	0.10	0.069	0.008
A4	0.10	0.106	0.012
A5	0.10	0.150	0.015
A6	0.10	0.212	0.021
A7	0.10	0.315	0.032
A8	0.10	0.466	0.047
A9	0.10	0.647	0.065
A10	0.10	0.806	0.081
A11	0.05	0.885	0.089

AVERAGE AIR CONCENTRATION = 0.395

*** Actual data was not taken at this point. Values at the depth of Y90 were determined from the graphs.

Table C5.1: Air concentration data, Station 2, 28.2 cfs/ft

POINT DEPTH CALCULATIONS			
DEPTH (ft)	AVERAGE VOLTAGE (VOLTS)	AIR CONCENTRATION	DIMENSIONLESS DEPTH
0.00	0.003	0.039	0.000
0.03	0.003	0.039	0.027
0.09	0.003	0.040	0.080
0.14	0.003	0.039	0.124
0.24	0.003	0.040	0.213
0.34	0.003	0.041	0.301
0.44	0.005	0.060	0.390
0.54	0.007	0.082	0.478
0.64	0.023	0.185	0.567
0.74	0.105	0.338	0.655
0.84	0.340	0.423	0.744
0.94	0.706	0.525	0.833
1.04	0.908	0.704	0.921
1.13	***	0.900	1.000
1.14	0.987	0.924	
1.24	0.996	0.972	

CALCULATION OF AVERAGES			
REGION	DEPTH OF REGION (ft.)	AVERAGE AIR CONCENTRATION	DEPTH X AVG. AIR CON.
A1	0.03	0.039	0.001
A2	0.06	0.039	0.002
A3	0.05	0.039	0.002
A4	0.10	0.039	0.004
A5	0.10	0.041	0.004
A6	0.10	0.051	0.005
A7	0.10	0.071	0.007
A8	0.10	0.133	0.013
A9	0.10	0.262	0.026
A10	0.10	0.380	0.038
A11	0.10	0.474	0.047
A12	0.10	0.615	0.061
A13	0.10	0.814	0.081
A14	0.10	0.948	0.095

CALCULATION OF AVERAGES (TO Y90 ONLY)			
REGION	DEPTH OF REGION (ft.)	AVERAGE AIR CONCENTRATION	DEPTH X AVG. AIR CON.
A1	0.03	0.039	0.001
A2	0.06	0.039	0.002
A3	0.05	0.039	0.002
A4	0.10	0.039	0.004
A5	0.10	0.041	0.004
A6	0.10	0.051	0.005
A7	0.10	0.071	0.007
A8	0.10	0.133	0.013
A9	0.10	0.262	0.026
A10	0.10	0.380	0.038
A11	0.10	0.474	0.047
A12	0.10	0.615	0.061
A13	0.09	0.802	0.071

AVERAGE AIR CONCENTRATION = 0.251

*** Actual data was not taken at this point. Values at the depth of Y90 were determined from the graphs.

Table C5.2: Air concentration data, Station 3, 28.2 cfs/ft

POINT DEPTH CALCULATIONS			
DEPTH (ft)	AVERAGE VOLTAGE (VOLTS)	AIR CONCENTRATION	DIMENSIONLESS DEPTH
0.00	0.003	0.043	0.000
0.03	0.003	0.043	0.024
0.10	0.004	0.044	0.080
0.20	0.005	0.059	0.159
0.30	0.007	0.079	0.239
0.40	0.013	0.124	0.319
0.50	0.016	0.144	0.398
0.60	0.033	0.221	0.478
0.70	0.081	0.315	0.558
0.80	0.168	0.374	0.637
0.90	0.409	0.437	0.717
1.00	0.670	0.510	0.797
1.10	0.876	0.656	0.876
1.20	0.971	0.861	0.956
1.26	***	0.900	1.000
1.30	0.988	0.931	

*** Actual data was not taken at this point. Values at the depth of Y90 were determined from the graphs.

CALCULATION OF AVERAGES			
REGION	DEPTH OF REGION (ft.)	AVERAGE AIR CONCENTRATION	DEPTH X AVG. AIR CON.
A1	0.03	0.043	0.001
A2	0.07	0.043	0.003
A3	0.10	0.051	0.005
A4	0.10	0.069	0.007
A5	0.10	0.102	0.010
A6	0.10	0.134	0.013
A7	0.10	0.183	0.018
A8	0.10	0.268	0.027
A9	0.10	0.345	0.034
A10	0.10	0.406	0.041
A11	0.10	0.474	0.047
A12	0.10	0.583	0.058
A13	0.10	0.759	0.076
A14	0.10	0.896	0.090

CALCULATION OF AVERAGES (TO Y90 ONLY)			
REGION	DEPTH OF REGION (ft.)	AVERAGE AIR CONCENTRATION	DEPTH X AVG. AIR CON.
A1	0.03	0.043	0.001
A2	0.07	0.043	0.003
A3	0.10	0.051	0.005
A4	0.10	0.069	0.007
A5	0.10	0.102	0.010
A6	0.10	0.134	0.013
A7	0.10	0.183	0.018
A8	0.10	0.268	0.027
A9	0.10	0.345	0.034
A10	0.10	0.406	0.041
A11	0.10	0.474	0.047
A12	0.10	0.583	0.058
A13	0.10	0.759	0.076
A14	0.05	0.880	0.048

AVERAGE AIR CONCENTRATION = 0.311

Table C5.3: Air concentration data, Station 4, 28.2 cfs/ft

POINT DEPTH CALCULATIONS			
DEPTH (ft)	AVERAGE VOLTAGE (VOLTS)	AIR CONCENTRATION	DIMENSIONLESS DEPTH
0.00	0.003	0.038	0.000
0.03	0.003	0.038	0.024
0.10	0.004	0.049	0.078
0.20	0.005	0.060	0.157
0.30	0.009	0.097	0.235
0.40	0.015	0.139	0.314
0.50	0.027	0.202	0.392
0.60	0.044	0.255	0.471
0.70	0.097	0.332	0.549
0.80	0.217	0.392	0.628
0.90	0.425	0.441	0.706
1.00	0.675	0.511	0.785
1.10	0.867	0.645	0.863
1.20	0.956	0.812	0.942
1.27	***	0.900	1.000
1.30	0.988	0.931	

*** Actual data was not taken at this point. Values at the depth of Y90 were determined from the graphs.

CALCULATION OF AVERAGES			
REGION	DEPTH OF REGION (ft.)	AVERAGE AIR CONCENTRATION	DEPTH X AVG. AIR CON.
A1	0.03	0.038	0.001
A2	0.07	0.043	0.003
A3	0.10	0.054	0.005
A4	0.10	0.078	0.008
A5	0.10	0.118	0.012
A6	0.10	0.171	0.017
A7	0.10	0.228	0.023
A8	0.10	0.293	0.029
A9	0.10	0.362	0.036
A10	0.10	0.416	0.042
A11	0.10	0.476	0.048
A12	0.10	0.578	0.058
A13	0.10	0.729	0.073
A14	0.10	0.872	0.087

CALCULATION OF AVERAGES (TO Y90 ONLY)			
REGION	DEPTH OF REGION (ft.)	AVERAGE AIR CONCENTRATION	DEPTH X AVG. AIR CON.
A1	0.03	0.038	0.001
A2	0.07	0.043	0.003
A3	0.10	0.054	0.005
A4	0.10	0.078	0.008
A5	0.10	0.118	0.012
A6	0.10	0.171	0.017
A7	0.10	0.228	0.023
A8	0.10	0.293	0.029
A9	0.10	0.362	0.036
A10	0.10	0.416	0.042
A11	0.10	0.476	0.048
A12	0.10	0.578	0.058
A13	0.10	0.729	0.073
A14	0.07	0.856	0.063

AVERAGE AIR CONCENTRATION = 0.328

Table C6.1: Air concentration data, Station 2, 32.2 cfs/ft

POINT DEPTH CALCULATIONS			
DEPTH (ft)	VOLTAGE (VOLTS)	AIR CONCENTRATION	DIMENSIONLESS DEPTH
0.00	0.000	0.000	0.000
0.08	0.000	0.000	0.069
0.19	0.000	0.001	0.075
0.29	0.000	0.001	0.157
0.39	0.000	0.004	0.239
0.49	0.001	0.011	0.321
0.59	0.003	0.033	0.402
0.69	0.009	0.097	0.484
0.79	0.040	0.244	0.566
0.89	0.221	0.393	0.648
0.99	0.586	0.481	0.730
1.09	0.843	0.618	0.811
1.19	0.973	0.868	0.893
1.22	***	0.900	1.000
1.29	0.994	0.957	

*** Actual data was not taken at this point. Values at the depth of Y90 were determined from the graphs.

CALCULATION OF AVERAGES			
REGION	DEPTH OF REGION (ft.)	AVERAGE AIR CONCENTRATION	DEPTH X AVG. AIR CON.
A1	0.08	0.000	0.000
A2	0.11	0.001	0.000
A3	0.10	0.001	0.000
A4	0.10	0.003	0.000
A5	0.10	0.007	0.001
A6	0.10	0.022	0.002
A7	0.10	0.065	0.006
A8	0.10	0.171	0.017
A9	0.10	0.319	0.032
A10	0.10	0.437	0.044
A11	0.10	0.549	0.055
A12	0.10	0.743	0.074
A13	0.10	0.913	0.091

CALCULATION OF AVERAGES (TO Y90 ONLY)			
REGION	DEPTH OF REGION (ft.)	AVERAGE AIR CONCENTRATION	DEPTH X AVG. AIR CON.
A1	0.08	0.000	0.000
A2	0.01	0.001	0.000
A3	0.10	0.001	0.000
A4	0.10	0.003	0.000
A5	0.10	0.007	0.001
A6	0.10	0.022	0.002
A7	0.10	0.065	0.006
A8	0.10	0.171	0.017
A9	0.10	0.319	0.032
A10	0.10	0.437	0.044
A11	0.10	0.549	0.055
A12	0.10	0.743	0.074
A13	0.13	0.884	0.115

AVERAGE AIR CONCENTRATION = 0.284

Table C6.2: Air concentration data, Station 3, 32.2 cfs/ft

POINT DEPTH CALCULATIONS			
DEPTH (ft)	AVERAGE VOLTAGE (VOLTS)	AIR CONCENTRATION	DIMENSIONLESS DEPTH
0.00	0.001	0.011	0.000
0.04	0.001	0.011	0.033
0.09	0.001	0.017	0.071
0.19	0.002	0.026	0.149
0.29	0.004	0.049	0.226
0.39	0.008	0.085	0.303
0.49	0.011	0.115	0.381
0.59	0.027	0.202	0.458
0.69	0.055	0.278	0.536
0.79	0.134	0.358	0.613
0.89	0.311	0.416	0.690
0.99	0.617	0.490	0.768
1.09	0.833	0.609	0.845
1.19	0.953	0.803	0.923
1.29	0.982	0.904	1.000
1.39	0.991	0.943	

CALCULATION OF AVERAGES			
REGION	DEPTH OF REGION (ft.)	AVERAGE AIR CONCENTRATION	DEPTH X AVG. AIR CON.
A1	0.04	0.011	0.000
A2	0.05	0.014	0.001
A3	0.10	0.022	0.002
A4	0.10	0.038	0.004
A5	0.10	0.067	0.007
A6	0.10	0.100	0.010
A7	0.10	0.159	0.016
A8	0.10	0.240	0.024
A9	0.10	0.318	0.032
A10	0.10	0.387	0.039
A11	0.10	0.453	0.045
A12	0.10	0.550	0.055
A13	0.10	0.706	0.071
A14	0.10	0.854	0.085
A15	0.10	0.924	0.092

CALCULATION OF AVERAGES (TO Y90 ONLY)			
REGION	DEPTH OF REGION (ft.)	AVERAGE AIR CONCENTRATION	DEPTH X AVG. AIR CON.
A1	0.04	0.011	0.000
A2	0.05	0.014	0.001
A3	0.10	0.022	0.002
A4	0.10	0.038	0.004
A5	0.10	0.067	0.007
A6	0.10	0.100	0.010
A7	0.10	0.159	0.016
A8	0.10	0.240	0.024
A9	0.10	0.318	0.032
A10	0.10	0.387	0.039
A11	0.10	0.453	0.045
A12	0.10	0.550	0.055
A13	0.10	0.706	0.071
A14	0.10	0.854	0.085

AVERAGE AIR CONCENTRATION = 0.302

Table C6.3: Air concentration data, Station 4, 32.2 cfs/ft

POINT DEPTH CALCULATIONS			
DEPTH (ft)	AVERAGE VOLTAGE (VOLTS)	AIR CONCENTRATION	DIMENSIONLESS DEPTH
0.00	0.002	0.024	0.000
0.03	0.002	0.024	0.022
0.09	0.003	0.039	0.069
0.19	0.004	0.045	0.143
0.29	0.006	0.071	0.218
0.39	0.011	0.111	0.292
0.49	0.020	0.170	0.367
0.59	0.040	0.243	0.441
0.69	0.082	0.316	0.516
0.79	0.168	0.374	0.591
0.89	0.347	0.424	0.665
0.99	0.579	0.479	0.740
1.09	0.809	0.588	0.814
1.19	0.919	0.724	0.889
1.29	0.971	0.860	0.963
1.34	***	0.900	1.000
1.39	0.990	0.938	

*** Actual data was not taken at this point. Values at the depth of Y90 were determined from the graphs.

CALCULATION OF AVERAGES			
REGION	DEPTH OF REGION (ft.)	AVERAGE AIR CONCENTRATION	DEPTH X AVG. AIR CON.
A1	0.03	0.024	0.001
A2	0.06	0.031	0.002
A3	0.10	0.042	0.004
A4	0.10	0.058	0.006
A5	0.10	0.091	0.009
A6	0.10	0.141	0.014
A7	0.10	0.207	0.021
A8	0.10	0.280	0.028
A9	0.10	0.345	0.034
A10	0.10	0.399	0.040
A11	0.10	0.451	0.045
A12	0.10	0.533	0.053
A13	0.10	0.656	0.066
A14	0.10	0.792	0.079
A15	0.10	0.899	0.090

CALCULATION OF AVERAGES (TO Y90 ONLY)			
REGION	DEPTH OF REGION (ft.)	AVERAGE AIR CONCENTRATION	DEPTH X AVG. AIR CON.
A1	0.03	0.024	0.001
A2	0.06	0.031	0.002
A3	0.10	0.042	0.004
A4	0.10	0.058	0.006
A5	0.10	0.091	0.009
A6	0.10	0.141	0.014
A7	0.10	0.207	0.021
A8	0.10	0.280	0.028
A9	0.10	0.345	0.034
A10	0.10	0.399	0.040
A11	0.10	0.451	0.045
A12	0.10	0.533	0.053
A13	0.10	0.656	0.066
A14	0.10	0.792	0.079
A15	0.05	0.880	0.043

AVERAGE AIR CONCENTRATION = 0.332

APPENDIX D

CONTINUITY CHECK DATA

Table D1: Continuity check at 16.6 cfs (3.3 cfs/ft)

STATION 2:

DEPTH (ft)	VELOCITY (fps)	AIR CONC.	WATER CONC.	DEPTH OF REGION (ft)	AVG.VEL. OF REGION (fps)	AVG. WTR. CONC.	AVG. WTR. VELOCITY (fps)	WTR. UNIT FLOW (cfs/ft)	FLOW RATE (cfs)
0.00	0.00	0.20	0.80						
0.03	18.47	0.20	0.80	0.03	9.24	0.80	7.41	0.22	1.11
0.13	24.36	0.32	0.68	0.10	21.41	0.74	15.90	1.59	7.95
0.23	33.31	0.63	0.37	0.10	28.83	0.53	15.21	1.52	7.60
0.32	33.31	0.90	0.10	0.09	33.31	0.24	7.86	0.68	3.42
								TOTAL:	20.09
								% DIFFERENCE:	20.3%

STATION 3:

DEPTH (ft)	VELOCITY (fps)	AIR CONC.	WATER CONC.	DEPTH OF REGION (ft)	AVG.VEL. OF REGION (fps)	AVG. WTR. CONC.	AVG. WTR. VELOCITY (fps)	WTR. UNIT FLOW (cfs/ft)	FLOW RATE (cfs)
0.00	0.00	0.25	0.75						
0.03	19.01	0.25	0.75	0.03	9.51	0.75	7.10	0.21	1.06
0.13	25.01	0.35	0.65	0.10	22.01	0.70	15.42	1.54	7.71
0.23	33.87	0.65	0.35	0.10	29.44	0.50	14.85	1.48	7.42
0.32	33.87	0.90	0.10	0.09	33.87	0.23	7.69	0.66	3.31
								TOTAL:	19.50
								% DIFFERENCE:	18.0%

Table D2: Continuity check at 48.5 cfs (9.7 cfs/ft)

STATION 2:

DEPTH (ft)	VELOCITY (fps)	AIR CONC.	WATER CONC.	DEPTH OF REGION (ft)	AVG.VEL. OF REGION (fps)	AVG. WTR. CONC.	AVG. WTR. VELOCITY (fps)	WTR. UNIT FLOW (cfs/ft)	FLOW RATE (cfs)
0.00	0.00	0.05	0.95						
0.03	19.79	0.05	0.95	0.03	9.90	0.95	9.35	0.28	1.40
0.13	24.16	0.09	0.91	0.10	21.98	0.93	20.36	2.04	10.18
0.23	27.45	0.15	0.85	0.10	25.81	0.88	22.72	2.27	11.36
0.33	30.93	0.24	0.76	0.10	29.19	0.81	23.57	2.36	11.79
0.43	33.45	0.42	0.58	0.10	32.19	0.67	21.57	2.16	10.79
0.53	38.26	0.67	0.33	0.10	35.86	0.45	16.22	1.62	8.11
0.63	38.26	0.87	0.13	0.10	38.26	0.23	8.79	0.88	4.39
0.67	38.26	0.90	0.10	0.04	38.26	0.12	4.45	0.17	0.85
								TOTAL:	58.86
								% DIFFERENCE:	17.6%

STATION 3:

DEPTH (ft)	VELOCITY (fps)	AIR CONC.	WATER CONC.	DEPTH OF REGION (ft)	AVG.VEL. OF REGION (fps)	AVG. WTR. CONC.	AVG. WTR. VELOCITY (fps)	WTR. UNIT FLOW (cfs/ft)	FLOW RATE (cfs)
0.00	0.00	0.08	0.92						
0.03	20.20	0.08	0.92	0.03	10.10	0.92	9.27	0.28	1.39
0.13	24.52	0.13	0.87	0.10	22.36	0.90	20.02	2.00	10.01
0.23	28.54	0.17	0.83	0.09	26.53	0.85	22.57	2.14	10.72
0.33	31.90	0.24	0.76	0.10	30.22	0.79	24.00	2.52	12.60
0.43	36.09	0.39	0.61	0.10	34.00	0.69	23.33	2.33	11.66
0.53	41.94	0.64	0.36	0.10	39.01	0.49	18.98	1.90	9.49
0.63	41.94	0.86	0.14	0.10	41.94	0.25	10.48	1.05	5.24
0.66	41.94	0.90	0.10	0.03	41.94	0.12	5.02	0.15	0.75
								TOTAL:	61.88
								% DIFFERENCE:	21.6%

Table D3: Continuity check at 90.0 cfs (18 cfs/ft)

STATION 2:

DEPTH (ft)	VELOCITY (fps)	AIR CONC.	WATER CONC.	DEPTH OF REGION (ft)	AVG.VEL. OF REGION (fps)	AVG. WTR. CONC.	AVG. WTR. VELOCITY (fps)	WTR. UNIT FLOW (cfs/ft)	FLOW RATE (cfs)
0.00	0.00	0.02	0.98						
0.03	19.82	0.02	0.98	0.03	9.91	0.98	9.71	0.29	1.46
0.13	23.83	0.03	0.97	0.10	21.82	0.97	21.25	2.13	10.63
0.23	27.39	0.06	0.94	0.10	25.61	0.95	24.40	2.44	12.20
0.33	32.02	0.13	0.87	0.10	29.71	0.90	26.78	2.68	13.39
0.43	38.42	0.28	0.72	0.10	35.22	0.79	27.99	2.80	14.00
0.53	47.77	0.46	0.54	0.10	43.10	0.63	27.33	2.73	13.67
0.63	47.77	0.68	0.32	0.10	47.77	0.43	20.72	2.07	10.36
0.73	47.77	0.83	0.17	0.10	47.77	0.25	11.76	1.18	5.88
0.80	47.77	0.90	0.10	0.07	47.77	0.13	6.42	0.44	2.21
								TOTAL:	83.79
								% DIFFERENCE:	-7.4%

STATION 3:

DEPTH (ft)	VELOCITY (fps)	AIR CONC.	WATER CONC.	DEPTH OF REGION (ft)	AVG.VEL. OF REGION (fps)	AVG. WTR. CONC.	AVG. WTR. VELOCITY (fps)	WTR. UNIT FLOW (cfs/ft)	FLOW RATE (cfs)
0.00	0.00	0.04	0.96						
0.03	5.32	0.04	0.96	0.03	2.66	0.96	2.55	0.08	0.38
0.11	24.17	0.05	0.95	0.08	14.74	0.95	14.04	1.12	5.61
0.21	27.81	0.08	0.92	0.10	25.99	0.93	24.20	2.42	12.10
0.31	31.68	0.13	0.87	0.10	29.75	0.89	26.59	2.66	13.29
0.41	35.61	0.17	0.83	0.10	33.64	0.85	28.61	2.86	14.30
0.51	39.69	0.25	0.75	0.10	37.65	0.79	29.67	2.97	14.83
0.61	44.77	0.38	0.62	0.10	42.23	0.68	28.91	2.89	14.46
0.71	48.97	0.55	0.45	0.10	46.87	0.53	25.02	2.50	12.51
0.81	48.97	0.74	0.26	0.10	48.97	0.35	17.26	1.73	8.63
0.96	48.97	0.90	0.10	0.15	48.97	0.18	8.80	1.29	6.47
								TOTAL:	102.59
								% DIFFERENCE:	12.3%

Table D4: Continuity check at 140.9 cfs (28.2 cfs/ft)

STATION 2:

DEPTH (ft)	VELOCITY (fps)	AIR CONC.	WATER CONC.	DEPTH OF REGION (ft)	AVG.VEL. OF REGION (fps)	AVG. WTR. CONC.	AVG. WTR. VELOCITY (fps)	WTR. UNIT FLOW (cfs/ft)	FLOW RATE (cfs)
0.00	0.00	0.04	0.96						
0.03	21.02	0.04	0.96	0.03	10.51	0.96	10.11	0.30	1.52
0.09	22.06	0.04	0.96	0.06	21.54	0.96	20.70	1.24	6.21
0.24	26.27	0.04	0.96	0.15	24.17	0.96	23.20	3.48	17.40
0.34	29.49	0.04	0.96	0.10	27.88	0.96	26.75	2.67	13.37
0.44	31.53	0.06	0.94	0.10	30.51	0.95	28.96	2.90	14.48
0.54	34.62	0.08	0.92	0.10	33.08	0.93	30.73	3.07	15.36
0.64	36.44	0.18	0.82	0.10	35.53	0.87	30.79	3.08	15.40
0.74	39.76	0.34	0.66	0.10	38.10	0.74	28.14	2.81	14.07
0.84	44.46	0.42	0.58	0.10	42.11	0.62	26.09	2.61	13.05
0.94	39.68	0.53	0.47	0.10	42.07	0.53	22.14	2.21	11.07
1.04	27.91	0.70	0.30	0.10	33.80	0.39	13.02	1.30	6.51
1.13	27.91	0.90	0.10	0.09	27.91	0.20	5.52	0.49	2.46
								TOTAL:	130.90
								% DIFFERENCE:	-7.0%

STATION 3:

DEPTH (ft)	VELOCITY (fps)	AIR CONC.	WATER CONC.	DEPTH OF REGION (ft)	AVG.VEL. OF REGION (fps)	AVG. WTR. CONC.	AVG. WTR. VELOCITY (fps)	WTR. UNIT FLOW (cfs/ft)	FLOW RATE (cfs)
0.00	0.00	0.04	0.96						
0.03	22.94	0.04	0.96	0.03	11.47	0.96	10.98	0.33	1.65
0.10	24.97	0.04	0.96	0.07	23.95	0.96	22.91	1.60	8.02
0.20	29.12	0.06	0.94	0.10	27.04	0.95	25.65	2.57	12.83
0.30	32.63	0.08	0.92	0.10	30.87	0.93	28.74	2.87	14.37
0.40	35.55	0.12	0.88	0.10	34.09	0.90	30.63	3.06	15.31
0.50	38.58	0.14	0.86	0.10	37.06	0.87	32.11	3.21	16.05
0.60	42.02	0.22	0.78	0.10	40.30	0.82	32.94	3.29	16.47
0.70	45.56	0.31	0.69	0.10	43.79	0.73	32.04	3.20	16.02
0.80	48.28	0.37	0.63	0.10	46.92	0.66	30.75	3.08	15.38
0.90	45.14	0.44	0.56	0.10	46.71	0.59	27.75	2.78	13.88
1.00	35.79	0.51	0.49	0.10	40.46	0.53	21.30	2.13	10.65
1.26	35.79	0.90	0.10	0.26	35.79	0.30	10.56	2.69	13.47
								TOTAL:	154.09
								% DIFFERENCE:	9.1%

Table D4 (continued): Continuity check at 140.9 cfs (28.2 cfs/ft)

STATION 4:

DEPTH (ft)	VELOCITY (fps)	AIR CONC.	WATER CONC.	DEPTH OF REGION (ft)	AVG.VEL. OF REGION (fps)	AVG. WTR. CONC.	AVG. WTR. VELOCITY (fps)	WTR. UNIT FLOW (cfs/ft)	FLOW RATE (cfs)
0.00	0.00	0.04	0.96						
0.03	20.16	0.04	0.96	0.03	10.08	0.96	9.70	0.29	1.45
0.10	24.04	0.05	0.95	0.07	22.10	0.96	21.14	1.48	7.40
0.20	29.23	0.06	0.94	0.10	26.64	0.95	25.20	2.52	12.60
0.30	34.01	0.10	0.90	0.10	31.62	0.92	29.14	2.91	14.57
0.40	37.40	0.14	0.86	0.10	35.71	0.88	31.48	3.15	15.74
0.50	40.68	0.20	0.80	0.10	39.04	0.83	32.38	3.24	16.19
0.60	42.85	0.25	0.75	0.10	41.76	0.77	32.23	3.22	16.11
0.70	46.59	0.33	0.67	0.10	44.72	0.71	31.60	3.16	15.80
0.80	48.94	0.39	0.61	0.10	47.77	0.64	30.49	3.05	15.24
0.90	46.52	0.44	0.56	0.10	47.73	0.58	27.86	2.79	13.93
1.00	34.09	0.51	0.49	0.10	40.31	0.52	21.11	2.11	10.56
1.27	34.09	0.90	0.10	0.27	34.09	0.29	10.03	2.75	13.75
								TOTAL:	153.35
								% DIFFERENCE:	8.7%

Table D5: Continuity check at 160.9 cfs (32.2 cfs/ft)

STATION 2:

DEPTH (ft)	VELOCITY (fps)	AIR CONC.	WATER CONC.	DEPTH OF REGION (ft)	AVG.VEL. OF REGION (fps)	AVG. WTR. CONC.	AVG. WTR. VELOCITY (fps)	WTR. UNIT FLOW (cfs/ft)	FLOW RATE (cfs)
0.00	0.00	0.00	1.00						
0.09	20.58	0.00	1.00	0.09	10.29	1.00	10.28	0.95	4.73
0.19	21.86	0.00	1.00	0.10	21.22	1.00	21.19	2.12	10.60
0.29	25.61	0.00	1.00	0.10	23.73	1.00	23.67	2.37	11.83
0.39	28.54	0.01	0.99	0.10	27.07	0.99	26.87	2.69	13.44
0.49	31.69	0.03	0.97	0.10	30.11	0.98	29.45	2.95	14.73
0.59	33.14	0.10	0.90	0.10	32.41	0.94	30.31	3.03	15.15
0.69	34.65	0.24	0.76	0.10	33.89	0.83	28.11	2.81	14.06
0.79	37.53	0.39	0.61	0.10	36.09	0.68	24.59	2.46	12.29
0.89	40.65	0.48	0.52	0.10	39.09	0.56	22.01	2.20	11.01
0.99	41.04	0.62	0.38	0.10	40.85	0.45	18.41	1.84	9.21
1.09	25.60	0.87	0.13	0.10	33.32	0.26	8.56	0.86	4.28
1.22	25.60	0.90	0.10	0.13	25.60	0.12	2.96	0.39	1.94
								TOTAL:	123.25
								% DIFFERENCE:	-29.8%

STATION 3:

DEPTH (ft)	VELOCITY (fps)	AIR CONC.	WATER CONC.	DEPTH OF REGION (ft)	AVG.VEL. OF REGION (fps)	AVG. WTR. CONC.	AVG. WTR. VELOCITY (fps)	WTR. UNIT FLOW (cfs/ft)	FLOW RATE (cfs)
0.00	0.00	0.01	0.99						
0.04	22.01	0.01	0.99	0.04	11.00	0.99	10.89	0.46	2.29
0.09	24.01	0.02	0.98	0.05	23.01	0.99	22.69	1.13	5.67
0.19	28.21	0.03	0.97	0.10	26.11	0.98	25.55	2.55	12.77
0.29	31.35	0.05	0.95	0.10	29.78	0.96	28.66	2.87	14.33
0.39	34.71	0.09	0.91	0.10	33.03	0.93	30.81	3.08	15.40
0.49	37.14	0.11	0.89	0.10	35.93	0.90	32.33	3.23	16.16
0.59	40.86	0.20	0.80	0.10	39.00	0.84	32.82	3.28	16.41
0.69	44.24	0.28	0.72	0.10	42.55	0.76	32.33	3.23	16.16
0.79	47.16	0.36	0.64	0.10	45.70	0.68	31.17	3.12	15.58
0.89	45.75	0.42	0.58	0.10	46.45	0.61	28.48	2.85	14.24
0.99	37.53	0.49	0.51	0.10	41.64	0.55	22.77	2.28	11.38
1.09	39.57	0.61	0.39	0.10	38.55	0.45	17.36	1.74	8.68
1.29	39.57	0.90	0.10	0.20	39.57	0.24	9.63	1.93	9.63
								TOTAL:	158.72
								% DIFFERENCE:	-0.8%

Table D5 (continued): Continuity check at 160.9 cfs (32.2 cfs/ft)

STATION 4:

DEPTH (ft)	VELOCITY (fps)	AIR CONC.	WATER CONC.	DEPTH OF REGION (ft)	AVG.VEL. OF REGION (fps)	AVG. WTR. CONC.	AVG. WTR. VELOCITY (fps)	WTR. UNIT FLOW (cfs/ft)	FLOW RATE (cfs)
0.00	0.00	0.02	0.98						
0.03	5.06	0.02	0.98	0.03	2.53	0.98	2.47	0.07	0.37
0.09	7.39	0.04	0.96	0.06	6.22	0.97	6.03	0.37	1.87
0.19	23.80	0.04	0.96	0.10	15.59	0.96	14.94	1.49	7.47
0.29	29.04	0.07	0.93	0.10	26.42	0.94	24.90	2.49	12.45
0.39	33.88	0.11	0.89	0.10	31.46	0.91	28.60	2.86	14.30
0.49	37.90	0.17	0.83	0.10	35.89	0.86	30.84	3.08	15.42
0.59	42.50	0.24	0.76	0.10	40.20	0.79	31.89	3.19	15.94
0.69	47.40	0.32	0.68	0.10	44.95	0.72	32.38	3.24	16.19
0.79	50.10	0.37	0.63	0.10	48.75	0.66	31.93	3.19	15.97
0.89	51.97	0.42	0.58	0.10	51.04	0.60	30.67	3.07	15.33
0.99	49.69	0.48	0.52	0.10	50.83	0.55	27.88	2.79	13.94
1.09	42.61	0.59	0.41	0.10	46.15	0.47	21.54	2.15	10.77
1.34	42.61	0.90	0.10	0.25	42.61	0.26	10.91	2.72	13.58

TOTAL: 153.61

% DIFFERENCE: -4.2%

APPENDIX E

DEPTH MEASUREMENT INSTRUMENT (DMI) DATA

Table E1: Depth Measurement Instrument (DMI) depth values

STATION	DMI DEPTH (ft)			
	3.2 cfs/ft	9.7 cfs/ft	18.0 cfs/ft	32.2 cfs/ft
1	0.82	1.27	1.77	2.93
2	0.95	1.06	1.03	1.46
3	0.76	1.07	1.10	1.08
4	0.70	1.04	1.12	1.59

APPENDIX F

FREEBOARD COMPARISON

This shows a comparison between the data taken for the current study, and the results of using the freeboard equation shown on page 92 as equation 4.6.

Equation 4.6

$$FB = 2 + (0.025)\, Vd^{(1/3)}$$

where FB is the freeboard in feet, V is the velocity, and d is the depth of unaerated flow in feet. Neglecting the 2 feet in this equation assuming it is a factor of safety, the freeboard at Station 3 for the 28.2 cfs/ft case would be:

$$FB = (0.025)(36)(0.87^{(1/3)})$$
$$= 0.86\ ft.$$

As stated on page 90, the average freeboard as determined from the data collected in the current study is approximately 0.25 feet.

The large difference in these values, approximately 71 %,makes any comparison difficult.